Università degli Studi di Milano-Bicocca

Dipartimento di Informatica, Sistemistica e Comunicazione

Corso di Laurea Magistrale in Informatica

Simulation of robot swarms for learning communication-aware coordination

Relatore: Dr. Alessandro Giusti
Co-relatore: Dr. Jèrôme Guzzi

Tesi di Laurea Magistrale di
Giorgia Adorni
Matricola 806787

Anno Accademico 2019–2020

I certify that except where due acknowledgement has been given, the work presented in this thesis is that of the author alone; the work has not been submitted previously, in whole or in part, to qualify for any other academic award; and the content of the thesis is the result of work which has been carried out since the official commencement date of the approved research program.

Giorgia Adorni
Lugano, 16 October 2020

To everyone who taught me something

“It has become appallingly obvious that our technology has exceeded our humanity.”

Albert Einstein

Abstract

In recent years, robotics research has dedicated extensive attention to cooperative multi-agent problems, in which agents have a common goal that requires them to collaborate, and possibly to communicate, to achieve it. We investigate imitation learning algorithms to address this issue, providing new insights and promising solutions. These methods learn a controller by observing demonstrations of an expert, such as the behaviour of a centralised omniscient controller, which can perceive the entire environment, including the state and observations of all agents.

Performing tasks with complete knowledge of the state of a system is relatively easy, but centralised solutions might not be feasible in real scenarios since agents do not have direct access to the state but only to their own observations. To overcome this issue, we train end-to-end Neural Networks (NNs), usually classifiers or regressors, that take as input local observations obtained from an omniscient centralised controller, in other words the agents' sensor readings, and the communications received, producing as output the action to be performed and the communication to be transmitted.

In this study, we focus on two different scenarios: distributing the robots in space such that they stand at equal distance from each other, and colouring the robots in space depending on their position with respect to the others in the group. Both are examples of cooperative tasks based on the use of a distributed controller. While the second cannot be solved without allowing an explicit exchange of messages between the agents, in the first one, a communication protocol is not necessary, although it may increase performance.

The experiments are run in Enki, a high-performance open-source simulator for planar robots, which provides collision detection and limited physics support for robots evolving on a flat surface. Moreover, it can simulate groups of robots hundreds of times faster than real-time.

The results show how applying a communication strategy improves the performance of the distributed model, letting it decide which actions to take almost as precisely and quickly as the expert controller.

Acknowledgements

I would like to thank my supervisors Alessandro Giusti and Jérôme Guzzi for their precious advice and help, my family who have never stopped believing in me and to Elia who shared with me this extraordinary journey, always encouraging and supporting me, despite all the difficulties.

A special thank goes also to Università della Svizzera Italiana and the University of Milano–Bicocca for allowing me to take part in this double degree program and to all those people who have accompanied me and made this experience special.

Contents

Figures

Tables

Equations

Listings

Introduction

In this work we consider cooperative multi-agent scenarios, in which multiple robots collaborate, and possibly communicate, to achieve a common goal [Ismail and Sariff, 2018]. Homogeneous Multi-Agent Systems (MAS) are composed of N interacting agents, which have the same physical structure and observation capabilities, so they can be considered to be interchangeable and cooperate to solve a given task [Stone and Veloso, 2000; Šošić et al., 2016]. This system is characterised by a state S — which can be decomposed in sets of local states for each agent and the set of possible observations O for each agent — obtained through sensors and the set of possible actions A for each agent.

The objective of this study is to use Imitation Learning (IL) approaches to learn decentralised solutions via imitation of an omniscient centralised control. To do so we train end-to-end NNs, either classifiers or regressors, that only exploit local observations and communications to decide the action to be performed. This controller is the same for each agent, which means that given an identical set of observations as input, likewise, for each of these the outputs will be equivalent [Ross et al., 2011; Tolstaya et al., 2020].

This research project focuses on two different multi-agent scenarios, in which N robots, all oriented in the same direction, are initially randomly placed along the x-axis. We consider the Thymio as holonomic, since their movements are limited in only one dimension. This premise simplifies our system, in which consequently we have to keep into account only geometric constraints and not kinematic.

In the first scenario, visualised in Figure 1, the objective is to distribute the robots in space such that they stand at equal distance from each other. To do so, each agent updates its state — its absolute position — by performing actions — moving forward and backwards along the x-axis — based on the observations received from the environment — the distances from neighbours. Perceiving the environment using its own sensors, in particular sensing the distances from the neighbours, each robot achieves the goal moving towards the target by minimising the difference between the values recorded by the front and rear sensors, trying to maintain the maximum achievable speed. This means that each robot is at the same distance from the one in front and the one behind, that should be the same distance among all the agents.

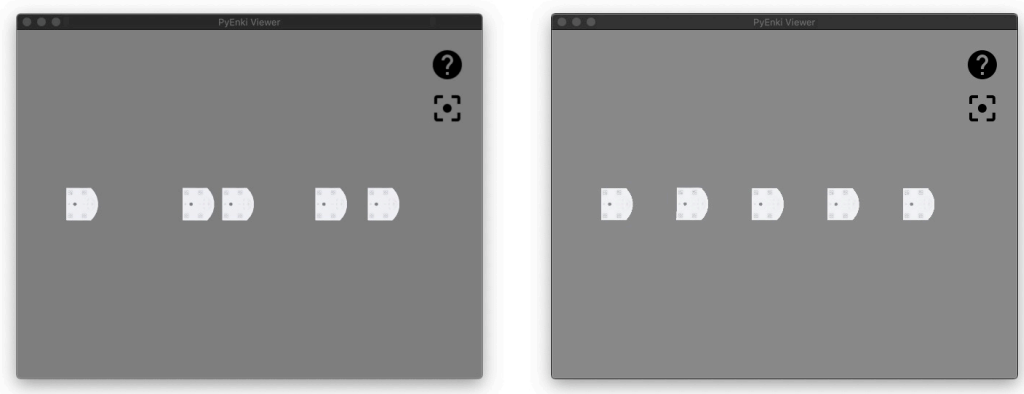

Figure 1. Visualisation of the initial and final configurations obtained simulating the first task.

In the second scenario, shown in Figure 2, assuming that the agents in space are divided into two sets, the objective is to colour them depending on their group membership. For the sake of simplicity, we decide the group each robot belongs to based on the total number of robots: in case of an even number of agents, those in the first half of the row belong to the first group and the remaining to the second, while in the case of an odd number of robots, the same reasoning is applied and the central agent is assigned to the first set. To perform this task, each agent performs actions — colouring the top Light Emitting Diode (LED) in red or blue — based on the observations received from the environment — the messages received from neighbours. This time, sensing

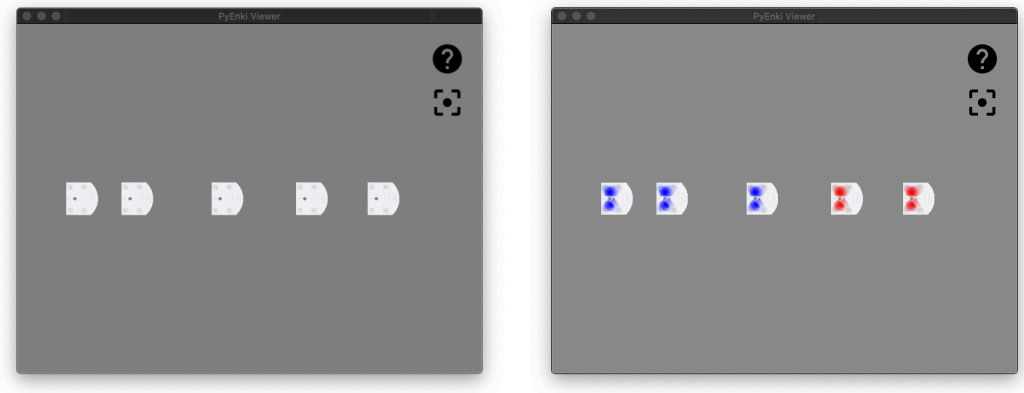

Figure 2. Visualisation of the initial and final configurations obtained simulating the second task.

the distance from neighbours does not provide useful information about the order of the agents, therefore they are not considered to accomplish this task. Instead, the only way for the robots to understand their ordering is necessarily using a communication protocol. For example, starting from the extreme agents, the first and the last in the

row, or those that cannot receive any communication respectively from back and front, all the robots retransmit the received value, increased by one. In this way, the agents will in a sense, learn to count in order to understand which is the correct value to transmit.

Both the scenarios are examples of cooperative tasks based on the use of a distributed controller. While the second cannot be solved without allowing an explicit exchange of messages between the agents, in the first one a communication protocol is not necessary, but it may nonetheless increase performance. To solve these tasks we have adopted two different methodologies, depending on whether the communication is used or not. First of all, we analyse typical supervised learning approaches, which directly learn a mapping from observations to actions. This method can be applied only to the first task, in which a very simple "distributed network" that takes as input an array containing the response values of the sensors — either `prox_values`, `prox_comm` or `all_sensors` — and produces as output an array containing one float that represents the speed of the wheels, which is assumed to be the same both right and left, so that the robot moves straight. After that, we concentrate on more challenging situations where the communication is not provided to the network, instead, it is a latent variable which has to be inferred [Le et al., 2017]. Throughout the experiments, we show the effectiveness of our methods, comparing approaches with and without communication. We also analyse the effects of varying the inputs of the networks, the initial distance between the robot and the number of agents chosen.

Outline

The thesis is composed of 6 chapters, whose main points are presented as follows:

- Chapter 1 summarises the previous research on the topic, evaluating the approaches adopted by the authors;
- Chapter 2 provides the background knowledge needed to properly understand the research contents;
- Chapter 3 presents the tools used for the data collection and all the additional frameworks we relied on;
- Chapter 4 thoroughly illustrates the methodology used, their benefits and limitations, also including descriptions of the kind of data used and how they are collected;
- Chapter 5 explores the analysis conducted and shows evaluation results;
- The Conclusion addresses the results of the experiments, concludes the thesis by discussing the implications of our findings, possible improvements and outlines future works.

Chapter 1

Literature review

This chapter discusses previous research about the topic, providing a brief introduction to the approach we adopted.

In recent years, the application of Artificial Intelligence (AI) and Deep Learning (DL) techniques to multi-agent cooperative problems has become increasingly successful. Gasser and Huhns, in *Distributed Artificial Intelligence* [Gasser and Huhns, 2014], have addressed the issue of coordination and cooperation among agents with the combination of distributed systems and AI, a discipline known as Distributed Artificial Intelligence (DAI).

Similarly, Panait and Luke, in their work *Cooperative multi-agent learning: The state of the art* [Panait and Luke, 2005], report that Multi-Agent Learning (MAL), the application of machine learning to problems involving multiple agents, has become a popular approach which deals with unusually large search spaces. In addition, they mention three of the most classic techniques used to solve cooperative Multi-Agent (MA) problems, that are Supervised and Unsupervised Learning, and Reinforcement Learning (RL). These methods are distinguished according to the type of feedback provided to the agent: the target output in the first case, no feedback is provided in the second, and reward based on the learned output in the last one.

Given these three options, the vast majority of articles in this field used reward-based methods to approach MAL scenarios, in particular RL, that make they possible to achieve sophisticated goals in complex and uncertain environments [Oliehoek, 2012]. However, this technique is notoriously known for being hard, in particular it is difficult to design a suitable reward function for the agents to optimise, which precisely leads to the desired behaviour in all possible scenarios. This problem is further exacerbated in multi-agent settings [Hadfield-Menell et al., 2017; Oliehoek, 2012].

Inverse Reinforcement Learning (IRL) addresses this problem by using a given set of expert trajectories to derive a reward function under which these are optimal. Nevertheless, this technique imposes often unrealistic requirements [Šošić et al., 2016].

IL is a class of methods that has been successfully applied to a wide range of domains

in robotics, for example, autonomous driving [Schaal, 1999; Stepputtis et al., 2019]. They aim to overcome the issues aforementioned and, unlike reward-based methods, the model acquires skills and provides actions to the agents by observing the desired behaviour, performed by an expert [Song et al., 2018; Zhang et al., 2018; Billard et al., 2008]. Using this approach the models learn how to extract relevant information from the data provided to them, directly learning a mapping from observations to actions. A more challenging situation occurs when the model also has to infer the coordination among agents that is implicit in the demonstrations, using unsupervised approaches to imitation.

In this direction, literature suggests that cooperative tasks sometimes cannot be solved using only a simple distributed approach, instead it may be necessary to allow an explicit exchange of messages between the agents. In *Multi-agent reinforcement learning: Independent vs. cooperative agents* [Tan, 1993], Tan affirms that cooperating learners should use communication in a variety of ways in order to improve team performance: they can share instantaneous informations as well as episodic experience and learned knowledge. Also Pesce and Montana propose the use of inter-agent communication for situations in which the agents can only acquire partial observations and are faced with a task requiring coordination and synchronisation skills [Pesce and Montana, 2019]. Their solution consists in an explicit communication system that allows agents to exchange messages that are used together with local observations to decide which actions to take.

Our work is based on *Learning distributed controllers by backpropagation* [Verna, 2020], which proposes an approach in which a distributed policy for the agents and a coordination model are learned at the same time. This method is based on an important concept introduced in *Coordinated multi-agent imitation learning* [Le et al., 2017]: the network has the ability to autonomously determine the communication protocol. Likewise, we use imitation learning approaches to solve the problem of coordinating multiple agents, introducing a communication protocol, which consists in an explicit exchange of messages between the robots. The communication is not provided to the network, instead, it is a latent variable which has to be inferred. The results show the effectiveness of this communication strategy developed, as well as an illustration of the different patterns emerging from the tasks.

Chapter 2

Background

This chapter provides some background concepts to understand the material presented in this thesis. We start Section 2.1 with a review about differential drive robots and their kinematics, providing some useful notions about the types of sensors used and finally summarising the theory of control. We conclude with a refresher on Neural Networks (NNs), in Section 2.2.

2.1 Differential drive robots

The robot we use for this study is Thymio II, a non-holonomic differential drive robot.

A differential wheeled vehicle is mobile robot, that typically consists of a rigid body

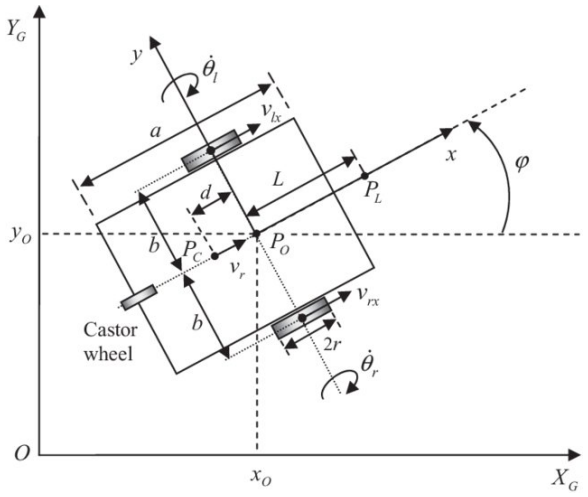

Figure 2.1. Configuration of a non-holonomic differential drive mobile robot [Shojaei et al., 2011].

and a mobile base with a system of wheels that allows movement in the environment. Its movements are based on two, independently powered and controlled, fixed wheels, placed on either side of the robot body, with a common axis of rotation, and one passive caster wheel, whose job is to keep the robot statically balanced. Thus, both drive and steering functions are provided. In fact, it is possible to impose different values of velocity for the two fixed wheels, allowing the robot to rotate and move back and forth [Siciliano et al., 2010]. It is important to note that the robot is non-holonomic since it cannot translate laterally.

The Instantaneous Center of Curvature (ICC), is the point which lies along the horizontal axis, common to the left and right wheels, perpendicular to the plane of each wheel. Its position changes over time as a function of the individual wheel velocities, in particular of their relative difference. Since the rate of rotation ω is the same for both wheels, the following expressions hold:

$$\omega\,(R+b) = V_{rx} \tag{2.1}$$

$$\omega\,(R-b) = V_{lx} \tag{2.2}$$

Equation 2.1. Right and left linear velocities of a differential drive robot, computed as function of the rotation rate, the distance between the wheels, and the distance from the ICC and the robot reference point.

where b is the distance between the centres of the two wheels, V_{rx} and V_{lx} are the right and left wheel velocities, and R is the signed distance from the ICC to the midpoint between the wheels P_O [Dudek and Jenkin, 2010]. Moreover, at any specific time instant t we can compute R and ω as follows:

$$R = b\,\frac{V_{rx}+V_{lx}}{V_{rx}-V_{lx}} \tag{2.3}$$

Equation 2.2. Function to compute R, the signed distance from the ICC to the midpoint between the wheels P_O, or robot reference point, using the right and left linear velocities and the distance between the centres of the two wheels.

$$\omega = \frac{V_{rx}-V_{lx}}{2b} \tag{2.4}$$

Equation 2.3. Function to compute ω, the angular velocity of the robot, using the right and left linear velocities and the distance between the centres of the two wheels.

As a consequence, by varying the speed of the two wheels, V_{rx} and V_{lx}, the trajectories that the robot takes changes as well:

- $V_{rx} = V_{lx}$: if the same speed is set to both wheels, we have a forward linear motion in a straight line. R becomes infinite, and there is effectively no rotation $\omega = 0$.
- $V_{rx} = -V_{lx}$: if both wheels are driven with equal speed but in the opposite direction, we have a rotation about the midpoint of the wheel axis, or in-place rotation. $R = 0$, the ICC coincide with P_O and $\omega = -\frac{V}{b}$.
- $V_{lx} = 0$: if the left wheel is not powered, we have a counter-clockwise rotation about the left wheel. $R = b$ and $\omega = \frac{V_{rx}}{2b}$.
- $V_{rx} = 0$: if the right wheel is not powered, we have a clockwise rotation about the right wheel. $R = -b$ and $\omega = -\frac{V_{lx}}{2b}$.

Differential drive robots, however, are sensitive to slight changes in velocity, and even small errors can affect the robot trajectory. Moreover, they are also susceptible to variations in the ground.

2.1.1 Sensors

A significant feature of the Thymio II robot, is the a large number of sensors with which it is equipped.

The adoption of external sensing mechanism is of crucial importance to allow a robot to interact with its environment and achieve high-performance [Fu et al., 1987; Siciliano et al., 2010].

It is possible to classify the sensors in two principal categories, according to their function: *proprioceptive* sensors, that measure the internal state and deal with the the detection of variables used for the control, such as the robot position, and *exteroceptive* sensors that measure the external state of the environment, dealing with the detection of variables such as range and proximity, often used for robot guidance as well as object detection.

For the purposes of this thesis we are interested in the study of proximity sensors, in particular the Infrared (IR) sensors, that used by Thymio II.

Proximity sensors are an example of exteroceptive sensors: they gather information from the environment around the robot, such as distance to objects. They are also *active* sensors: they emit their own energy, usually light, and measure the reflection. Among the advantages of this type of sensors is the fact that the infrared beams generated by the sources can be used unobtrusively, since they are invisible to the human eye.

IR sensors are composed of an emitter, which radiates invisible infrared light, and a receiver, that measures the intensity of the reflection and the quantity of light that comes back. If the reflection is strong enough — a large part of the light is reflected from

the object and returns to the robot — it can be inferred that the obstacle is relatively close and lies within a certain range of the sensor, depending on the received intensity. If the object is farther away, only a small part of the light comes back [Fu et al., 1987]. However, this estimate can be significantly affected by some property of the obstacle, such as its colour and reflectivity, but also by the presence of external light sources and the temperature of the environment — e.g. a black object reflects less light than a white one, placed at the same distance [Ben-Ari and Mondada, 2018].

2.1.2 Control theory

The problem of controlling a robot is of a primary importance: to achieve a given task, an agent must acts based on the perception received from the environment. To do so, robots use a controller that takes decisions according to algorithms developed to accomplish the goal.

We can distinguish two main techniques of control: *open-loop control* sets in advance the parameters of the algorithm and never observes the result of its actions to adjust them to the actual state, *closed-loop control* or feedback-based control, measures the error between the desired state of the system and the actual one, and uses this feedback to to adjust the control and decide the next action to take [Ben-Ari and Mondada, 2018].

These methods can be used to compute trajectories that lead the robot from an initial configuration to a final one. To achieve a more appropriate behaviour we are interested in the use of closed-loop control systems [Siegwart et al., 2011].

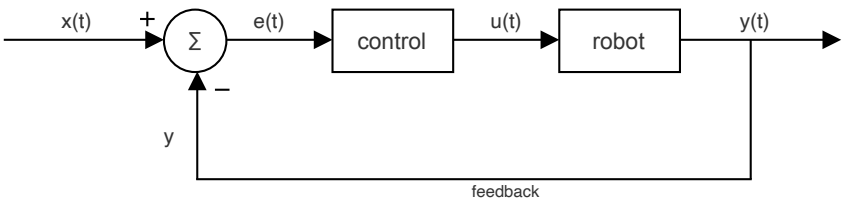

Figure 2.2. Closed-loop control system.

This model can be formally defined using the variables introduced below:

- $x(t)$, called command or set point (SP), represents the reference value, or a desired output. It cannot be imposed directly on the robot, instead it is transformed into a control value $u(t)$.
- $u(t)$, called control variable, is the output of the control and the input of the robot.
- $y(t)$, called process variable (PV), represents an observable part of the the actual state of the robot. It is the feedback signal combined with the set point to compute the error value.

- $e(t)$ is the error. It is computed as the difference between the value of the set point and the process variable, as shown in Equation 2.4. The error is used to generate the new control signal $u(t)$.

$$e(t) = x(t) - y(t) \tag{2.5}$$

Equation 2.4. Calculation of the error value $e(t)$ of the system.

The closed-loop control algorithms sometimes can be very sophisticated. For the purpose of this study, we design two algorithms, the first one is a Proportional–Integral–Derivative (PID) controller, while the second a Bang Bang controller.

The implementation of any feedback controller requires the availability of the robot configuration at each time instant.

2.1.2.1 Proportional (P) controller

Considering real situations in which agents do not have access to their states but only to their local observations, the controller we design for achieve the goal of the first task is a Proportional (P) Controller, a particular variant of PID Controller, with only the K_p term, more details are provided in the Section 4.5.2.1.

The closed-loop control uses a feedback to adjust the control while the action takes place in proportion to the existing error. This function, given a desired output $x(t)$, or set point, produces an output $y(t)$, or process variable, such that the error $e(t)$ is obtained as the difference between the value of the set point and the process variable. Finally, the control variable $u(t)$ is the output of the PID controller and is computed as follows:

$$u(t) = K_p * e(t) \tag{2.6}$$

Equation 2.5. Proportional PID controller.

The value of the proportional gain can be tuned to yield satisfactory performance so that the system is stable.

2.1.2.2 Bang-bang controller

The controller we design to achieve the goal of the first task, of which more details are provided in the Section 4.5.1.1, is a variant of the Bang-bang algorithm.

In this case we considered instead a situation in which agents have access to their states: given the set point and the variable measured, the goal and the actual position

of the robot, the error is computed as the difference between the two quantities. What we want to achieve is that the error is 0, to do so, when the error is negative, the robot should move forward to reach the goal, on the contrary if is positive it should move backwards. Its main feature is that the motor powers are turned to full forwards or full backwards depending on the sign of the error.

This approach has many advantages, such as its simplicity and no need for calibration. However, since this controller is not always precise, especially when a derivative term is needed to avoid oscillations or when we are in steady-state, close to desired value, we implemented a variant that moves the the robot at full speed unless they are closer than a certain value, avoiding to approach the goal at full speed and overshoot it.

2.2 Artificial Neural Networks

In the field of Machine Learning (ML), ANNs are mathematical models based on the simplification of Biological Neural Networks [Zou et al., 2008].

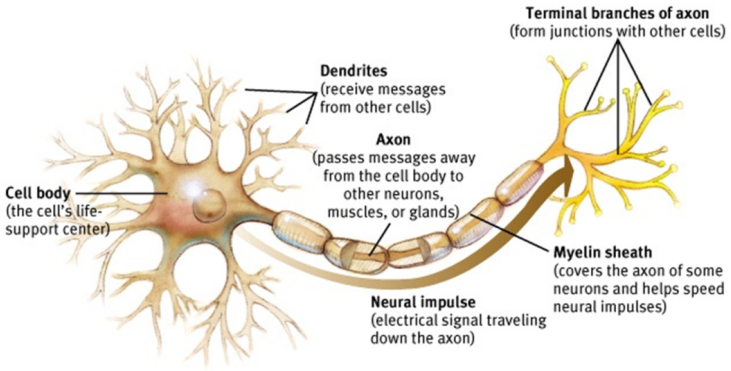

Figure 2.3. Structure of a Biological Neuron.

A NN can be considered as a dynamic system having the topology of an oriented graph, whose nodes model the neurons in a biological brain, while the edges represent the synapses — interconnections of information. Each connection can transmit a signal from one artificial neuron to another, which are typically aggregated in layers. The stimuli are received by a level of input nodes, called processing unit, which processes the signal and transmits it to other neurons connected to it.

As we anticipated, NNs can be seen as mathematical models that define a function $f : X \to Y$. The network function of a neuron $f(x)$ is defined as a composition of other functions $g_i(x)$, which can in turn be decomposed into others. A widely used representation for the description of traditional ANNs is the weighted sum, shown in Equation 2.6.

$$f(x) = \phi\left(\sum_i w_i x_i + \theta\right) \tag{2.7}$$

Equation 2.6. Function that describes mathematically the traditional ANNs in terms of weighted sum.

Each input signal x_i is multiplied by its corresponding weight w_i, which assumes a positive or negative value depending on whether you want to excite or inhibit the neuron. The bias θ varies according to the propensity of the neuron to activate, influencing its output. Additionally, a predefined function ϕ can be applied, also called activation function, which is explained in the following paragraph.

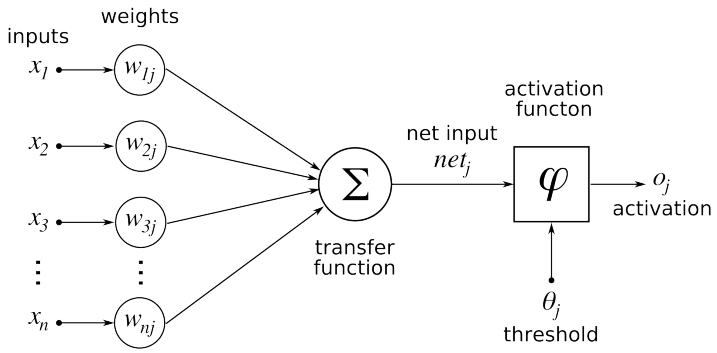

Figure 2.4. Mathematical model of an Artificial Neuron.

2.2.1 Activation functions

An activation function is a fundamental component of the model. It allows the network to learn non-linear transformations, in order to be able to compute non-trivial problems. In the course of this study, we used two of the most popular activation functions in deep learning, the hyperbolic tangent (Tanh) [Kalman and Kwasny, 1992] and the sigmoid [Han and Moraga, 1995], visualised in Figure 2.5.

Tanh The tanh is a zero-centred function, whose range lies between $(-1, 1)$, and its output is given by the following formula:

$$f(x) = \frac{\sinh(x)}{\cosh(x)} = \left(\frac{e^x - e^{-x}}{e^x + e^{-x}}\right) \tag{2.8}$$

Equation 2.7. Hyperbolic Tangent Function (Tanh).

Sigmoid The sigmoid models the frequency of the stimuli emitted by an inactive neuron, $\sigma(x) = 0$, to one fully saturated with the maximum activation frequency, $\sigma(x) = 1$. Its output is given by the following formula:

$$\sigma(x) = \frac{1}{1 + e^{-x}} \tag{2.9}$$

Equation 2.8. Sigmoid Function.

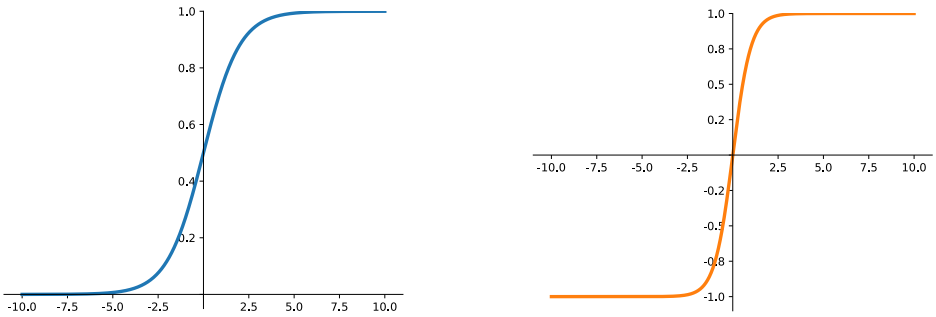

(a) Tanh activation function. **(b)** Sigmoid activation function.

Figure 2.5. Trends of two non-linear activation functions.

2.2.2 Loss functions

The learning process is structured as a non-convex optimisation problem in which the aim is to minimise a cost function, which measures the distance between a particular solution and an optimal one.

In the course of this study we used two different objective functions, depending on the strategy to be adopted: to solve the first task, that can be modelled as a regression problem, we used the Mean Squared Error (MSE) [Wang and Bovik, 2009], while for the second, that is a binary classification problem, we used the Binary Cross Entropy (BCE) [Gómez, 2018].

Mean Squared Error The MSE computes the deviation between the values observed $\hat{y}_i$ and those predicted by the network y_i, over the number of predictions n, as shown in Equation 2.9. Formally, this criterion measures the average of squared error between predictions and targets, and learns to reduce it by penalising big errors in the model predictions.

$$\texttt{MSE} = \frac{\sum_{i=1}^{n}(y_i - \hat{y}_i)^2}{n} \tag{2.10}$$

Equation 2.9. Mean Squared Error (MSE) loss function.

Binary Cross Entropy The BCE is a combination of the sigmoid activation and the Cross Entropy (CE). It sets up a binary classification problem between two classes, with the following formulation:

$$\texttt{BCE} = -\frac{1}{n}\sum_{i=1}^{n} y_i \cdot \log(\hat{y}_i) + (1 - y_i) \cdot \log(1 - \hat{y}_i) \tag{2.11}$$

Equation 2.10. Binary Cross Entropy (BCE) loss function [Sadowski, 2016].

where $\hat{y}_i$ is the i-th scalar value in the model output, y_i is the corresponding target value, and n is the number of scalar value in the model output[1].

This loss function should return high values for bad predictions and low values for good ones.

2.2.3 Optimisation algorithms

Optimisation algorithms are needed to minimise the result of a given objective function, which depends on the parameters the model has to learn during training. They strongly influence the effectiveness of the learning process as they update and calculate the appropriate and optimal values of that model. In particular, the extent of the update is determined by the learning rate, which guarantees convergence to the global minimum, for convex error surfaces, and to a local minimum, for non-convex surfaces.

Adam The optimiser we have chosen for this thesis project is Adam, an algorithm for first-order gradient-based optimisation of stochastic objective functions, based on adaptive estimates of lower-order moments [Kingma and Ba, 2014; Loshchilov and Hutter, 2017].

[1] `https://peltarion.com/knowledge-center/documentation/modeling-view/build-an-ai-model/loss-functions/binary-crossentropy`

Chapter 3

Tools

This chapter introduces the tools used in this work, starting from the description of the target platform in Section 3.1, then describing the simulator in Section 3.2 and finally mentioning the frameworks used for the implementation in Section 3.3.

3.1 Thymio II

The target platform is Thymio II, a small differential drive mobile robot developed in the context of a collaboration between the MOBOTS group of the Swiss Federal Institute of Technology in Lausanne (EPFL) and the Lausanne Arts School (ECAL).

Thymio runs the Aseba open-source programming environment, an event-based modular architecture for distributed control of mobile robots, designed to enable beginners to program easily and efficiently [Magnenat et al., 2010; Mondada et al., 2017], making it well-suited for robotic education and research.

Another particularity of this tool is the integration with the open-source Robot Operating System (ROS) [Quigley et al., 2009], through asebaros bridge [Magnenat, 2010].

The Thymio II includes sensors that can measure light, sound and distance. It can perform actions such as move using two wheels, each powered by its own motor, but also turning lights on and off.

3.1.1 Motors

The robot is equipped with two motors, each connected to one of the two wheels, which allow the robot to move forward, backwards but also turn by setting the velocity of the wheels at different speeds. The maximum speed allowed to the agent is 16.6cm/s.

3.1.2 Sensors

Thymio II possesses a large number of sensors, but for the purpose of this study we focused only on usage of the horizontal proximity ones.

Around the robot periphery are positioned 7 distances sensors, five on the front and two on the rear. These sensors can measure the distances to nearby objects thanks to

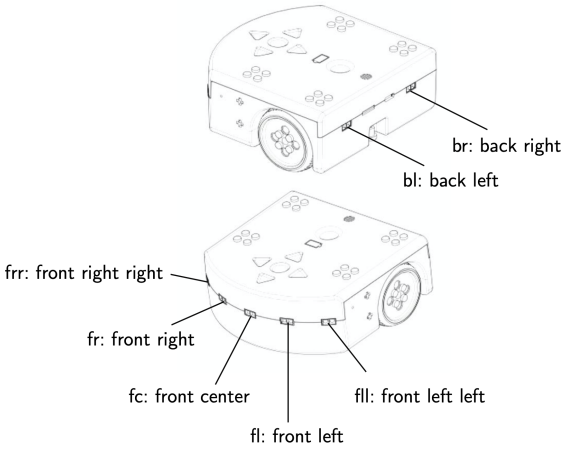

Figure 3.1. Thymio II sensors

the use of Infrared (IR), addressed in Section 2.1.1.

3.1.3 Communication

Thymio II can employ its horizontal IR sensors to communicate a value to robots within a range of about 48cm. In particular, the robot can enable the proximity communication and send an integer payload of 11 bits at 10 Hz, one value transmitted every 0.1s. This message is received by other agents if at least one of their proximity sensors is visible by one of the emitter's LEDs and if they have enabled the proximity communication. Every time that a message is received by some robot, an event is created containing the message, payload data and intensities data.

3.1.4 LEDs

Thymio II holds many LEDs scattered around its body, most of them are associated with sensors and can highlight their activations.

In this study, specifically for the objectives of Task 2 introduced later in Section 5.2, two Red Green Blue (RGB) LEDs on the top of the robot are used and driven together. It is possible to set the intensities of the top LEDs, in particular choosing the value for each channel (red, green and blue) in a range from 0 (off) to 32 (fully lit).

3.2 Enki simulator

Enki is the open-source robot simulator used in this project. It provides collision and limited physics support for robots evolving on a flat surface and can simulate groups of

robots a hundred times faster than real-time [Magnenat et al., 1999].

In this project, we exploit the PyEnki package [Guzzi, 2020] that provides Python bindings to the Enki simulator using Boost::Python [Seefeld, 2002-2015]. Moreover, it adds some functionalities to the original simulator such as the support for the proximity communication between Thymio II. Another peculiarity is that the simulated world can be run in real time inside a Qt application or even without the Graphical User Interface (GUI) as fast as possible.

In the simulator, the environment is represented as a three-dimensional (3D) Cartesian coordinate system, defined by three pair-wise perpendicular axes, x, y and z, that go through the origin in $(0, 0, 0)$.

In the following sections, the functioning of motors and sensors are explored in detail, as well as the concept of communication, anticipated in Section 3.1.3, giving particular attention to the explanation of their use in the simulator.

3.2.1 Motors

As for the motors, they are used to establish the speed of the wheels. The target wheels' speed can be set by writing the variables `motor_{left,right}_target`. The velocity is a float value specified in centimetres per second (cm/s). The wheels at maximum maximum allowed speed can provide a velocity of 16.6cm/s.

Another important element used for the construction of the model constraints is the distances between the left and right driving wheels, that is fixed to 9.4 cm.

Finally, a little amount of relative noise, about 0.027, is added to the target wheel speed at each control step.

3.2.2 Sensors

In Enki, it is possible to access the Thymio sensor readings in two different ways, by using `prox_values` and `prox_comm_events`.

`prox_values` an array of floats that holds the values of 7 horizontal distance sensors around its periphery [`fll` (front left left), `fll` (front left), `fc` (front centre), `fr` (front right right), `frr` (front right), `bl` (back left), `br` (back right)]. These values can vary from 0 — when the robot does not see anything — up to 4505 — when the robot is very close to an obstacle. Thymio II updates this array at a frequency of 10 Hz, generating the `prox event` after every update. The maximum range of these sensors is 14cm.

`prox_comm_events` a list of events, one for every received message collected during the last control step of the simulation. After enabling the proximity communication, using `prox_comm_enable` command, the robot can use the horizontal IR distance sensors to communicate a value to peer robots within a range of about 48cm. The integer payload to be sent is contained in the variable `prox_comm_tx`, while the value received is

contained in the variable `prox_comm_events.rx` of the fired event. In addition, the IRCommEvent stores, in the variable `prox_comm_events.payloads`, a list of 7 payloads, one for each sensor and a list of 7 intensities [`fll`, `fll`, `fc`, `fr`, `frr`, `bl`, `br`], saved in the variable `prox_comm_events.intensities`. The readings of the latter array, together with those contained in `prox_values`, are those that will be used in the course of this study.

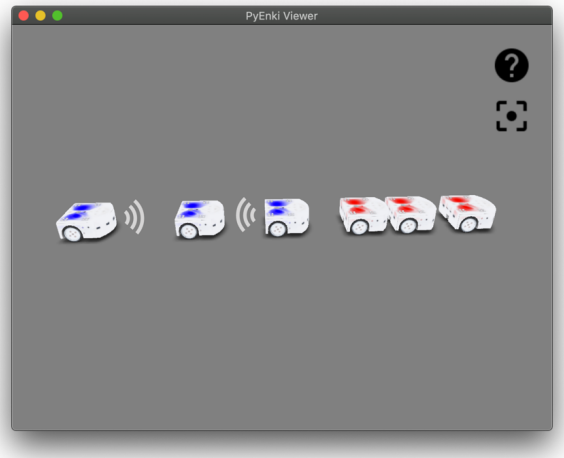

Figure 3.2. The PyEnki simulator viewer showing an example of communication, where the second Thymio is receiving messages from the nearest agents.

3.3 Frameworks

The proposed imitation learning approaches have been implemented in `Python` and all the models have been trained on an NVIDIA Tesla V100-PCIE-16GB Graphics Processing Unit (GPU). For this purpose, we used different tools which we briefly mention below.

`PyTorch` is an open source machine learning framework for tensor computation with strong GPU acceleration, uses also to build Deep Neural Networks (DNNs)[1].

`NumPy` is a package for scientific computing that provides support for a range of utilities for linear algebra and matrix manipulation[2].

[1] `https://pytorch.org`
[2] `https://numpy.org`

Pandas is an open source library providing high-performance, easy-to-use data structures and data analysis tools[3]. We used it in particular for building and working on the datasets generated for training the models.

Matplotlib is a comprehensive package for creating static, animated, and interactive visualisations in `Python`[4].

scikit-learn is a library that provides simple and efficient tools for predictive data analysis, built on `NumPy`, `Scipy`, and `Matplotlib`[5].

[3] `https://pandas.pydata.org`
[4] `https://matplotlib.org`
[5] `https://scikit-learn.org`

Chapter 4

Methodologies

This chapter illustrates the methodology used to approach the development process of this work. We start Section 4.1 by analysing the domain of the problem and then defining in Section 4.2 the learning method. We continue with a presentation of the approaches considered in Section 4.3, followed by Section 4.4 that describes the type of data used for this purpose and how they are generated. We conclude Section 4.5 with a detailed explanation of the controllers used and of the models implemented.

4.1 Multi-agent systems

In this work, we investigate collaborative scenarios in a homogeneous Multi-Agent System (MAS).

In a given simulated one-dimensional (1D) environment, we consider a team of N interacting agents, that are assumed to be interchangeable since they have the same physical structure and observation capabilities, which collaborate to solve a given common goal [Stone and Veloso, 2000; Šošić et al., 2016].

This system, containing agents also called "swarming agents", in principle is an extension of a Decentralised partially observable Markov decision process (Dec-POMDP) [Oliehoek, 2012], and can be formally defined as a tuple (S, O, A, R, π), [Schaal, 1999], where:

- S is the state of the system, or the set of local states for each agent, composed of all the possible combinations of positions and observations.
- O is the set of possible observations for each agent, obtained through the sensors.
- A is the set of possible actions for each agent.
- R is the reward function $S \times A \rightarrow \mathbb{R}$.
- π is the policy $S \rightarrow A$ which determines the action to execute in a given state for every single agent.

As introduced in Chapter Introduction, through the course of this study we tackle two MA scenarios. In both of them, the agents have a common goal that requires them to cooperate to achieve it.

Three popular approaches used to solve cooperative MA problems are Supervised and Unsupervised learning, and Reinforcement Learning (RL), which are distinguished according to the type of feedback provided to the agent: the target output in the first case, no feedback is provided in the second, and reward based on the learned output in the last one [Panait and Luke, 2005]. However, in reward-based methods, it is notoriously hard to design a suitable reward function, able to lead to the desired behaviour in all possible scenarios, even for complex tasks [Hadfield-Menell et al., 2017]. Imitation Learning (IL) methods can be used to overcome this problem by learning a policy from expert demonstrations without access to a reward signal [Song et al., 2018].

4.2 Imitation learning

Imitation Learning (IL) is a class of methods that has been successfully applied to a wide range of domains in robotics, for example, autonomous driving. Unlike reward-based methods, IL acquires skills by directly observing demonstrations of the desired behaviour in order to provide a learning signal to the agents [Zhang et al., 2018].

A typical approach to IL, also called Behavioural Cloning [Torabi et al., 2018], is a supervised technique that consists in collecting a certain amount of data, corresponding to a sequence of encountered observations and actions performed by a teacher agent which acts according to an unknown policy in order to achieve a certain goal. Then, the demonstrations of the expert's behaviour are used to learn a controller, by training usually a classifier or regressor, that predict behaviour to correctly achieve the same goal in a certain environment [Ross et al., 2011]. The machine learning model should be able to learn how to extract relevant information from the data provided to it, directly learning a mapping from observations to actions.

Instead, an unsupervised approach collects only the data that correspond to a sequence of encountered observations performed by a teacher agent, and the learned controller should be able to infer the correspondence from observations to actions and find a way to accomplish the same task [Stadie et al., 2017]. In this case, learning a good model is more challenging since the coordination, that is implicit in the demonstrations, has to be inferred as a latent variable [Le et al., 2017].

4.3 Approaches

Given the two scenarios presented in Chapter Introduction, distributing the robots in space such that they stand at equal distance from each other and colouring the robots in space depending depending on their position with respect to the others in the group,

through the course of this study we tackle two MA scenarios. In both of them, the agents have a common goal that requires them to cooperate to achieve it.

While both are excellent examples of distributed tasks, they have an important difference: the first problem can be solved without using communication, while for the second one it is necessary. A full explanation of how communication works for Thymio II is covered in Section 3.1.3.

4.3.1 Distributed approach

As stated before, the first task can be accomplished with a distributed approach without communication. The agents share the same goal: arrange themselves uniformly along the line between the two "dead" robots, in such a way they stand at equal distances from each other. This problem represents an example of a cooperative task, for this reason, it will be desirable for the agents to cooperate [Barrett et al., 2017].

On the one hand, when communication is not possible, they can achieve their goal without directly interact with each other. As stated by Holland in *Multiagent systems: Lessons from social insects and collective robotics* [Holland, 1996], since the agents exist in the same environment, they can affect each other indirectly in several ways. For instance, they can be sensed from the other robot's or they can even change the state of an agent by applying a force on it, for example, by colliding with it. The work of Grassè about Stigmergy Theory provides additional details about active and passive stigmergy [Grassé, 1959].

On the other hand, the difficulty of the problem we consider is that the agent does not have full knowledge of its mates' behaviours. Although a communication protocol is not necessary, allowing an explicit exchange of messages between the agents may nonetheless increase agent performance: they use the exchange of message in order to coordinate more effectively and distribute more accurately, finally reaching a more efficient solution [Panait and Luke, 2005].

4.3.2 Distributed approach with communication

In the second task also, the agents share a common goal: assuming that they are divided into groups, which are unknown to them, their objective is to determine their group membership and to colour themselves accordingly. For this kind of problems, allow explicit communication is not a plus but a necessity.

An important aspect that needs to be considered is the decision of what to communicate and when, so that no issues arise.

Regarding the communication content, the agents can, for example, inform the others of their current state by sharing the sensor readings, or even information about the past [Guestrin et al., 2002; Panait and Luke, 2005]. For this purpose, we used an unsupervised approach in which we do not have to specify the communication content, which instead has to be inferred by the network as a latent variable.

Of great importance is also the moment in which transmit a message. In fact, if the communication is delayed, it can become useless or even cause unwanted behaviour [Stone and Veloso, 2000]. As we have already said in Section 3.1.3, each robot transmits a message every 0.1s and likewise receives one for each of the sensors. In our case, we expect each agent to receive two communications, one from each of its respective neighbours. With real robots, but also in simulation, what we want to attain is a synchronous communication update protocol. Formally, each robot n, given the observations at time t, that corresponds to the sensor readings $S_n(t)$, and the communications at time $t-1$, in particular $C_{n-1}(t-1)$ and $C_{n+1}(t-1)$, calculates the control $V_n(t)$ and the message to transmit $C_n(t)$ at time t. Adopting this technique, it is not important to keep track of the order of the robots and it is as if the agents operate simultaneously. Ideally, the frequency of updates must be lower than that with which the robots exchange messages, however, it can happen that due to delays or noise in the sensor readings the communication of some robots is not received or transmitted. In this case, the array is not updated and the last received message is kept instead, without causing undesired behaviour but simply a slowdown.

4.4 Data collection

In this work, N robots, all oriented in the same direction, are initially randomly placed along the x-axis, avoiding collisions and in such a way the average gap among them is included in the proximity sensors' ranges. All agents act in collaboration to achieve a common goal, except the first and last in the row that behave like walls.

Each robot can be considered as a point on the plane, formally described by a homogeneous vector with respect to the world coordinate frame W, obtained multiplying the homogeneous vector of the point w.r.t. the robot coordinate frame A, by a homogeneous transformation. The relative pose A of each agent is identified by a 3×3 matrix $\mathbf{T}$, with respect to the world reference frame W. However, since they are arranged on a line,

$$ {}^{W}\xi_A = {}^{W}\mathbf{T}_A = \begin{pmatrix} {}^{W}\mathbf{R}_A & {}^{W}\mathbf{t}_A \\ 0,0 & 1 \end{pmatrix} = \begin{pmatrix} \cos\theta & -\sin\theta & t_x \\ \sin\theta & \cos\theta & t_y \\ 0 & 0 & 1 \end{pmatrix} \tag{4.1} $$

Equation 4.1. The homogeneous transformation matrix, ${}^{W}\mathbf{T}_A$, includes ${}^{W}\mathbf{R}_A$, a 2×2 rotation matrix and ${}^{W}\mathbf{t}_A$, a 2×1 translation vector.

the environment can be considered 1D, hence, the y coordinate is equal to 0 and also the orientation angle θ must be zero as all the agents are oriented as the world frame. Moreover, we can consider the agents as holonomic, since their movements are limited to only one dimension. This premise simplifies our system, in which consequently we

have to keep into account only geometric constraints and not kinematic.

Of fundamental importance is the approach adopted for the generation of the starting positions of the robots. The initial configurations need to be randomly generated, verifying that there is no bias towards those close to the target. In particular, once established the number of agents to spawn and the average gap between them, a vector containing samples, each representing a random gap in $\mathbb{R}$, is drawn from a uniform distribution in the interval $[0, 2 * \texttt{avg\_gap})$. The length of the Thymio, that is 10.9 cm, is added to each gap, then the final positions are obtained by returning the cumulative sum of the elements in the generated vector.

Another premise regards the sensors of the Thymio: as introduced in Section 3.2.2, we have available `prox_values` and `prox_comm_events.intensities`. Before being used, the `prox_comm_events.intensities` should be flattened to obtain a single array containing the intensities of all recorded events. To do so, we decided to create a new array, called `prox_comm`, by keeping for each element only the value with the maximum intensity among the possible values in the corresponding position of the original vectors – for this purpose maximum 2. In addition, we define another variable, named `all_sensors`, which is an array of 14 intensities resulting from the combination of the `prox_values` and `prox_comm` vectors.

The data that we use to train our machine learning models are generated through Enki, the simulator introduced in Section 3.2. In particular, two datasets containing 1000 simulation runs each are built using the omniscient and the manual controllers, that will be explained in Sections 4.5.1 and 4.5.2. Each run, that differs from the others for the initial positions of the agents, sets up a world containing N Thymio. In particular, for all the simulations the number of agents N is chosen randomly within the range $[5, 10]$, and the `avg_gap`, that is the average distance among the robot in the final configuration of the run, that can be in the range $[5, 24]$. A simulation run is stopped either immediately after all the robots reach the target pose, with a certain tolerance, or after 4s (40 time steps). At each time step, all the useful information regarding the agents is stored in the dataset, such as the sensor readings, the pose of the robot, the motors target, the communication transmitted and received and its colour.

All the original datasets are shuffled, based on the single run, in order to improve the generalisation on the samples, and then split the resulting collection into train, validation and test sets, containing respectively 60-20-20% of the data. The dataset generated using the expert controller is the one used to train the networks, while the one generated with the manual controller is used as a baseline for the comparison with the learned model.

4.5 Controllers

In a Multi-Agent System (MAS), each agent can perceive the environment through sensors acquiring a total or partial knowledge of it. The observations can be used by a

controller, the key component of the system introduced in Section 2.1.2, together with the current state of the agents, to determine actions, draw inferences and finally solve tasks.

For the two scenarios that we consider in this study, the state of the agent is the combination of four elements: its position on the x-axis, the observations, i.e., the distances from neighbours recorded in the sensor readings, communication messages, one transmitted to the two nearest neighbours, one on the left and the other on the right, and two received from peer robots, and finally its colour. Instead, the set of actions that agents can perform are different depending on the task: in the first scenario the agents move forward and backwards along the x-axis, therefore the set includes the range of velocity that they can assume; in the second one, the agents can turn on their top RGB LED in red or blu, so the set this time is composed by the two possible colours.

In an Imitation Learning (IL) setting, there are two main controllers involved: an omniscient controller, which decide the best action exploiting its perfect knowledge of the state of the system, and a learned controller, which imitate the behaviour of the expert. Undoubtedly, one of the main advantages of adopting a ML model to solve these tasks is that the algorithm must learn how to extract relevant information from the data it receives, sidestepping the difficulty of manually implementing the perception part. However, for the tasks that we are going to face, we introduce three controllers: in addition to the two mentioned before, we also use a manual controller, which can observe only parts of the system. As a consequence, its decisions do not depend on the state of the whole swarm [Šošić et al., 2016].

4.5.1 Expert controller

As just described, the first element involved in an imitation learning problem is the omniscient controller, also called expert. This is a centralised controller that perceives the environment and observes the state and the observations of all agents, obtaining a global knowledge of the state of the system. In this way, it can use all the information to decide the best action to perform for all the agents.

As the goals to be achieved vary, the controllers should act differently. For this reason, in the following paragraphs we define the approaches used for the implementation of the controllers in the two scenarios.

4.5.1.1 Task 1: Distributing the robots in space

In the first scenario, the omniscient controller, based on the current poses of the robots, moves the agents at a certain speed to reach the target positions. In particular, the linear velocity of each agent is computed as a “signed distance“ between the current and the goal position of the robot, along its theta.

Formally, given the current pose, defined by the triple (x, y, θ) and the target pose $(\overline{x}, \overline{y}, \overline{\theta})$, the signed distance d is computed as follow:

$$d = (\overline{x} * \cos(\theta) + \overline{y} * \sin(\theta)) - (x * \cos(\theta) + y * \sin(\theta)) \tag{4.2}$$

Equation 4.2. Function used to compute the "signed distance" between the current and the goal position of a robot.

To obtain the final velocity of the agent, this quantity is multiplied by a constant, we choose 10 to keep the controller as fast as possible, and then clipped to the maximum value supported by Thymio II, 16.6cm/s.

This controller can be considered as a variant of a Bang Bang controller, introduced in Section 2.1.2.2, since the optimal controller moves the robot at maximum speed towards the target unless the target is closer than `control_step_duration` × `maximum_speed`. In this case, the agent is moved slower than maximum speed so that at the end of the time step it is located exactly at the target.

4.5.1.2 Task 2: Colouring the robots in space

In this scenario, the omniscient controller, based on the current poses of each robot, is able to determine the order of the agents and turn on their top LED in one time step. For this reason, we decided to use the same dataset obtained for the previous task, but adding to it the colour of the robot, in order to provide the network with examples consisting of multiple time steps from which it can learn.

4.5.2 Manual controller

Unfortunately, centralised solutions for distributed problems are not feasible in real situations since agents do not have access to their states but only to their local observations. The global state of the system, accessible to a centralised controller, in this case, is hidden from each agent who therefore cannot understand its absolute position. Instead, we are interested in situations in which is used a local controller to decide the next action, based on the individual agent's observations, or even cases in which the programming part of the controller is automated. In fact, the main purpose of this controller is to draw conclusions about the quality of the controller learned.

As before, to different goals to be achieved correspond different controllers that should act differently. For this reason, in the following paragraphs we define the approaches used for the implementation of the controllers in the two scenarios.

4.5.2.1 Task 1: Distributing the robots in space

In the first scenario, the controller is in charge of moving the robots towards the target by minimising the difference between the values recorded by the front and rear sensors, trying to maintain the maximum achievable speed.

For each agent, the controller is the same and, if given an identical set of observations as input, likewise, the outputs will be equivalent.

The kind of controller we decided to implement for this purpose is a Proportional (P) controller, a particular variant of the Proportional–Integral–Derivative (PID) controller with only the K_p term, described in detail in Section 2.1.2.1. In particular, the value of the proportional gain has been tuned to yield satisfactory performance so that the system is stable, as shown in Figure 4.1.

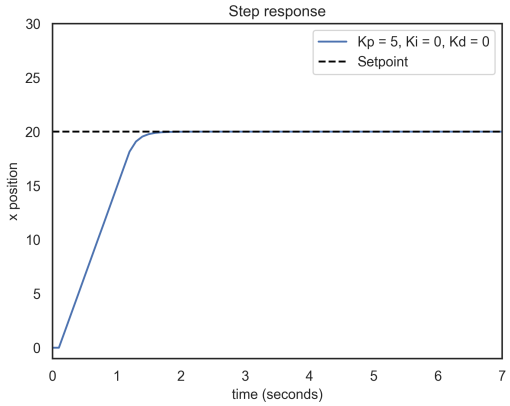

Figure 4.1. Visualisation of the step-response of a P controller with proportional gain 5.

It is important to notice that the speed returned by the controller is used to set the `motor_{left, right}_target`, both with the same value, in order to move the robots straight ahead. Moreover, the first and the last robots of the line, whose sensors never receive a response respectively from the back and from the front, never move.

4.5.2.2 Task 2: Colouring the robots in space

In this scenario, the robots observations, in particular, the sensor readings, do not provide useful information about the order of the agents, therefore they are not considered to accomplish this task. On the other hand, if an omniscient controller is not employed, it is impossible to solve the problem without using communication, since it is the only way for the agents to understand their ordering.

Thus, by initially making all robots transmit the same value, i.e.,0, we are able to establish which are the first and the last robots in the row, or those that do not receive any communication respectively from back and front. These two agents can at this point start the actual communication by transmitting the value they received, increased by 1, that is 1. The following robots will in turn transmit the value they have received, increased by one. Since the messages received by each of them are two, the agents will in a sense, learn to count in order to understand which is the correct value to transmit.

The protocol used to decide the communication and the colour, which also depends on the amount of robots N, or if there are even or odd numbers, is shown in Listing

4.1. The colour of each agent in the initial configuration is randomly chosen between the two possible colours, red and blue.

```
    c_left, c_right = get_received_communication(state)

    if N % 2 == 1:  # if the number of robots is odd

    # Case 1: no communication received from left
    if c_left == 0:
    if c_right > N // 2:
    # the agent is in the first half of the row, so its colour is blue
    message = c_right - 1
    colour = 1
    elif c_right == N // 2:
    # the agent is the central one, so its colour is blue
    message = c_right + 1
    colour = 1
    else:
    # the agent is in the second half of the row, so its colour is red
    message = c_right + 1
    colour = 0

    # Case 2: no communication received from right
    elif c_right == 0:
    if c_left > N // 2:
    # the agent is in the second half of the row, so its colour is red
    message = c_left - 1
    colour = 0
    elif c_left == N // 2:
    # the agent is the central one, so its colour is blue
    message = c_left + 1
    colour = 1
    else:
    # the agent is in the first half of the row, so its colour is blue
    message = c_left + 1
    colour = 1

    # Case 3: communication received from both sides
    else:
    if c_left > c_right:
    # the agent is in the second half of the row, so its colour is red
    message = c_right + 1
    colour = 0
    else:
    # the agent is in the first half of the row, so its colour is blue
    message = c_left + 1
    colour = 1


    elif self.N % 2 == 0:  # if the number of robots is even
```

```
    # Case 1: no communication received from left
    if c_left == 0:
    if c_right > N // 2:
    # the agent is in the first half of the row, so its colour is blue
    # the situation is ambiguous the message to transmit could be c_right or
    # even c_right - 1
    message = c_right
    colour = 1
    else:
    # the agent is in the second half of the row, so its colour is red
    message = c_right + 1
    colour = 0

    # Case 2: no communication received from right
    elif c_right == 0:
    if c_left < N // 2:
    # the agent is in the first half of the row, so its colour is blue
    message = c_left + 1
    colour = 1
    else:
    # the agent is in the second half of the row, so its colour is red
    # the situation is ambiguous the message to transmit could be c_left or
    # even c_left - 1
    message = c_left
    colour = 0

    # Case 3: communication received from both sides
    else:
    if c_left > c_right:
    # the agent is in the second half of the row, so its colour is red
    message = c_right + 1
    colour = 0
    elif c_left < c_right:
    # the agent is in the first half of the row, so its colour is blue
    message = c_left + 1
    colour = 1
    else:
    # the agent is in the second half of the row, so its colour is red
    message = c_left
    colour = 0
```

Listing 4.1. Protocol used by the manual controller to decide, for each robot, the message to transmit and the colour.

4.5.3 Learned controller

Usually, to train a network that learns a controller, the states and the actions, provided by an expert, need to be observable. For this study, we have decided to use the observations of the robots instead of the state, i.e.,the positions. The reason behind this

decision is that in most environments, agents are never actually exposed to the full state of this system. Instead, they receive partial observations, often local or incomplete. In addition, it is frequently too expensive to provide the agent with the full state of the system, and sometimes it is not even clear how to represent it [Juliani, 2018].

As the goals to be achieved vary, the controllers should act differently. For this reason, we define distinct approaches for the implementation of the controllers in the two scenarios. Regarding the first task, we consider two different networks: one distributed that act in a supervised way, and one that, in addition to predicting the control output, infers a communication protocol between the agents. In the second task, we trained one network that predicts the colour output and in addition, as before, infers the communication between the robots.

4.5.3.1 Task 1: Distributing the robots in space without using communication

Using the data collected through the simulator using the expert controller, it is possible to train a very simple "distributed network" that takes as input an array containing the response values of the sensors – which can be either `prox_values`, `prox_comm` or `all_sensors` – and produces as output an array containing one float that represents the speed of the wheels, which is assumed to be the same both right and left.

The training dataset then contains a fixed number of simulation runs, each composed of a variable quantity of time steps. It is important to notice that for this approach, unlike the one with communication, it is neither necessary to preserve the order of the sequence of time steps, nor to know the exact number of agents in the simulation since the network input is the sensing of a single robot.

For this reason, the model is independent of the number of agents and consequently it is possible to prove its generalisation capacity, regardless the number of robots, by training the networks first on datasets each with a different but fixed value of N and then evaluating them on simulations with a variable N. It is easy to show that, although the value of N changes, the network structure does not, as it is sufficient during the input preprocessing to change the dimension of the input in such a way that all the tensors have the same length, fixed at the maximum possible value of N, padding those tensors with a lower number of agents.

The architecture of the network, displayed in Figure 4.2, is straightforward: there are three linear layers of size $\langle$`input_size`$, 10\rangle$, $\langle 10, 10\rangle$ and $\langle 10, 1\rangle$, where `input_size` is the shape of the sensing that can be either 7 or 14.

The Tanh non-linear activation function introduced in Section 2.2.1, is applied to the first and second layer.

As optimiser, we chose Adam, introduced in Section 2.2.3, implemented in the `torch.optim` package, with a learning rate of 0.01.

Instead of performing gradient descent on the entire dataset, the training set is split in mini-batches of size 100. In this way, an approximation of the gradient is produced, which makes the algorithm faster and at the same time, for sufficiently large batches,

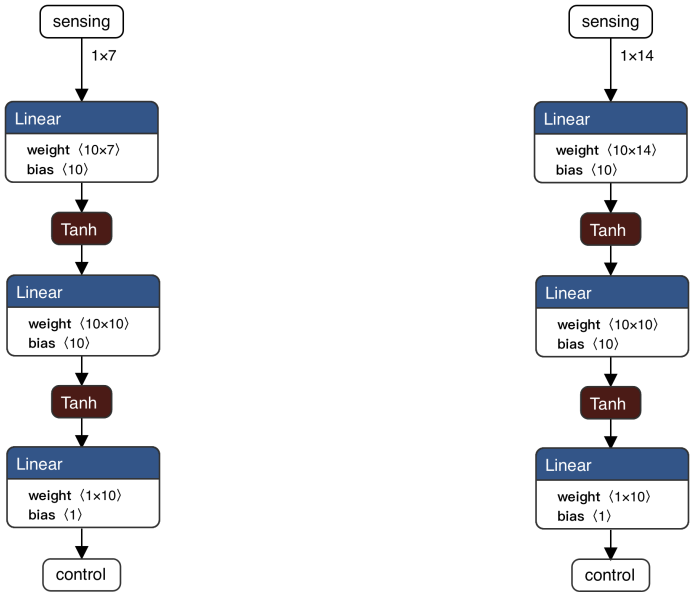

(a) Network with 7 input sensing. **(b)** Network with 14 input sensing.

Figure 4.2. Visualisation of the network architecture chosen for the distributed approach.

the result is indistinguishable. Gradient descent algorithms are susceptible to "getting stuck" in local minima. Mini-batches shuffle facilitate to avoid this problem by enabling the gradient to "bounce" out of eventual local minimum, making it more variable by exploiting randomness, thereby helping convergence [Meng et al., 2019].

All the models are trained for 50 epochs and evaluated using the MSE loss function, defined in Section 2.2.2, implemented in the `torch.nn` package.

4.5.3.2 Task 1: Distributing the robots in space using communication

An alternative to the previous approach involves training a distributed network that also exploits a communication protocol between agents to decide the output control more reliably. Thus, using the same data collected before, we build a model that at each time step takes as input an array containing the response values of the sensors for each robot – `prox_values`, `prox_comm` or `all_sensors` – and the messages received in the previous time step, communicated by the nearest agents (on the left and on the right), and produces 2 floats as output: the control, which is the speed of the wheels as before, and the communication, i.e.,the message transmitted by the robot to its two neighbouring agents.

Even for this purpose, the model is independent of the number of agents in the simulations. Instead, now it is important to keep track of the time steps order since the input of the network requires the communication received which corresponds to the messages transmitted in the previous time step. To do so, preprocessing is applied to the

dataset to combine consecutive time steps into a set of sequences. Therefore, we divide each simulation in sequences of length 2, composed of two successive observations for each robot, using a stride of 1. Accordingly, the shape of the model input has been transformed from $1 \times$ `input_size` to `seq_length` $\times$ `N` $\times$ `input_size`, where `seq_length` is fixed at 2, N is variable and `input_size` can be 7 or 14.

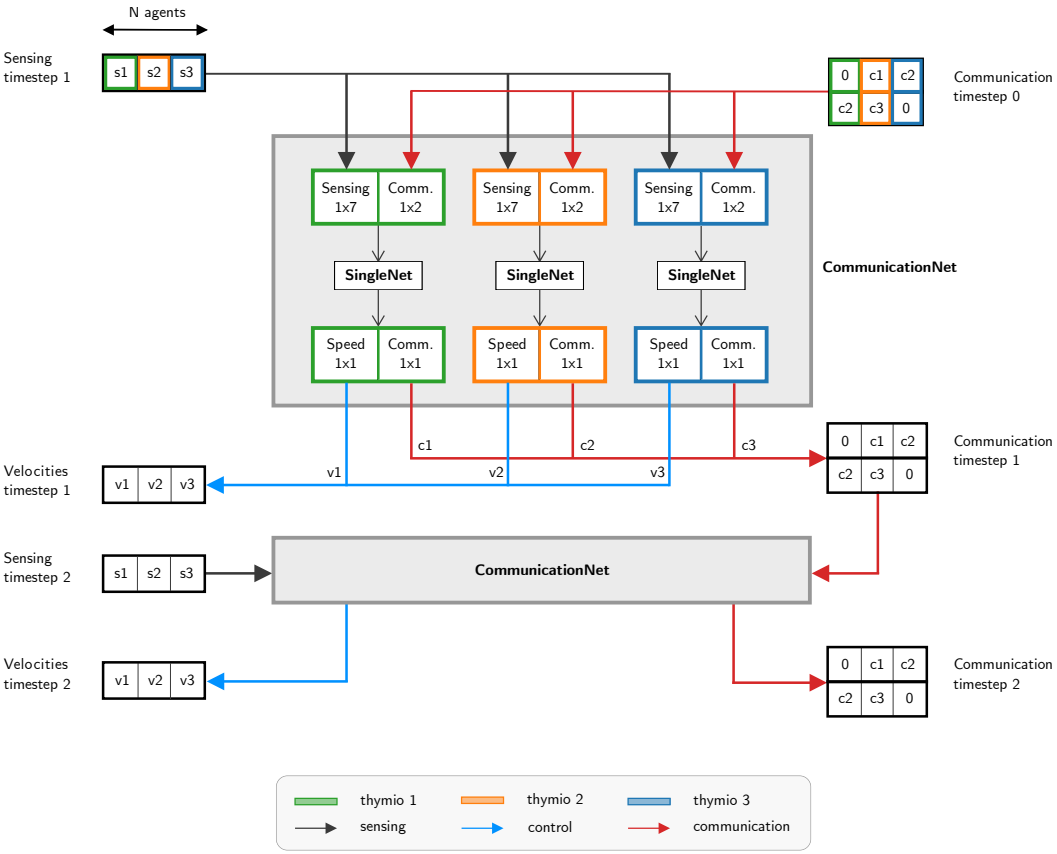

Figure 4.3. Visualisation of the forward pass of the communication network with three agents and a sequence composed by two time steps.

It is important to notice that the communication is not in the input since it is not contained in the original dataset, instead is treated as a hidden variable to be inferred. At the beginning of each sequence, there are no previous time steps to consider since no messages have been received yet. Therefore, a placeholder is randomly initialised, filled with float values in the range $[0, 1]$. The size of this array corresponds to the number of agents plus two elements, one at the beginning and one at the end of the vector, always set to 0 since they are used to store the fact that the two extreme robots never receive messages respectively from the left or from the right. The random initialisation of this vector is essential to increase the generalization capabilities of the network during its training, showing it different starting situations.

As a consequence, we define a recurrent structure of the communication network, shown in Figure 4.3. It is composed by two nested modules: in the outer level operates the `CommNet` that handles the sensing of all the agents, while in the inner the `SingleNet` that works on the sensing and the communication received by a single agent in a certain time step, producing as output the control and the communication to transmit. Therefore, this corresponds to a static unroll of a Recurrent Neural Network (RNN).

The architecture of the `SingleNet`, displayed in Figure 4.4, is almost the same as the one of the distributed model without communication: there are three linear layers each of size $\langle \texttt{input\_size}, 10 \rangle$, $\langle 10, 10 \rangle$ and $\langle 10, 2 \rangle$, where `input_size` is the sum of the shape of the sensing and the two communication values received, one from the left and one from the right.

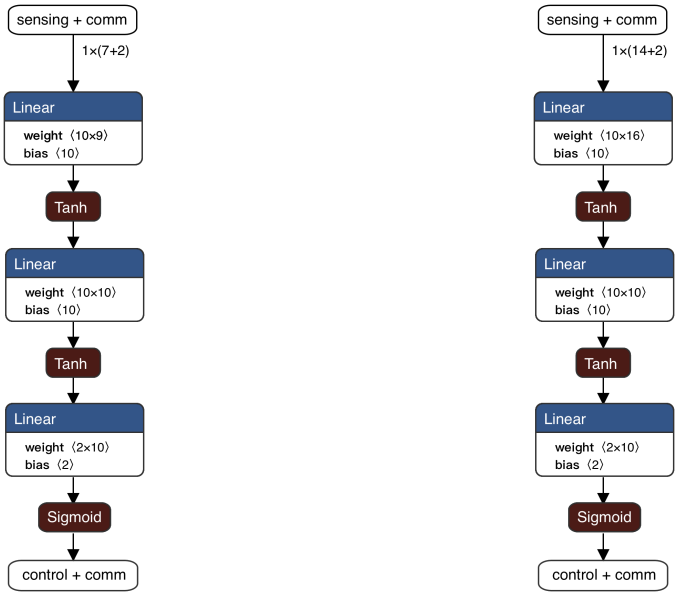

(a) `SingleNet` with 7 input sensing. **(b)** `SingleNet` with 14 input sensing.

Figure 4.4. Visualisation of the network architecture chosen for the distributed approach with communication in case of 7 or 14 inputs.

As before, a Tanh non-linear activation function is applied to the first and second layer, while a sigmoid, introduced in Section 2.2.1, is applied to the second dimension of the output in order to normalise it in the range $[0, 1]$.

As before, we use Adam optimiser, addressed in Section 2.2.3, but with a smaller learning rate, 0.001. We split the dataset in mini-batches, this time of size 10 and then we train the models for 500 epochs. Finally, we evaluate the goodness of the predicted control using the MSE loss function, while the communication has to be inferred by the network. Since the network is fully connected, the communication affects directly the output, and consequently, the error minimised. Improving the loss has an impact also on the communication latent variable, since the error is propagated through the

internal network, in order to update the weight during the back-propagation step.

4.5.3.3 Task 2: Colouring the robots in space

In this scenario, it is possible to implement a network very similar to the one used for the previous task, that is the distributed approach with communication, described in Paragraph 4.5.3.2, but this time ignoring the sensors readings. Thus, using the same data collected before we build a model that at each time step takes as input for each robot only the messages received in the previous time step, communicated by the nearest agents (on the left and on the right), and produces as output an array of 2 floats, the first one is the probability of the agent top LED to be blue and the second is the communication, i.e.,the message to be transmitted by the robot.

The communication network, whose structure is shown in Figure 4.6, is composed by two nested modules: in the outer-level operates the `CommNet` that handle the sensing of all the agents, while in the inner-level the `SingleNet` that works on the communication received by a single agent in a certain time step, producing as output the colour and the communication to transmit.

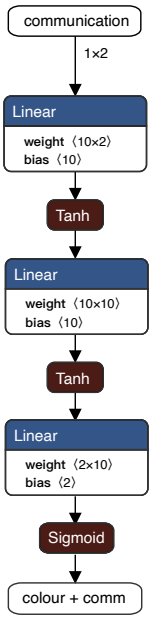

Figure 4.5. Visualisation of the network architecture chosen for the communication approach.

The `SingleNet`, displayed in Figure 4.5, is composed by three linear layers of size $\langle$`input_size`$, 10\rangle$, $\langle 10, 10\rangle$ and $\langle 10, 2\rangle$, where `input_size` corresponds to the two communication values received, one from the left and one from the right.

The activation functions used for this purpose are two, and are introduced in Section 2.2.1. To the first and second layer is applied a Tanh non-linear activation function,

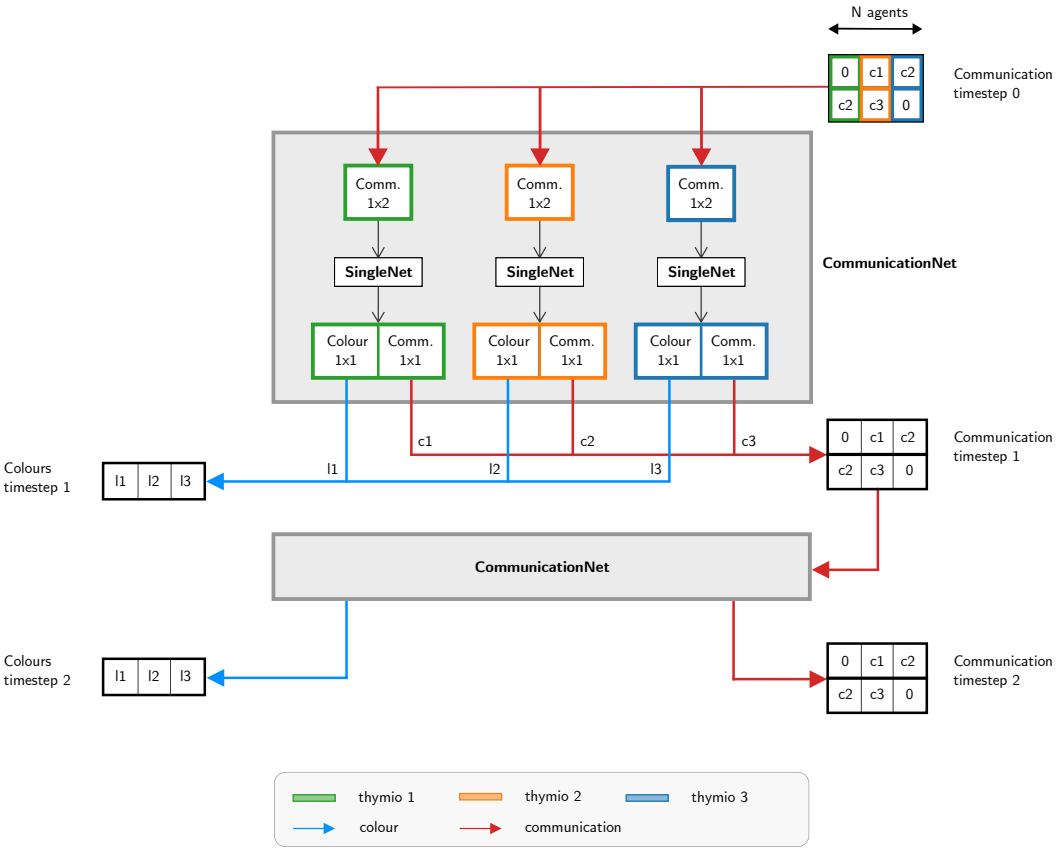

Figure 4.6. Visualisation of the forward pass of the communication network with three agents and a sequence composed by two time steps.

while a sigmoid to the output, in order to normalise it in the range $[0, 1]$.

As before, we use Adam optimiser but with a smaller learning rate, 0.001. We split the dataset in mini-batches of size 10 and then we train the models for 100 epochs.

In order to decide the metric to evaluate the goodness of the prediction, it is necessary to analyse the output of the network. As we said, the model returns, in addition to the communication, the colour that is actually the probability of the agent top LED to be blue. This means that, when the network produces a 0, the probability that the LED is blue is equal to 0, i.e.,it is red; in the same way, 1 means that instead, this will be blue. In this way, we define a simple policy function that returns the colour blue when the probability is between 0.5 and 1, and red otherwise, or when the probability is less than 0.5. For this reason, instead of using the MSE loss function, as this is a binary classification problem we choose the BCE, defined in Section 2.2.2, implemented in the `torch.nn` package. It is important to remember that communication is still inferred as a latent variable.

Chapter 5

Evaluation

In this chapter we present the results of our research. For this purpose, we use the tools presented in Chapter 3 and the environment set up provided in Chapter 4. We briefly describe the tasks we face respectively in Sections 5.1 and 5.2, and then we proceed with the evaluation of the results of the experiments.

Throughout the experiments we compare different models, varying the input of the network, either `prox_values`, `prox_comm` or `all_sensors`, the number of agents and the average gap between them, either fixed to a certain value or variable.

5.1 Task 1: Distributing the robots in space

The first scenario tackles an interesting multi-agent coordination task, distributing the robots in space in such a way they stand at equal distance from each other. In particular, they have arrange themselves uniformly along the line between the two "dead" robots.

We focus on two approaches to solve to problem, one distributed that act in a supervised way in order to predict the target velocity of the agents, and one that in addition to predict the control infers a communication protocol between the agents.

In both cases, we train DNNs that receive sensor inputs and produce commands for the motors, but for the second alternative, the network has an addition input – the received communication transmitted by the neighbouring agents in the previous time step – and an extra output – the message to be sent.

5.1.1 Distributed approach

5.1.1.1 Experiment 1: fixed number of agents

The first group of experiments, summarised in Table 5.1, examines the behaviour of the control learned in the case of the three different inputs, `prox_values`, `prox_comm` or `all_sensors`, for a number of robots N and an `avg_gap` both fixed at 5 and the second chosen between 8, 13 and 24.

Model	network_input	input_size	avg_gap
net-d1	prox_values	7	8
net-d2	prox_values	7	13
net-d3	prox_values	7	24
net-d4	prox_comm	7	8
net-d5	prox_comm	7	13
net-d6	prox_comm	7	24
net-d7	all_sensors	14	8
net-d8	all_sensors	14	13
net-d9	all_sensors	14	24

Table 5.1. List of the experiments carried out with 5 agents.

First of all we start by showing in Figure 5.1 an overview of the models performance in terms of train and validation losses. It is immediately evident that, in case of

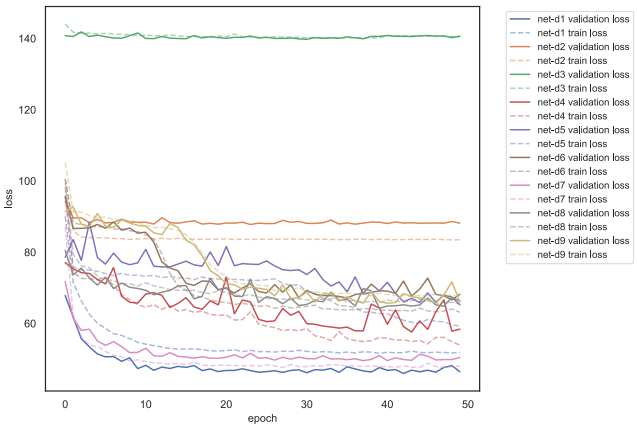

Figure 5.1. Comparison of the losses of the models carried out with 5 agents.

prox_values inputs, the experiment performed with an avg_gap of 24 is not remarkable since the gap exceeds the maximal range of the sensor. In fact, from this analysis we generally expect a more stable behaviour using both types of input together, i.e., all_sensors, as they are able to perform with both small and large gaps.

Results using prox_values input We start the analysis by exploring the results of the experiments obtained using the prox_values readings alone as input of the network, continuing the with prox_comm and concluding with all_sensors.

The performance of net-d1 are shown in the following images. In particular, in Figure 5.2 is visualised a comparison of the R^2, or coefficient of determination, of the manual and the learned controllers, on the validation set. This score function evidences

how well the regression predictions approximate the real data points (groundtruth). Since a model which perfectly predicts the data has a score of 1, we assume that a higher score corresponds to a model that performs better. From these figures we expect

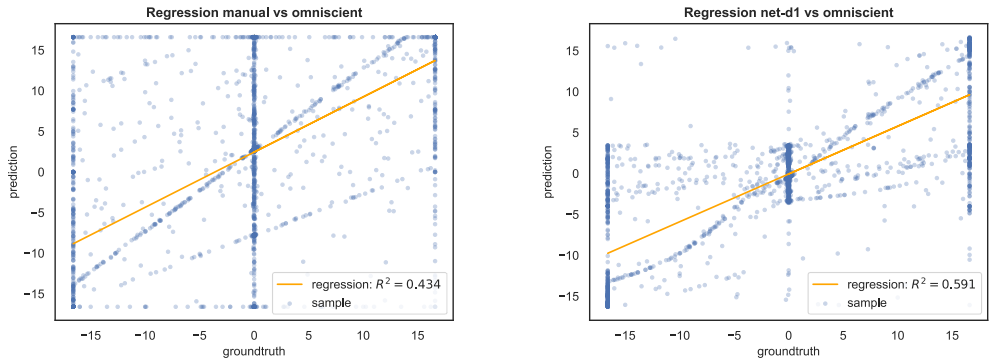

Figure 5.2. Comparison of the R^2 coefficient of the manual and the controller learned from `net-d1` with respect to the omniscient one.

that the robots' behaviour using the learned controller instead of the manual one is a bit better, even if far from the omniscient controller.

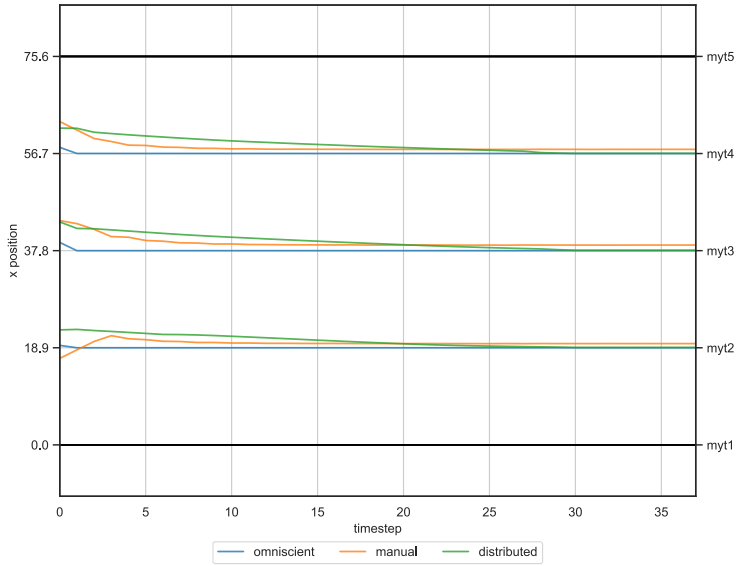

Figure 5.3. Comparison of trajectories, of a single simulation, generated using three controllers: the expert, the manual and the one learned from `net-d1`.

In Figure 5.3 we first show a sample simulation: on the y-axis is represented the position of each agent, while on the x-axis the simulation time steps. We compare the trajectories obtained from the three controllers, in particular visualising the omniscient

one in blue, the manual in orange and the learned one in green. The extreme robots are passive. The agents moved using the omniscient controller reach the target very quickly, in a couple of time steps. Those moved using the manual controller are slower, they approach the goal position on average in 10 time steps but never reach it. Instead, the learned controller is even slower than the previous one, but in about 25 time steps, the agents manage to arrive in the correct final configuration.

In Figure 5.4 we show a comparison of the expert and the learned trajectories, and then between the manual and the learned ones, this time summarising the performance over all the validation runs: at each time step, the position of each agent is presented

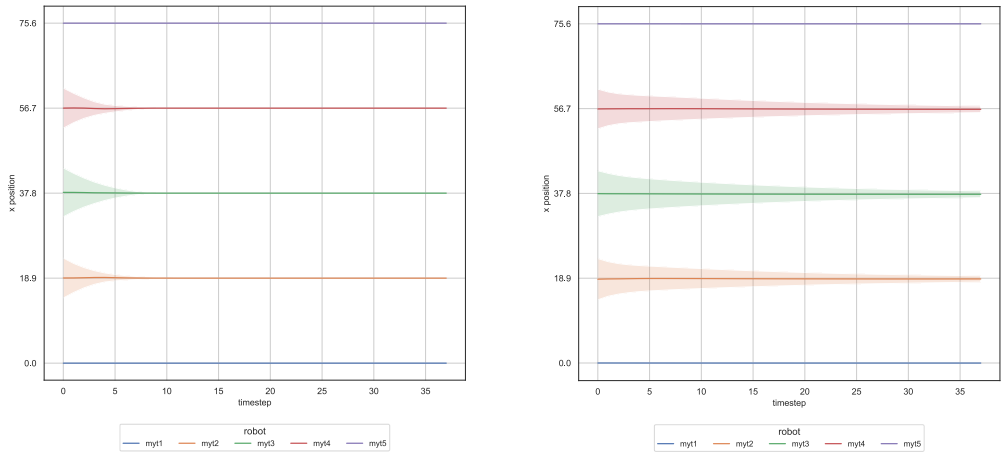

(a) Expert controller trajectories.

(b) Distributed controller trajectories.

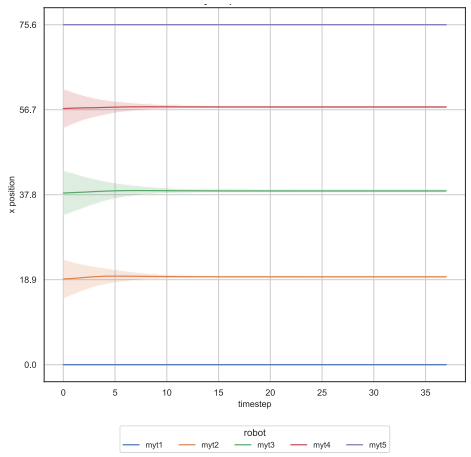

(c) Manual controller trajectories.

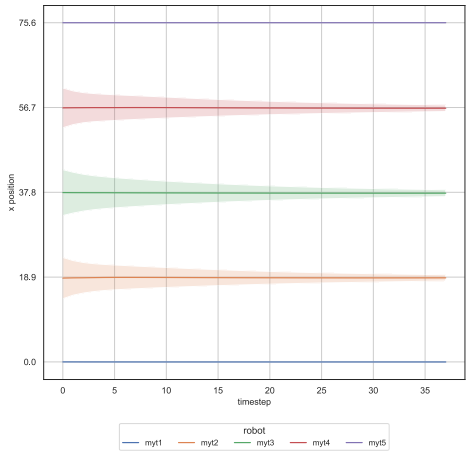

(d) Distributed controller trajectories.

Figure 5.4. Comparison of trajectories, of all the simulation runs, generated using three controllers: the expert, the manual and the one learned from `net-d1`.

as an average over all the simulation runs, and besides is shown this average minus and plus the standard deviation. As expected, the convergence of the robots to the target using the omniscient controller is much faster than with the manual or the learned one. Generally, the learned trajectories require a higher number of time steps to converge to the correct configuration, sometimes even 40 may be necessary, compared to the two other controllers that need less than 10.

Indeed, analysing in Figure 5.5 the evolution of the control over time, it is possible to notice that the omniscient in the first time steps uses a higher speed than that chosen by the manual controller or the one predicted by the network. After about 10 time steps the expert reaches the target while the manual need about 15 time steps to arrive to the goal with a certain tolerance, maintaining then the speed constant at 0. Instead, the distributed controller decreases the speed of the agents as the time steps pass, reaching zero speed but with a certain variance, probably caused by oscillations.

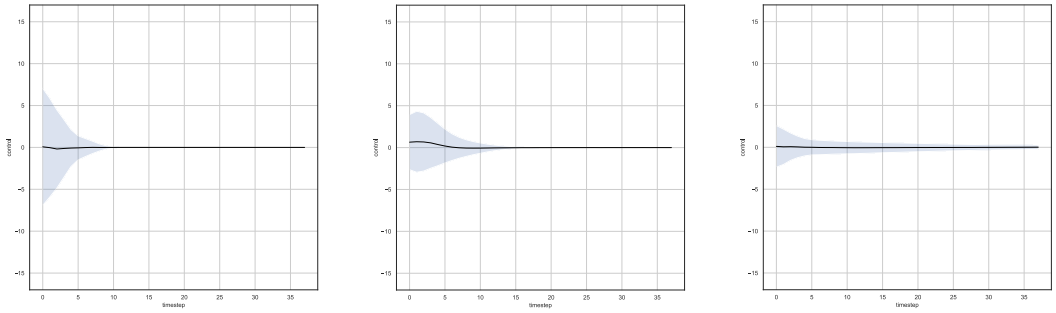

(a) Expert controller. **(b)** Manual controller. **(c)** Distributed controller.

Figure 5.5. Comparison of output control decided using three controllers: the expert, the manual and the one learned from `net-d1`.

In Figure 5.6 is visualised the response of the learned controller as the input sensing changes. In particular we analyse two cases. The first one shows the control predicted by the network when the robot sees only in front and nothing behind, more specifically when the given input is $([0,0,x,0,0,0,0])$, with x varying in the range $[0,4500]$. The second shows the control predicted by the network when the robot instead sees nothing in front, more specifically when the given input is $([0,0,0,0,0,x,x])$, with x varying in the range $[0,4500]$. The behaviour is almost as expected. When the robot sees nothing behind but something in front, the model returns a negative speed, since the robot has to move backwards. The absolute value of control increases as the proximity to the obstacle increases. A complementary behaviour is obtained when the robot sees only behind but not in front.

In Figure 5.7 is displayed the behaviour of a robot located between two stationary agents which are already in their place, showing the response of the controllers, on the y-axis, by varying the position of the moving robot, visualised on the x-axis. The output control is computed as an average over 100 measures in which the pose of the

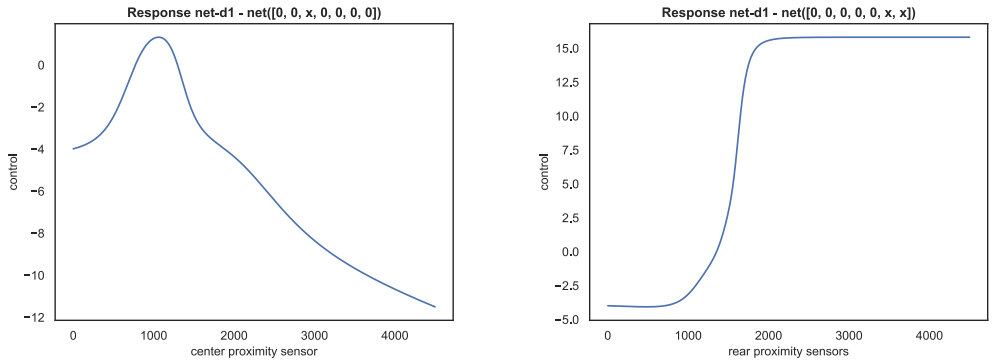

Figure 5.6. Response of `net-d1` by varying the input sensing.

agent (x, y, θ) differs by a certain epsilon uniformly distributed in the range $[-0.5, 0.5]$, thus to avoid the effects of noise that would be obtained on a single measurement and unrealistic artefacts in which the sensors are not continuous. Besides, are shown the bands which represent plus and minus standard deviation. As expected, the output is a high value, positive or negative respectively when the robot is close to an obstacle on the left or on the right, or it is close to 0 when the distance from right and left is equal.

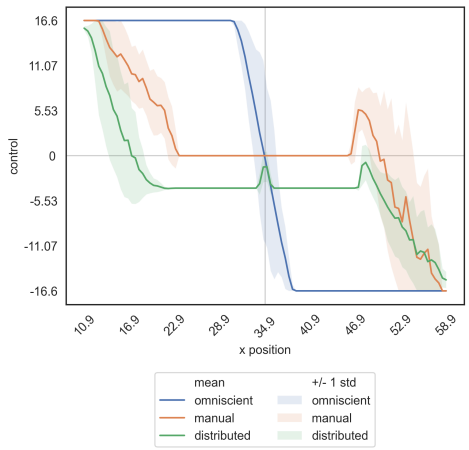

Figure 5.7. Response of `net-d1` by varying the initial position.

Finally, in Figure 5.8 is presented another useful metric that measures the absolute distance of each robot from the target, visualised on the y-axis, over time. This value is averaged on all robots among all the simulation runs. The median value is shown as well as the interquartile and interdecile ranges. On average, the distance from goal of the learned controller is lower than the one obtained with the manual controller, meaning that in the final configuration the robots moved following the learned controller are

closer to the target than those moved with the manual one, which are on average at a distance of about 1cm from the goal position.

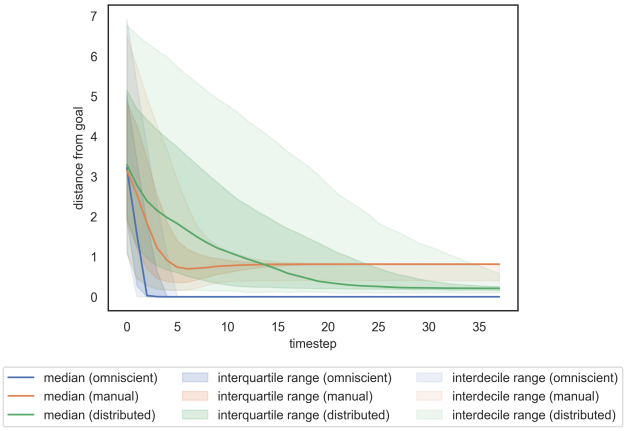

Figure 5.8. Comparison of performance in terms of distances from goal obtained using three controllers: the expert, the manual and the one learned from `net-d1`.

As mentioned before, in case of `prox_values` inputs the experiment performed with an `avg_gap` of 24 is not meaningful since this value exceeds the maximal range of the sensor. Similarly, since 14 is the maximum range, it is difficult to use this type of input when the `avg_gap` is 13, as shown by the losses in Figure 5.9.

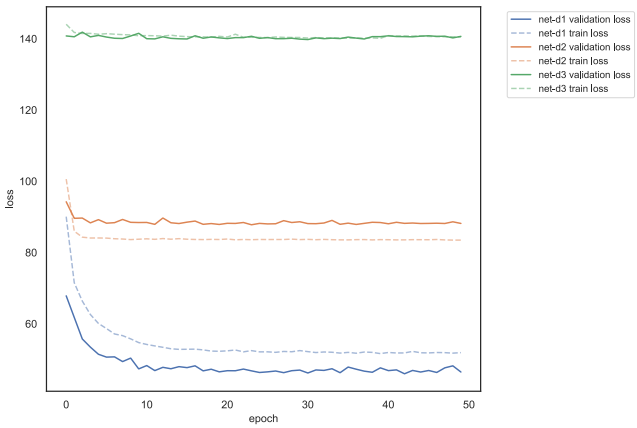

Figure 5.9. Comparison of the losses of the models that use `prox_values` readings.

Results using `prox_comm` input Following are shown the results of the experiments obtained using the `prox_comm` readings. In Figure 5.10, we analyse the losses by varying the average gap. From a first observation, the network seems to be able to work with all the gaps.

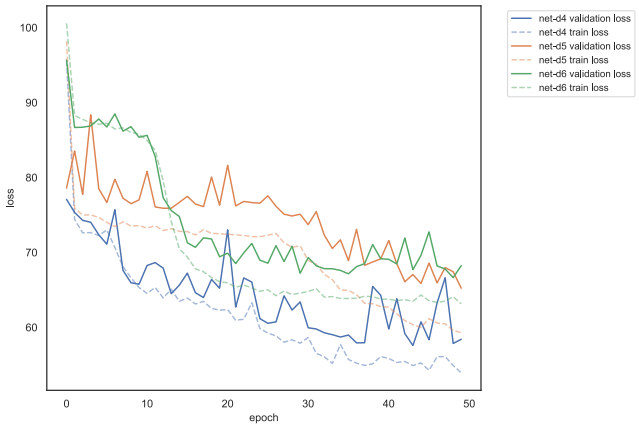

Figure 5.10. Comparison of the losses of the models that use `prox_comm` readings.

For the assumptions made before, we believe that the model obtained from `net-d6`, the has a higher average gap, is the more promising. Moreover, as shown from the R^2 coefficients in Figure 5.11, we expect that the robots' behaviour using the learned instead of the manual controller is better, even if far from the expert.

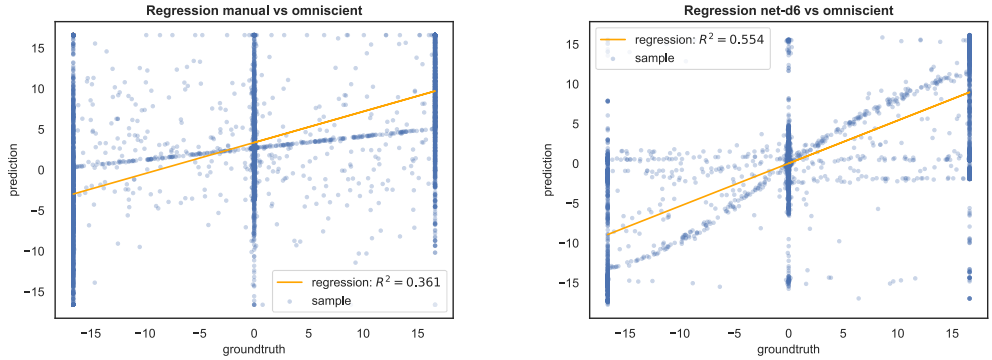

Figure 5.11. Comparison of the R^2 coefficient of the manual and the controller learned from `net-d6` with respect to the omniscient one.

In Figure 5.12, we show a comparison of the trajectories obtained for a sample simulation, using the three controllers. We immediately see that the agents moved using the omniscient controller reach the target in less then 15 time steps. Those moved using the manual controller did not approach the goal, even if they try to position themselves at equal distances. Instead, the learned controller lets the robots arrive in the correct final configuration in 10 time steps, faster than the expert. This because, in this case, the initial positions of the agents moved with the omniscient controller are farther than in the other case, so it takes longer to reach the goal.

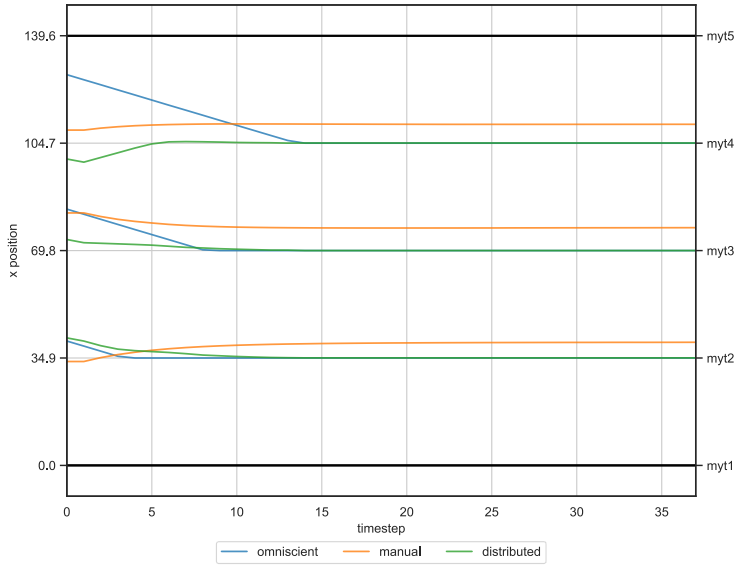

Figure 5.12. Comparison of trajectories, of a single simulation, generated using three controllers: the expert, the manual and the one learned from `net-d6`.

In Figure 5.13 are shown the trajectories obtained employing the three controllers, averaged over all the runs. As expected, the convergence to the target is slower than before, even for the expert, since the distance between the robots is greater, but it is still much faster than with the other two controllers. The manual controller has serious

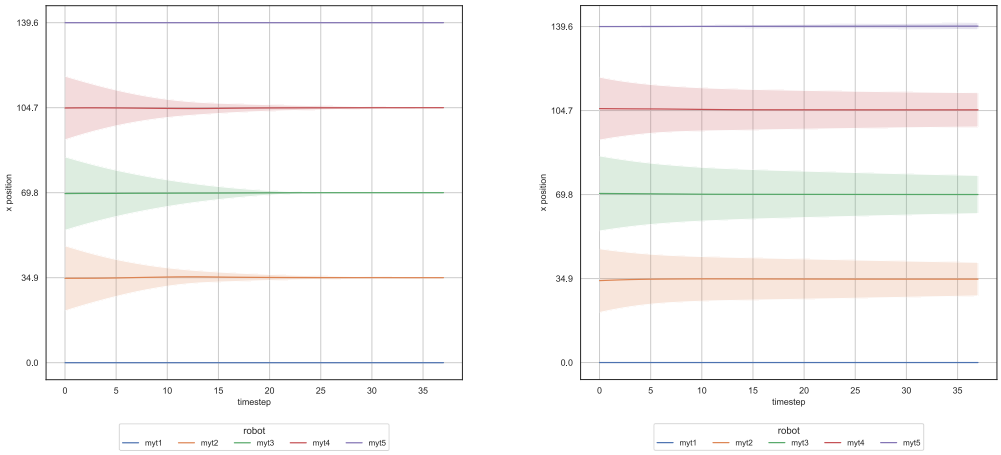

(a) Expert controller trajectories.

(b) Distributed controller trajectories.

Figure 5.13. Comparison of trajectories, of all the simulation runs, generated using three controllers: the expert, the manual and the one learned from `net-d6`.

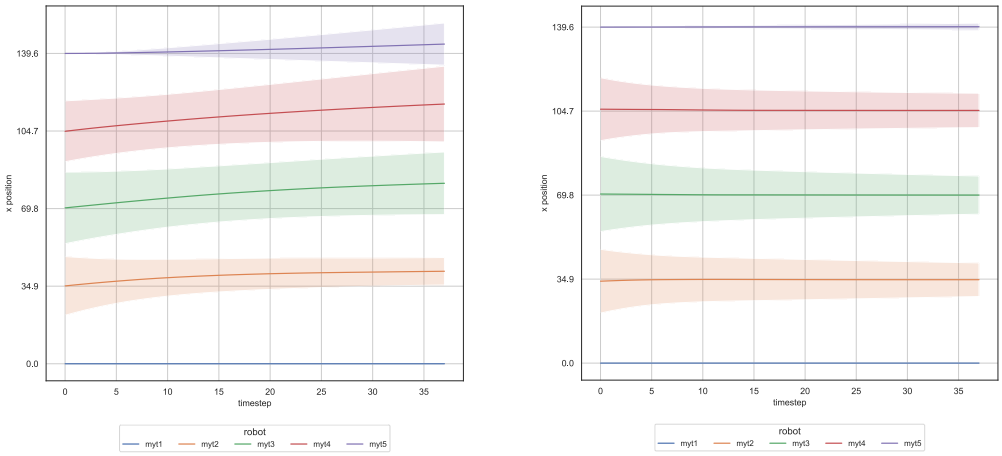

(c) Manual controller trajectories. **(d)** Distributed controller trajectories.

Figure 5.13. Comparison of trajectories, of all the simulation runs, generated using three controllers: the expert, the manual and the one learned from `net-d6` (cont.).

problems in reaching the goal: even if the agents try to position themselves at equal distances, they tend to increase the average gap between them, creating situations in which the last robot in motion hits the fixed one. Surprisingly, the learned controller allows the agents to converge to the correct configuration by taking more time than the expert does.

An immediate examination of the evolution of the control over time, in Figure 5.14, highlights the speed of the expert controller, which in all the simulation runs, after 25 time steps, has reached 0. In addition, the manual controller always sets a positive speed, which leads to the wrong behaviour mentioned earlier, while the slowness of the distributed control is explained by the usage of a low speed.

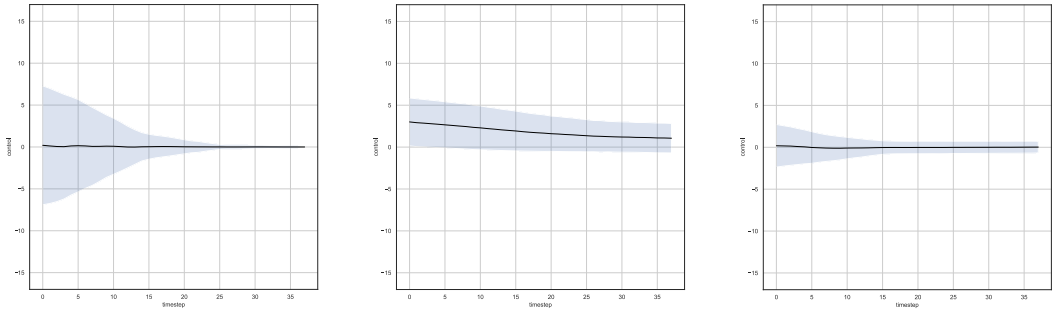

(a) Expert controller. **(b)** Manual controller. **(c)** Distributed controller.

Figure 5.14. Comparison of output control decided using three controllers: the expert, the manual and the one learned from `net-d6`.

Figure 5.15 visualises the response of the learned controller as the input sensing changes, analysing the same two cases as before. Despite the behaviour is the same obtained using `prox_values` when the robot sees only behind, this time the trend is different when the robot sees nothing behind: since the robot has to move backwards, a negative speed is always returned, that is higher when the obstacle is far.

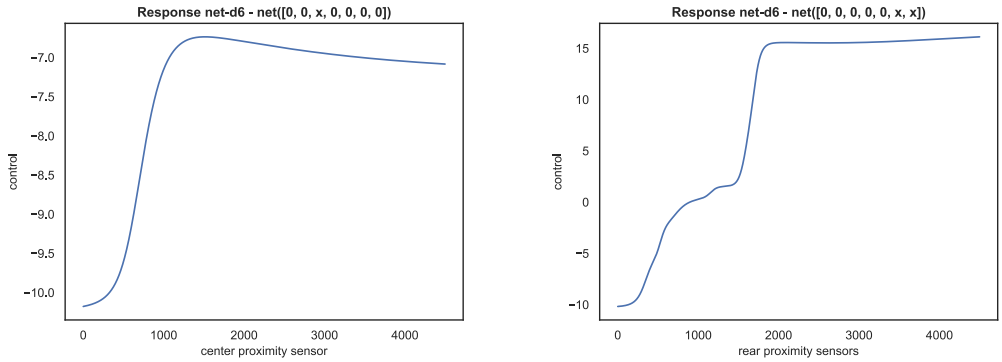

Figure 5.15. Response of `net-d6` by varying the input sensing.

In Figure 5.16, the behaviour of a robot located between other two that are already in their place is displayed. It visualises the response of the learned controller by vary-

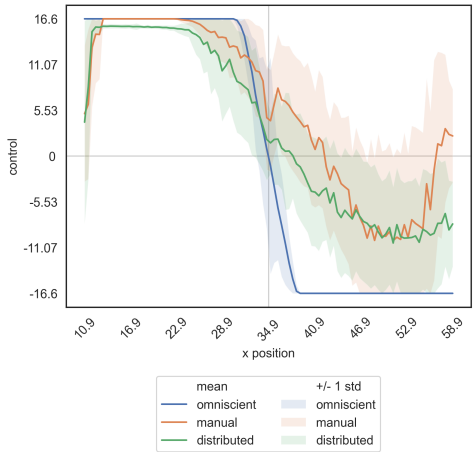

Figure 5.16. Response of `net-d6` by varying the initial position.

ing the distance between two stationary agents and a robot located among them. As expected, the output is a high positive value when the robot is close to an obstacle on the left, it decreases and reaches 0 when the distance from right and left is equal, and finally becomes negative when there is an obstacle in front and not behind.

Finally, in Figure 5.17, is presented the average distance of the robots from the target among all the simulations. The performance of the learned and the manual controllers are similar: in the final configuration they both are at about 5cm from the target.

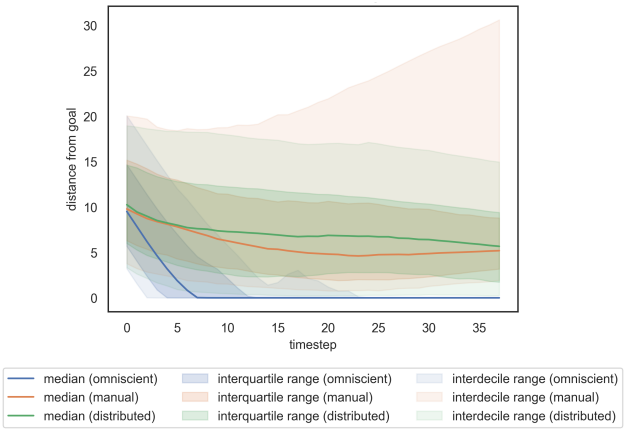

Figure 5.17. Comparison of performance in terms of distances from goal obtained using three controllers: the expert, the manual and the one learned from `net-d6`.

We conclude the first group of experiments presenting the results obtained using both types of input together from which we expect a more stable and robust behaviour.

Results using `all_sensors` input In Figure 5.18, an analysis of the losses shows that using `all_sensors` inputs the network is able to work well with all the gaps.

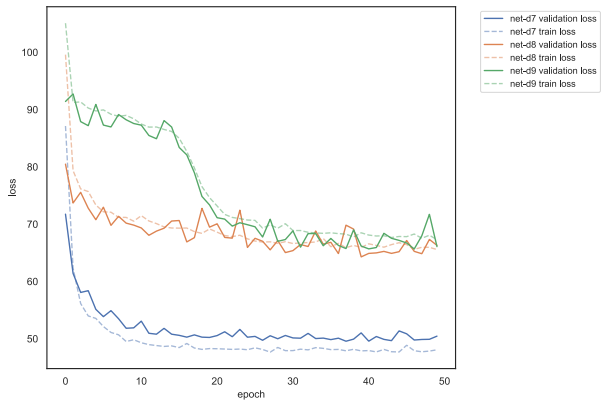

Figure 5.18. Comparison of the losses of the models that use `all_sensors` readings.

Examining the R^2 coefficients in Figure 5.19, the behaviour obtained with `net-d7` and `net-d9` are the more promising.

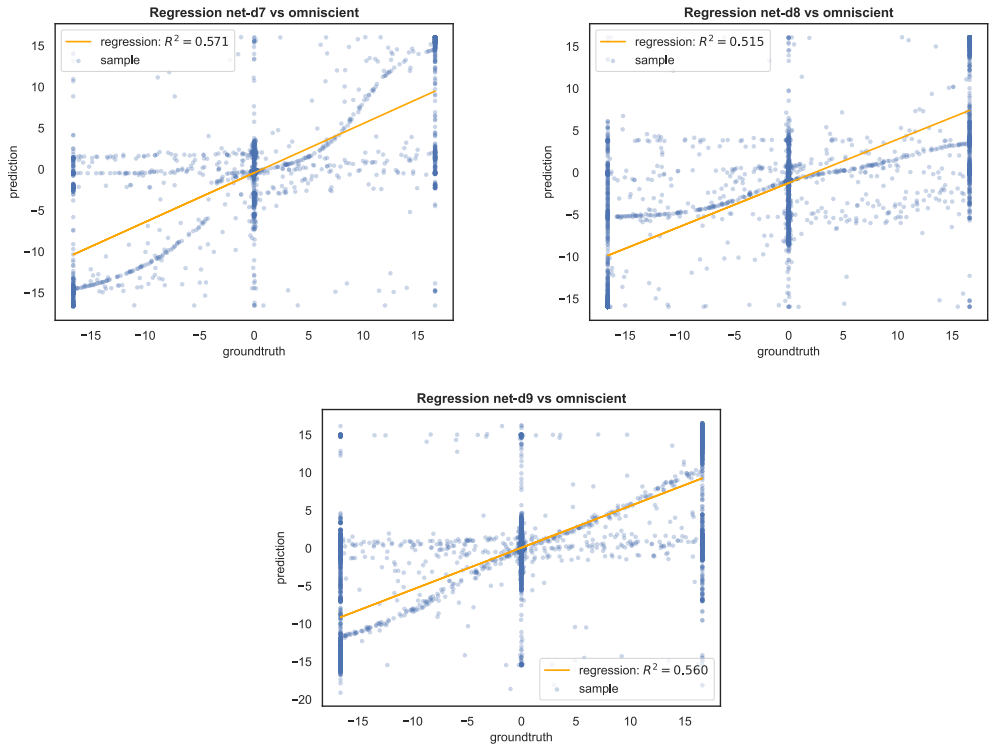

Figure 5.19. Comparison of the R^2 coefficients of the models that use `prox_comm` readings.

Considering the more complex case, that is the one with the greatest average gap, the superiority of this controller is further supported by the comparisons in Figure 5.20.

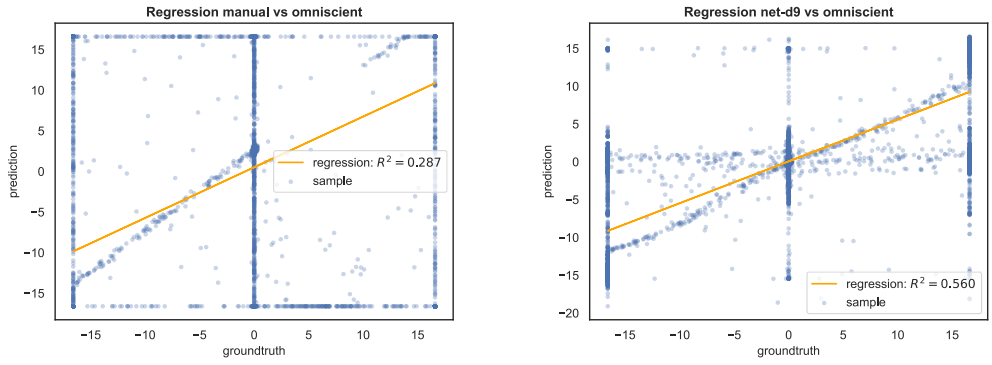

Figure 5.20. Comparison of the R^2 coefficient of the manual and the controller learned from `net-d9` with respect to the omniscient one.

In Figure 5.21 is shown a comparison of the trajectories for a sample simulation. As before, the performance obtained using the omniscient and the learned controllers are comparable: both are very fast and in less than 10 time steps they reach the target. Instead, when the agents moved using the manual controller have almost approached the target, they start to oscillate. This problem is not surprising, since the parameters of the manual controller have been tuned on some specific cases and are always the same for all datasets, sometimes it does not work correctly.

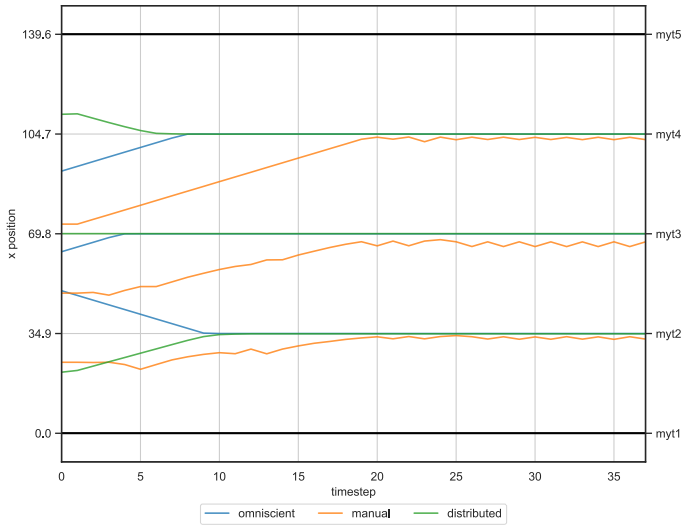

Figure 5.21. Comparison of trajectories, of a single simulation, generated using three controllers: the expert, the manual and the one learned from `net-d9`.

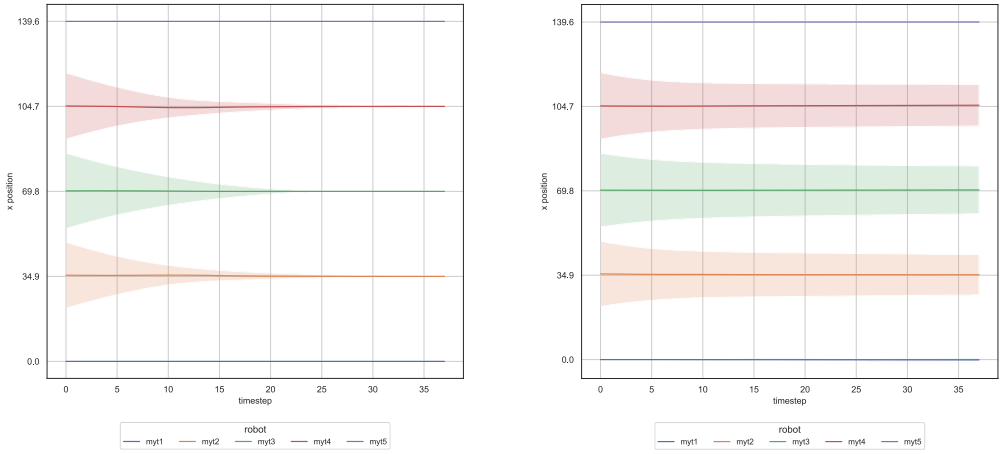

(a) Expert controller trajectories. **(b)** Distributed controller trajectories.

Figure 5.22. Comparison of trajectories, of all the simulation runs, generated using three controllers: the expert, the manual and the one learned from `net-d9`.

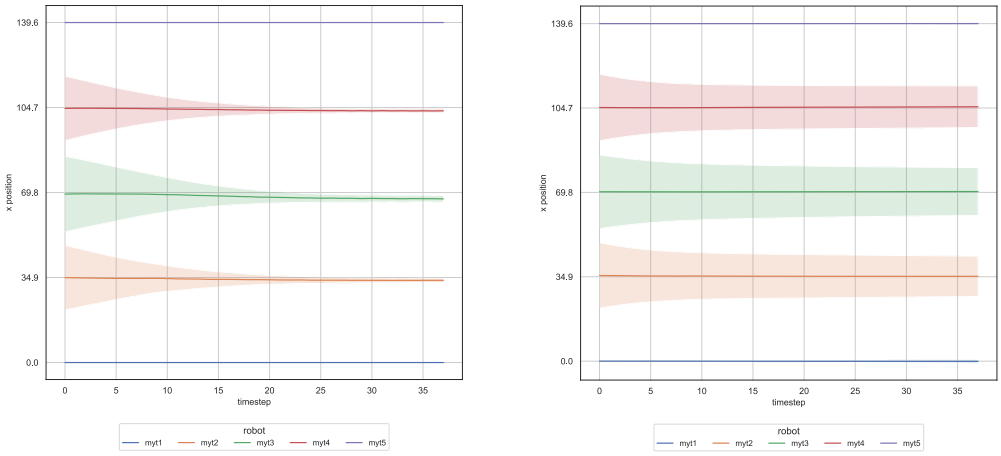

(c) Manual controller trajectories.

(d) Distributed controller trajectories.

Figure 5.22. Comparison of trajectories, of all the simulation runs, generated using three controllers: the expert, the manual and the one learned from `net-d9` (cont.).

In Figure 5.22 are shown trajectories obtained employing the three controllers. The convergence to the target is still slow, even if this time the expert needs less time steps than before. The manual controller does not show the same problem as before, while the learned controller is still the slowest to end up in the correct configuration.

Examining the evolution of the output control, in Figure 5.23, the plots of the expert and the learned controllers are similar, although the speed in the second is much lower.

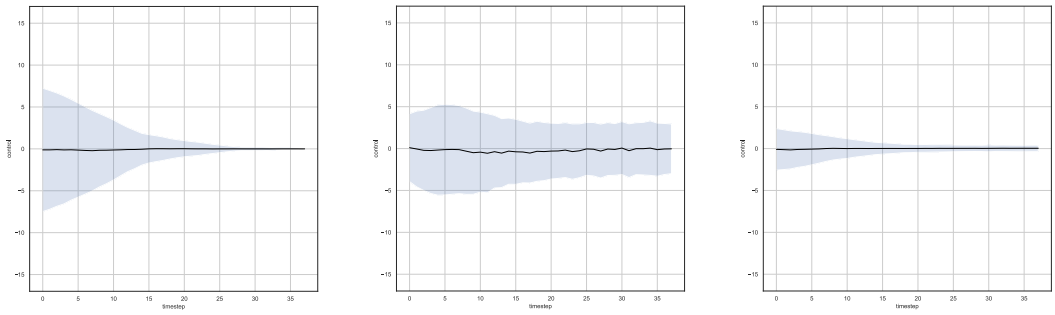

(a) Expert controller.

(b) Manual controller.

(c) Distributed controller.

Figure 5.23. Comparison of output control decided using three controllers: the expert, the manual and the one learned from `net-d9`.

In Figure 5.24 is displayed the behaviour of a robot located between other two that are already in their place. This time the trend of the three curves shows how the behaviour of the model learned and of the manual controller are similar to that of the expert.

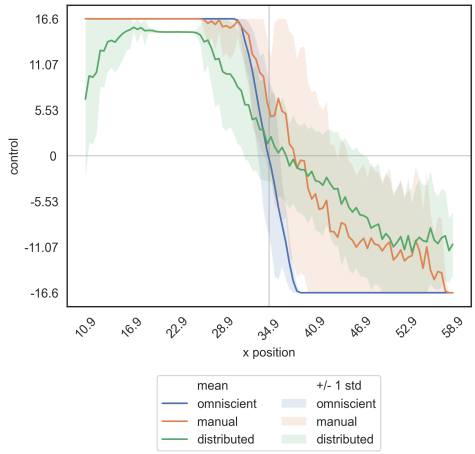

Figure 5.24. Response of `net-d9` by varying the initial position.

Finally, in Figure 5.25, is presented the absolute distance of each robot from the target, averaged on all robots among all the simulation runs. The median value is shown as well as the interquartile and interdecile ranges. As anticipated by the trajectories in

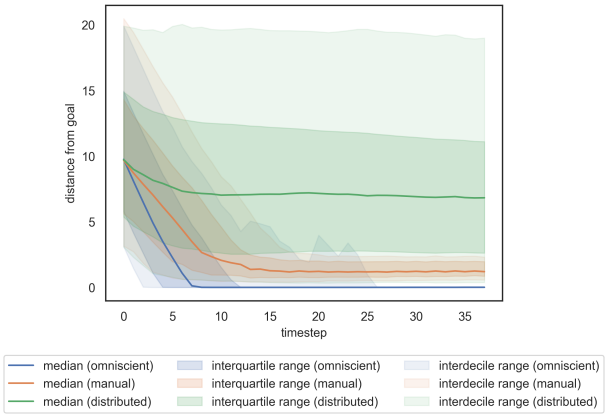

Figure 5.25. Comparison of performance in terms of distances from goal obtained using three controllers: the expert, the manual and the one learned from `net-d9`.

Figure 5.22, the controller learned from `net-d9` is slower to converge than the manual one. In fact, this plot confirms that the agents moved following a manual controller in the final configuration are closer to the target than those moved by the distributed controller: they are on average 2 or 7cm away from the goal position respectively.

Summary We show in the figures below the losses of the trained models as the different inputs of the network vary, in particular, we represent with the blue, the orange and the green lines `prox_values`, `prox_comm` and `all_sensors` inputs respectively.

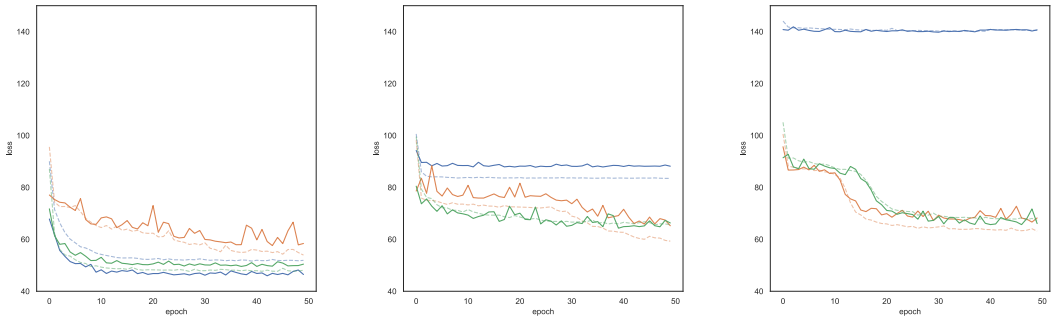

(a) `avg_gap` of 8cm. **(b)** `avg_gap` of 13cm. **(c)** `avg_gap` of 24cm.

Figure 5.26. Comparison of the losses by varying the input of the networks for the three gaps.

In case of an `avg_gap` of 8cm, the model trained using `prox_values` has a lower loss, following is the network that employ `all_sensors`, with similar results, and finally the model that works with `prox_comm`. This performance is expected, as well as the fact that `all_sensors` cannot perform better than `prox_values` with small gaps, since in this case the data coming from `prox_comm` contains only zeros in the the second half of the array, making it unusable. In a complementary way, by increasing the gap to 13cm, `prox_values` alone is not able to achieve satisfactory results, while used together with `prox_comm`, `all_sensors` reaches good performances that on the validation set are comparable to those obtained using `prox_comm` alone. Finally, by increasing the gap even more, up to 24cm, `prox_values` becomes completely unusable, while `prox_comm` and `all_sensors` still have excellent performances similar to each other.

5.1.1.2 Experiment 2: variable number of agents

The second group of experiments we carried out using a distributed approach, examines the behaviour of the control learned using `all_sensors` inputs.

Model	network_input	input_size	avg_gap	N
net-d10	all_sensors	14	8	5
net-d11	all_sensors	14	20	5
net-d12	all_sensors	14	variable	5
net-d13	all_sensors	14	8	8
net-d14	all_sensors	14	20	8
net-d15	all_sensors	14	variable	8
net-d16	all_sensors	14	8	variable
net-d17	all_sensors	14	20	variable
net-d18	all_sensors	14	variable	variable

Table 5.2. List of the experiments carried out using a variable number of agents and of gaps.

In this situation, the simulation runs use a different number of robots N, that can be fixed at 5 or 8 for the entire simulation, or even vary in the range $[5, 10]$. The same reasoning is applied to the choice of the `avg_gap`, that can be a fixed value in all the runs, chosen between 8 or 20, but also vary in the range $[5, 24]$. The objective of this set of experiments, summarised in Table 5.2, is to verify the robustness of the models, proving that it is possible to train networks that handle a variable number of agents.

First of all, we start by showing in Figure 5.27 an overview of the models performance in terms of train and validation losses.

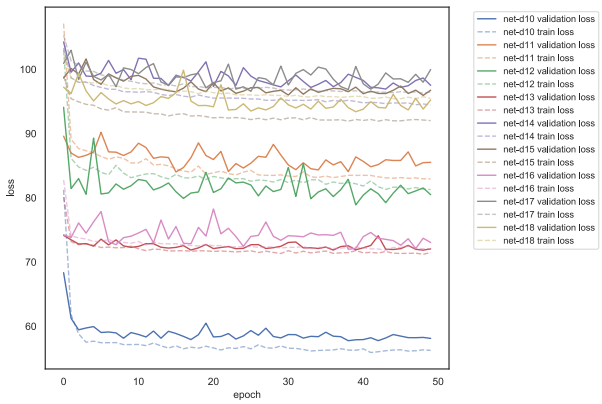

Figure 5.27. Comparison of the losses of the models carried out using a variable number of agents and of average gap.

Results using 5 agents In Figure 5.28 are analysed the experiments performed using a fixed number of agents, the same used for the group of experiments presented above, i.e., 5, in order to show the difference of performance using a gap that is first small, then large and finally variable.

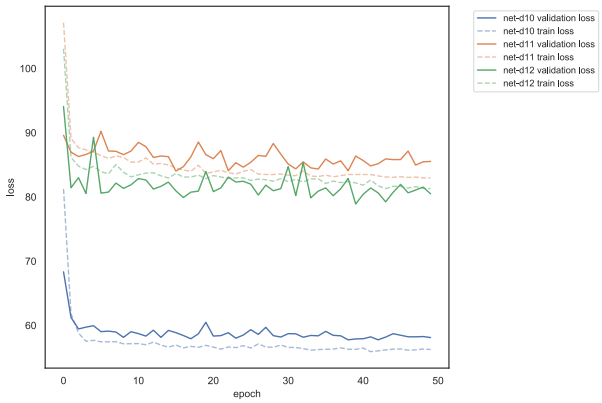

Figure 5.28. Comparison of the losses of the models that use 5 agents as the gap varies.

Examining more in detail the case in which the model is trained using a variable average gap, in Figure 5.29 is visualised a comparison of the R^2 of the manual and the learned controllers, on the validation set. The robots' behaviour using the learned instead of the manual controller is a bit better, even if far from the expert.

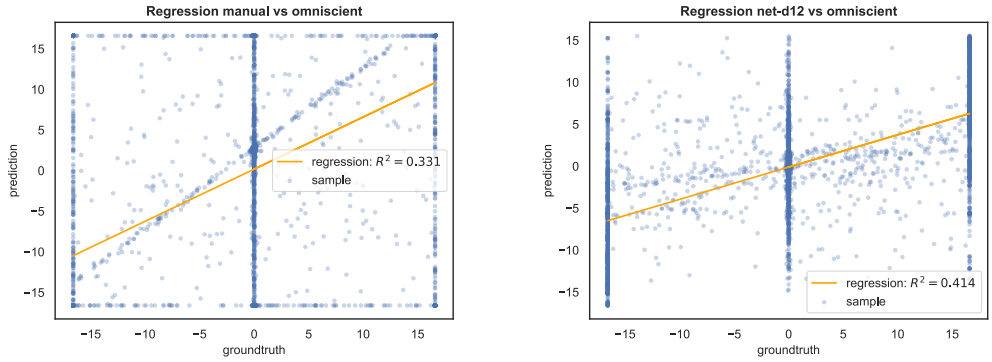

Figure 5.29. Comparison of the R^2 coefficients of the manual and the controller learned from `net-d12` with respect to the omniscient one.

In Figure 5.30, we first show a sample simulation: on the y-axis are visualised the positions of the agents, while on the x-axis the simulation time steps. The agents moved

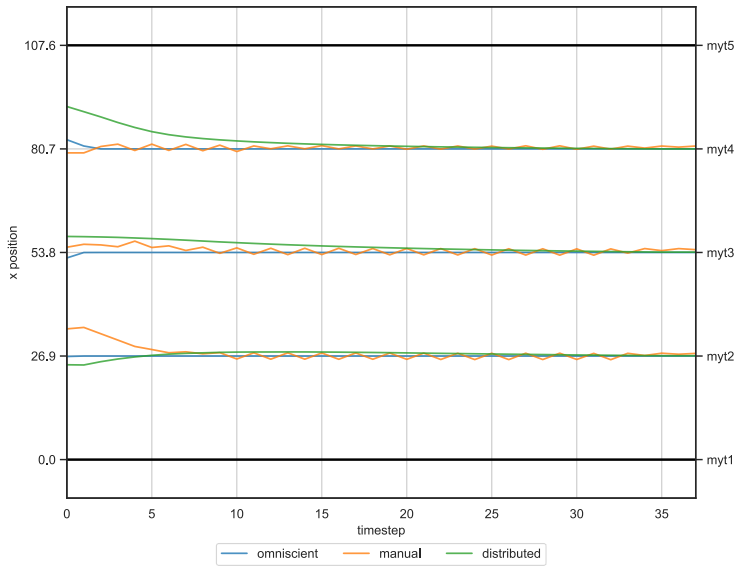

Figure 5.30. Comparison of trajectories, of a single simulation, generated using three controllers: the expert, the manual and the one learned from `net-d12`.

using the omniscient controller are, as expected, those that reach the target faster. Those moved using the manual controller are slower and moreover, as for the case

shown in Figure 5.21, they start to oscillate when they approach the target. Instead, the learned controller, even if is slower than the other two, is able to reach the correct configuration.

In Figure 5.31, we show first a comparison of the expert and the learned trajectories, and then between the manual and the learned ones. In particular, on the y-axis is visualised the position of each agent over time, averaged over all the simulation runs, while on the x-axis the simulation time steps. It is important to note that there is a difference in these graphs compared to those of the previous group of experiments.

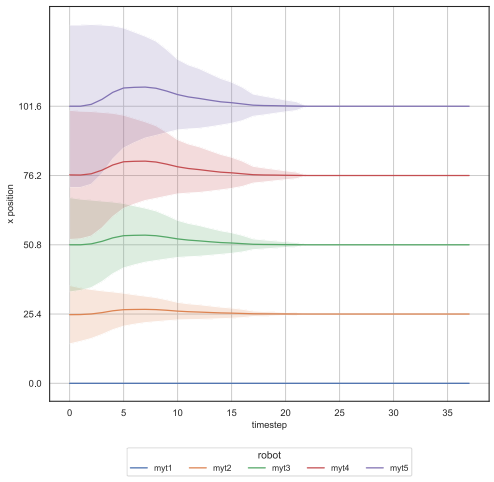

(a) Expert controller trajectories.

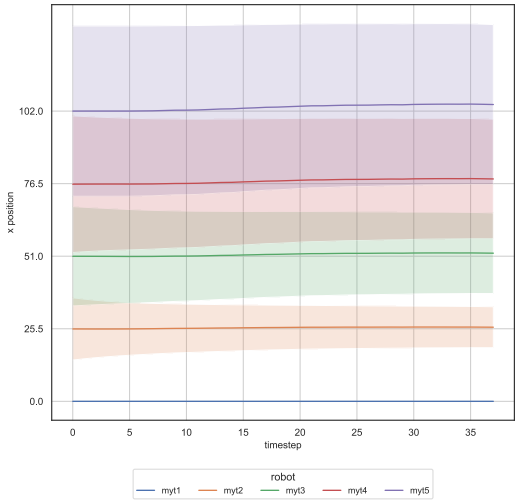

(b) Distributed controller trajectories.

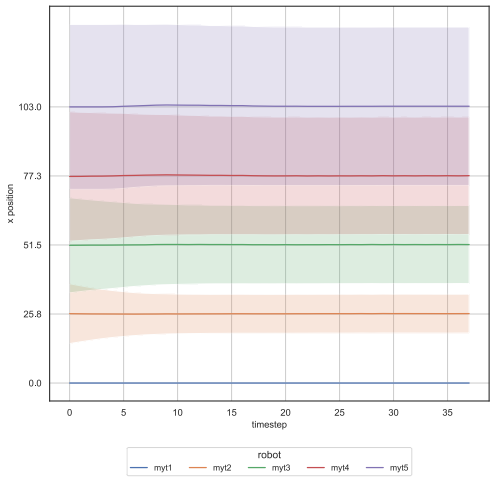

(c) Manual controller trajectories.

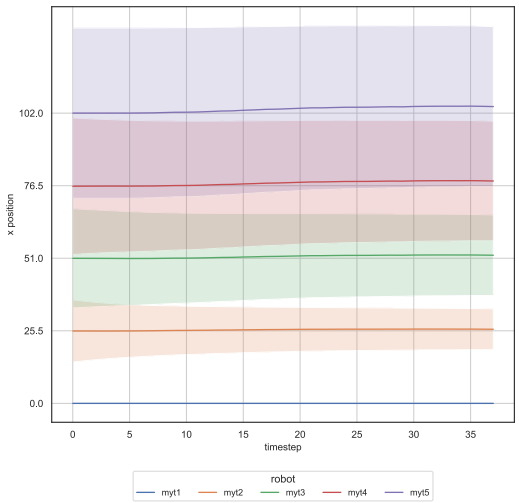

(d) Distributed controller trajectories.

Figure 5.31. Comparison of trajectories, of all the simulation runs, generated using three controllers: the expert, the manual and the one learned from `net-d12`.

Observing the deviation of the position of the robots with respect to the average, the last agent of the row did not maintain the same initial and goal positions throughout the simulations since the average gap set is different for every run. The convergence of the robots to the target is guaranteed in 20 time steps using the expert, while the manual and learned controller still manage to reach the correct configuration with more time.

Analysing the evolution of the control over time, in Figure 5.32, we observe that the speeds set by the manual controller and the one learned from the network are significantly lower and therefore do not allow to reach the target in a satisfactory time.

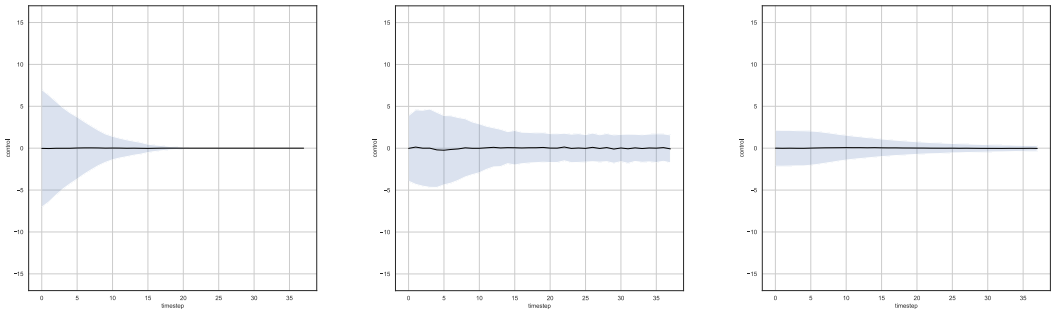

(a) Expert controller. **(b)** Manual controller. **(c)** Distributed controller.

Figure 5.32. Comparison of output control decided using three controllers: the expert, the manual and the one learned from `net-d12`.

In Figure 5.33, another informative plot displays the behaviour of a robot located between other two that are already in their place. As expected, the trend of the three curves shows how the behaviour of the model learned and of the manual controller are similar. However, the performance of the manual controller, when the robot is close to

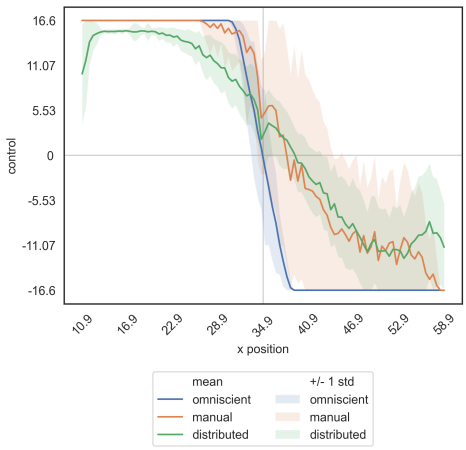

Figure 5.33. Response of `net-d12` by varying the initial position.

the one that preceded it, is practically comparable to that obtained by the expert. In contrast, when the agent is close to the following one, it worsens and presents a lot of variability.

Finally, in Figure 5.34, is shown the absolute distance of each robot from the target, averaged on all robots among all the simulation runs, over time. Despite we expected performances similar to those presented in the Figure 5.25, in this circumstance the agents moved following the distributed controller are closer to the target, in particular in the final configuration they are on average 2cm away from the goal position. Furthermore, it is shown that there are far fewer cases away from the average behaviour.

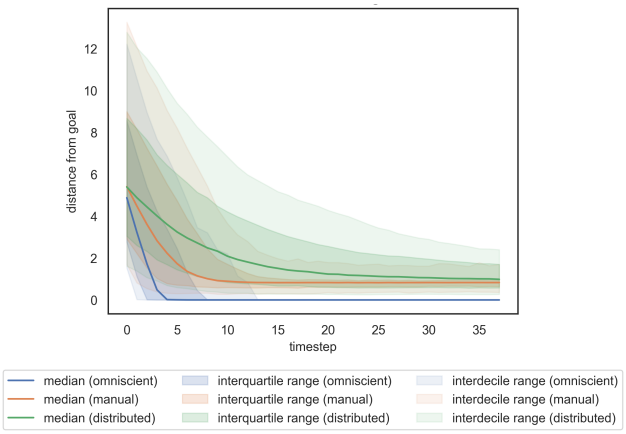

Figure 5.34. Comparison of performance in terms of distances from goal obtained using three controllers: the expert, the manual and the one learned from `net-d12`.

Results using 8 agents Following are shown the losses of the models trained using an higher number of agents, i.e.,8, by varying the average gap. From a first observation,

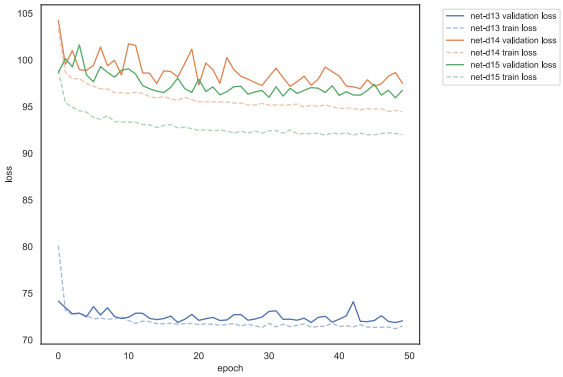

Figure 5.35. Comparison of the losses of the models that use 8 agents as the gap varies.

the network seems to be able to work with all the gaps. As before, for the network it is easier to perform a task using a smaller gap. For this reason, it is more interesting to analyse the case in which the model is trained using a variable gap.

In Figure 5.36 is visualised a comparison of the R^2 coefficients of the manual and the learned controller. In both cases, the coefficients are very low, since in most of the cases in which the controllers have to decide a zero or maximum speed a wrong value is predicted, however, the coefficient obtained from the network is slightly better.

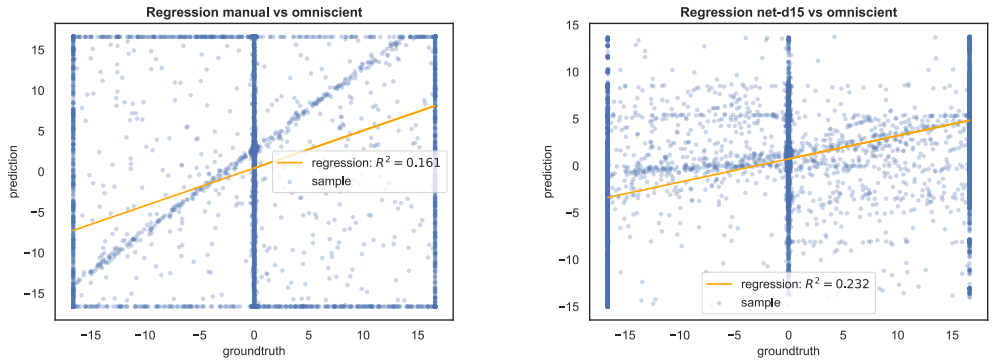

Figure 5.36. Comparison of the R^2 coefficients of the manual and the controller learned from `net-d15` with respect to the omniscient one.

In Figure 5.37 is displayed a sample simulation that shows on the y-axis position of

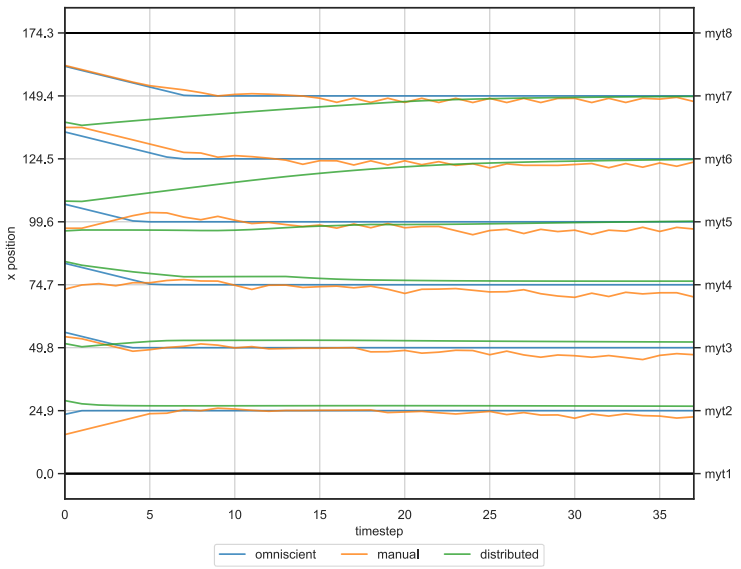

Figure 5.37. Comparison of trajectories, of a single simulation, generated using three controllers: the expert, the manual and the one learned from `net-d15`.

each agent, while on the x-axis the simulation time steps. The agents moved using the learned controller, even if in the initial configuration are far from the target, they are able to reach the goal. Instead, the agents moved using the manual controller, when have almost approached the target, they start to oscillate.

In Figure 5.38 are shown the trajectories obtained employing the three controllers, averaged over all the simulation runs. Compared to the previous case, a greater number of robots implies a slowdown in reaching the correct position, even when using an expert controller. As before, the convergence of the robots using the manual and learned controllers needs more time.

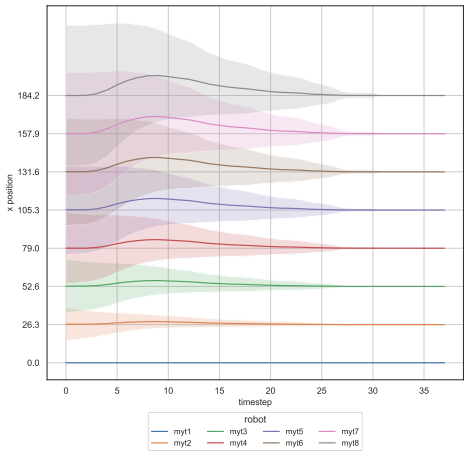

(a) Expert controller trajectories.

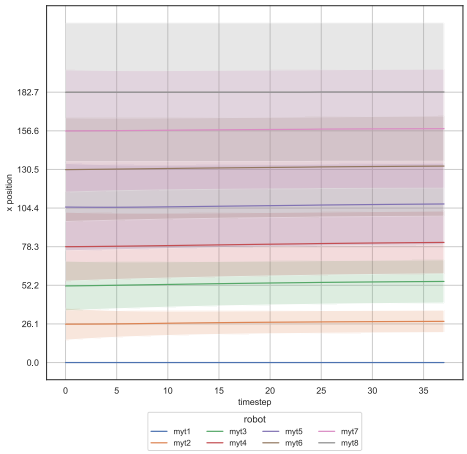

(b) Distributed controller trajectories.

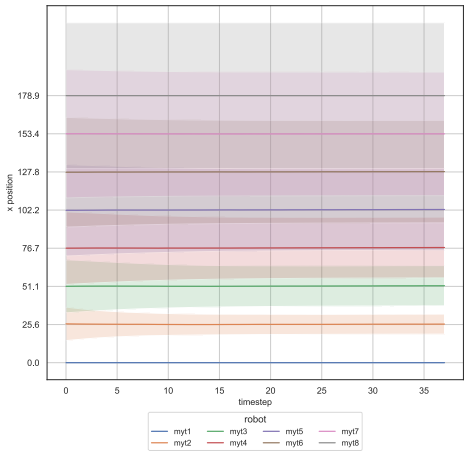

(c) Manual controller trajectories.

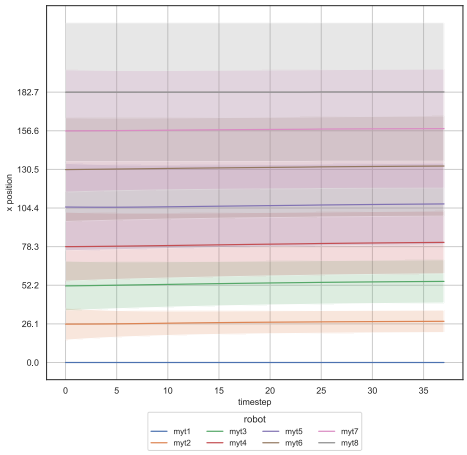

(d) Distributed controller trajectories.

Figure 5.38. Comparison of trajectories, of all the simulation runs, generated using three controllers: the expert, the manual and the one learned from `net-d15`.

Examining in Figure 5.39 the evolution of the control over time, the graph of the distributed controller highlights how the speed decided by the model has further decreased due to the increase in the amount of agents in the simulation.

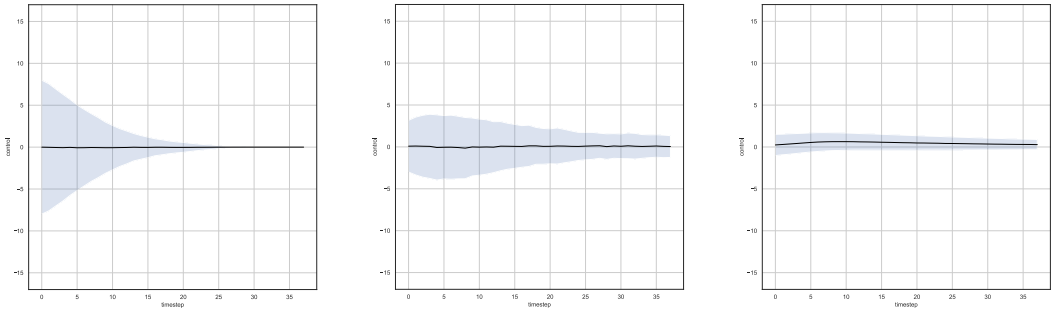

(a) Expert controller. **(b)** Manual controller. **(c)** Distributed controller.

Figure 5.39. Comparison of output control decided using three controllers: the expert, the manual and the one learned from `net-d15`.

Figure 5.40 displays the behaviour of a robot located between other two that are already in their place. Analysing the way of acting of the three controllers for this experiment, from the plot arises an important difference in the decisions taken by the distributed and the manual controllers. The learned controller, whether a robot is closer to the one that precedes it or to the one following it, sets a proportional speed, lower than the optimal one, that leads it to move respectively back and forth to reach the desired position. Instead, the manual controller when an agent is closer to the one in front sets a very high speed to move quickly to the desired position, just like the expert does, unlike when the robot is closer to the one following it, where it sets a negative speed but not high enough, a bit like the distributed controller does.

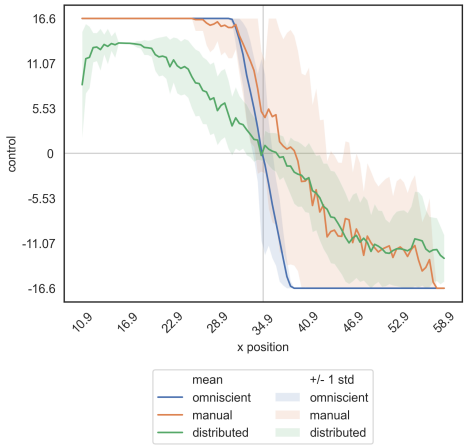

Figure 5.40. Response of `net-d15` by varying the initial position.

Finally, in Figure 5.41 is presented the average distance of the robots from the target among all the simulations. The performance of the learned and the manual controllers are different from before: `net-d15` is slower to converge. In fact, this plot confirms that the agents moved following a manual controller in the final configuration are closer to the target than those moved by the distributed controller, respectively, they are on average 2 or 3.5cm away from the goal position. Moreover, observing the coloured bands we see that there is a lot of variance in the distributed controller final positions, in fact there are runs in which some agents can be even 10cm far from the target.

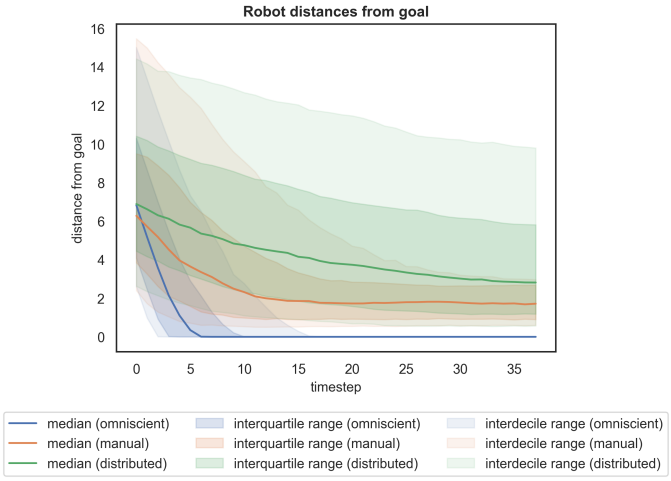

Figure 5.41. Comparison of performance in terms of distances from goal obtained using three controllers: the expert, the manual and the one learned from `net-d15`.

Results using variable agents We conclude the experiments performed using a distributed approach by presenting the results obtained with a variable number of agents.

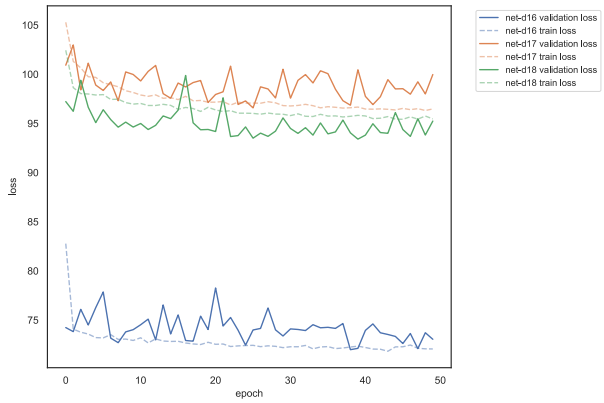

Figure 5.42. Comparison of the losses of the models that use variable agents and gaps.

In Figure 5.42, are analysed the losses by varying the average gap. As before, for the network it is easier to perform a task using a smaller gap and in general training the model on a variable gap performs better than on a fixed but big gap.

Dwelling on the most interesting case, the one in with both average gap and number of agents variable, the R^2 coefficients shown in Figure 5.43 are still very low.

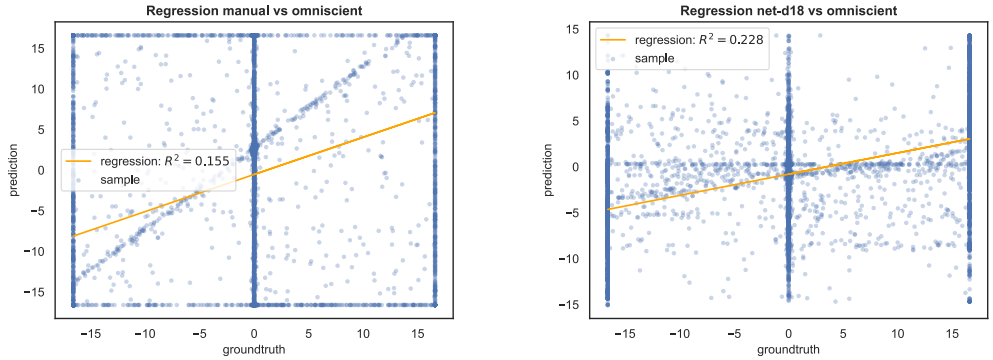

Figure 5.43. Comparison of the R^2 coefficient of the manual and the controller learned from `net-d18` with respect to the omniscient one.

In Figure 5.21 is shown a comparison of the trajectories obtained for a sample simulation. In this example, in the simulation there are 10 agents that are always able

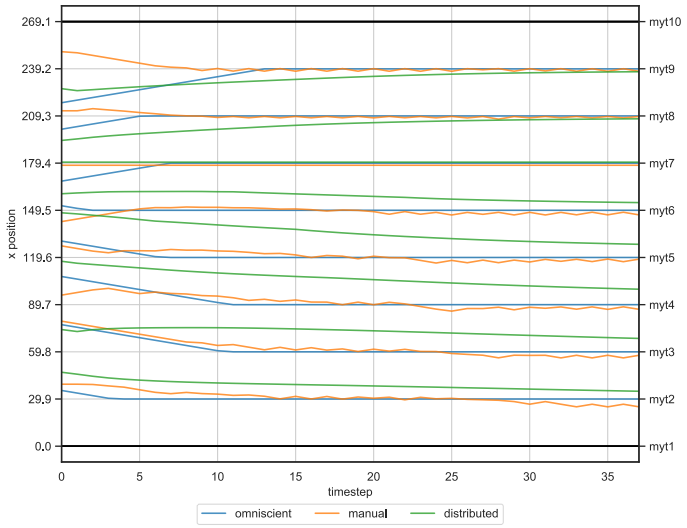

Figure 5.44. Comparison of trajectories, of a single simulation, generated using three controllers: the expert, the manual and the one learned from `net-d18`.

to reach the target when moved using an omniscient controller. When they use the manual controller, the same oscillation issue occurs in proximity to the goal. Instead,

the learned controller is certainly the slowest, and after 38 time steps not all robots are in the correct position.

Since the number of agents is variable, we show different plots, depending on this quantity, for the trajectories obtained employing the three controllers: we analyse, in the following figures, cases with 5, 8 and 10 agents. From a first observation it is

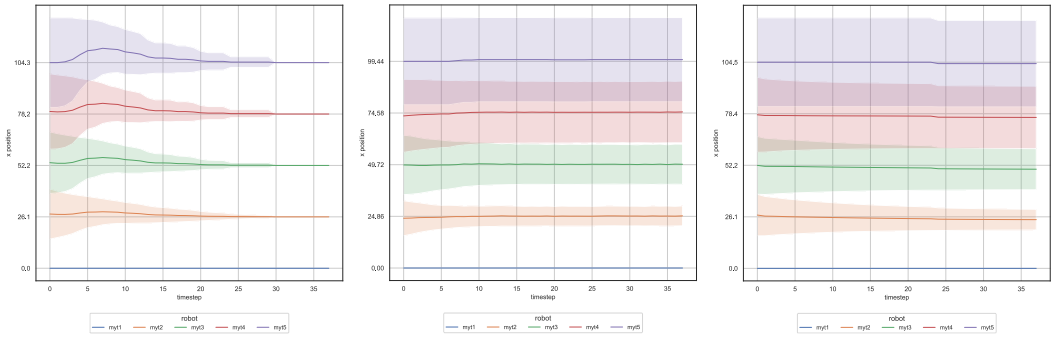

(a) Expert controller. **(b)** Manual controller. **(c)** Distributed controller.

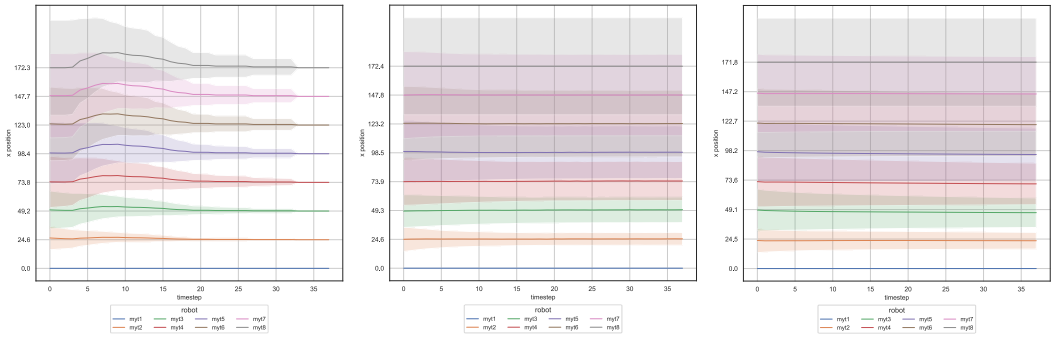

(d) Expert controller. **(e)** Manual controller. **(f)** Distributed controller.

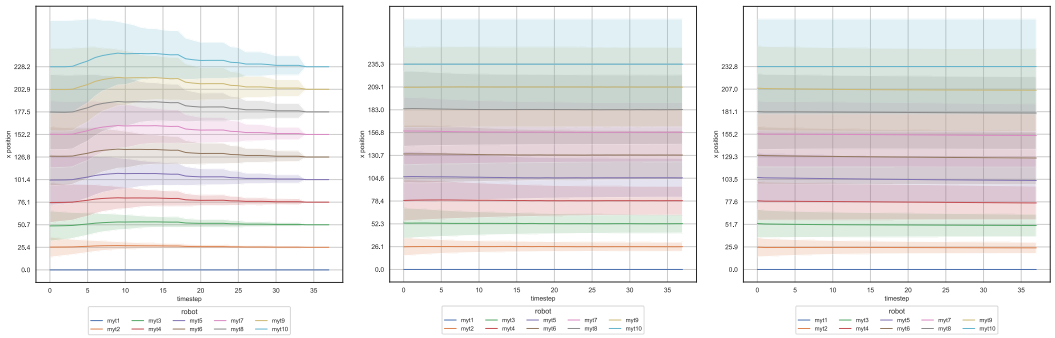

(g) Expert controller. **(h)** Manual controller. **(i)** Distributed controller.

Figure 5.45. Comparison of trajectories, of all the simulation runs, of 5, 8 and 10 agents generated using three controllers.

confirmed that increasing the number of robots in the simulation implies a greater number of time steps to reach the final configuration. Furthermore, with a large number of agents it is common for biases to add up and for the error to become more significant, in particular the one of the central robot of the group. The convergence is still slow, even if this time the expert need less time steps than before. The learned controller is still the slowest to end up in the correct configuration.

Examining the evolution of the output control, in Figure 5.46, the graph of the distributed controller highlights how the speed decided by the model has decreased due to the increase in the amount of agents in the simulation.

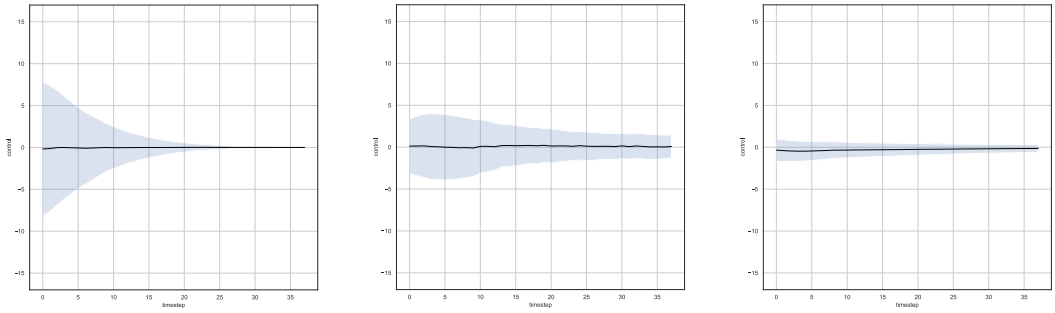

(a) Expert controller. **(b)** Manual controller. **(c)** Distributed controller.

Figure 5.46. Comparison of output control decided using three controllers: the expert, the manual and the one learned from `net-d18`.

In Figure 5.47 is displayed the behaviour of a robot located between other two that are already in their place. In this case the same reasoning made for Figure 5.40 applies.

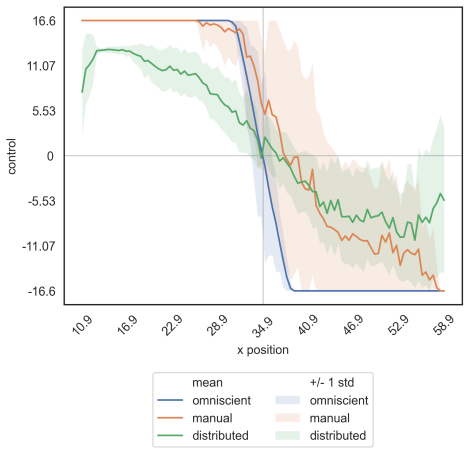

Figure 5.47. Response of `net-d18` by varying the initial position.

Focusing on the absolute distance of each robot from the target, presented in Figure 5.48, we observe once again that the agents moved following a manual controller in

the final configuration are closer to the target than those moved with the learned one.

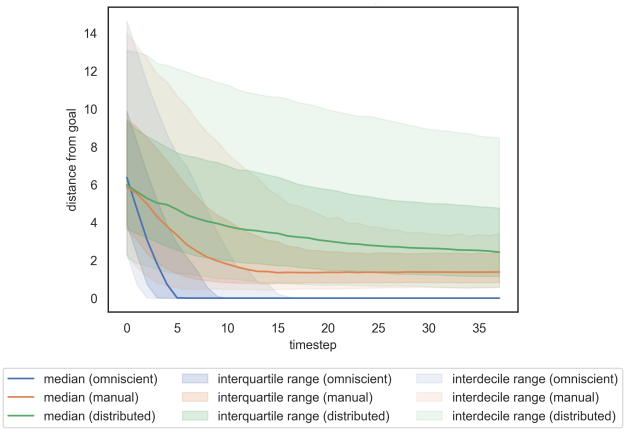

Figure 5.48. Comparison of performance in terms of distances from goal obtained using three controllers: the expert, the manual and the one learned from `net-d18`.

Summary To summarise the performance, as the number of agents vary for each gap, we show once again in the figures below the losses of the trained models. In case of an `avg_gap` of 8cm, the model trained using a minor number of agents, as expected has a lower loss, following, with very similar values the model that employs 8 robots and that with a variable number of agents. Finally, by choosing a variable gap and number of agents the performance are better than those generated with fixed but high number of robots. While again, the results obtained using fewer agents are the best.

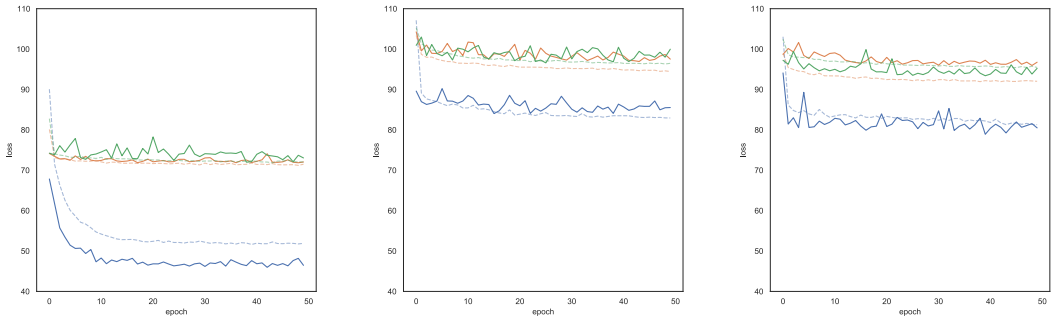

(a) `avg_gap` of 8cm. **(b)** `avg_gap` of 20cm. **(c)** `avg_gap` variable.

Figure 5.49. Comparison of the losses by varying the input of the networks for different gaps.

5.1.1.3 Experiment 3: increasing number of agents

Multi-agent systems present interesting scalability challenges. For this reason, the objective of the last group of experiments is to show the behaviour of a network trained

using `all_sensors` input, variable gaps and number of agents, applied on simulations with a higher number of robots, from 5 up to 50. In Figure 5.50 is visualised, for 5 dif-

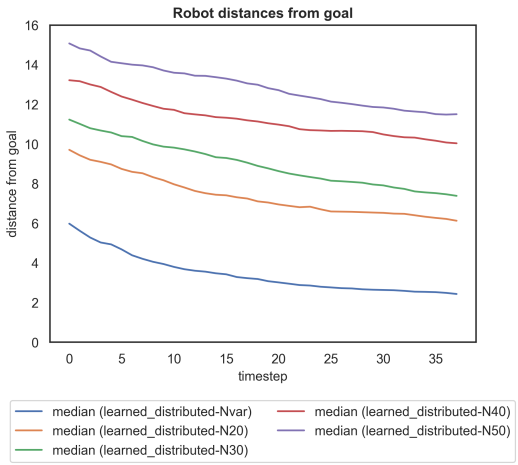

Figure 5.50. Comparison of performance in terms of distances from goal obtained on simulations with an increasing number of robots.

ferent experiments, the absolute distance of each robot from the target over time. This value is averaged on all robots among all the simulation runs. In general, as expected, the complexity grows rapidly as the number of agents increases and it is common for biases to add up and for the error to become more significant. In the experiment performed with a variable number of agents, i.e.,in the range $[5, 10]$, in the final configuration the robots are on average at about 3cm from the goal position. Increasing the number of agents, first to 20, then 30, 40 and finally 50, the robots are more and more distant, in the worst case 13cm from the target.

5.1.1.4 Remarks

In this section, we have shown that using a distributed controller learned by imitating an expert it is possible to obtain results more or less comparable to those reached employing a manual controller. The problem presents interesting scalability challenges, and in general, a greater number of robots implies a slowdown in reaching the correct positions. However, this approach is not enough to achieve satisfactory performance. In the following section we are going to describe a second approach that solve the problem by exploiting a communication protocol between agents.

5.1.2 Distributed approach with communication

5.1.2.1 Experiment 1: fixed number of agents

In this section we explore the same experiments carried out for the distributed approach without communication, addressed in Section 5.1.1.1, paying more attention to the cases with variable gaps and robots.

Model	network_input	input_size	avg_gap
net-c1	prox_values	7	8
net-c2	prox_values	7	13
net-c3	prox_values	7	24
net-c4	prox_comm	7	8
net-c5	prox_comm	7	13
net-c6	prox_comm	7	24
net-c7	all_sensors	14	8
net-c8	all_sensors	14	13
net-c9	all_sensors	14	24

Table 5.3. List of the experiments carried out with 5 agents using communication.

The first analysis, summarised in Table 5.3, concerns the behaviour of the learned controllers in case of the three different inputs, `prox_values`, `prox_comm` or `all_sensors`, for a number of robots N and an `avg_gap` both fixed respectively at 5 and the second chosen between 8, 13 and 24. The performance of these model in terms of train and validation losses are shown in Figure 5.51. It is immediately evident that the trend of the curves are very similar to that obtained with the distributed approach.

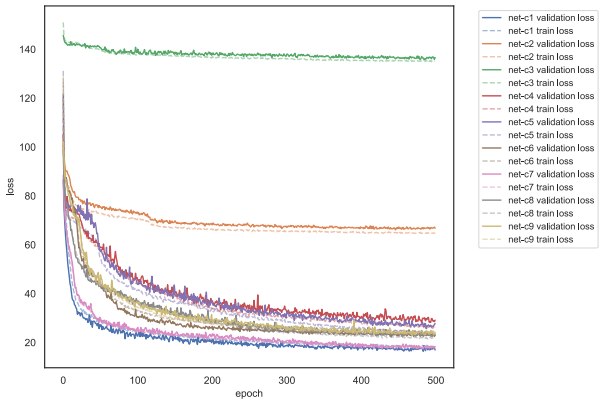

Figure 5.51. Comparison of the losses of the models carried out using a variable number of agents and of average gap.

Results using `prox_values` input We continue by analysing and comparing the performances obtained from these experiments and those in Section 5.1.1.1.

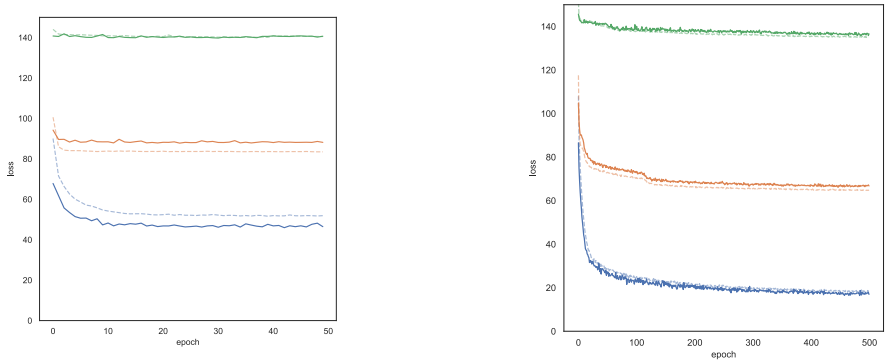

(a) Distributed approach.

(b) Distributed approach with communication.

Figure 5.52. Comparison of the losses of the models that use `prox_values` readings.

In Figure 5.52 is shown an overview of the performance, in terms of loss, of the models trained using `prox_values` and varying the average gap: the blue, orange and green lines represent respectively gaps of 8, 13 and 24cm. The loss in case of the smaller gap is decreased from 40 to 20, meaning an improvement over the previous approach.

Focusing on the models that use the `prox_values` readings as input and the dataset generated using 8cm as average gap, in Figure 5.53 we observe the R^2 of the manual and the learned controllers, in both cases, i.e.,with and without communication, on the validation sets. From these figures, as previously mentioned, we expect that the behaviour of the robots using the distributed controller is better than the manual one, even if far from the expert. On the other hand, adding the communication to the model produces an increase in the coefficient R^2 from 0.59 to 0.85, thus promising superior performance and an attitude more similar to that of the omniscient controller.

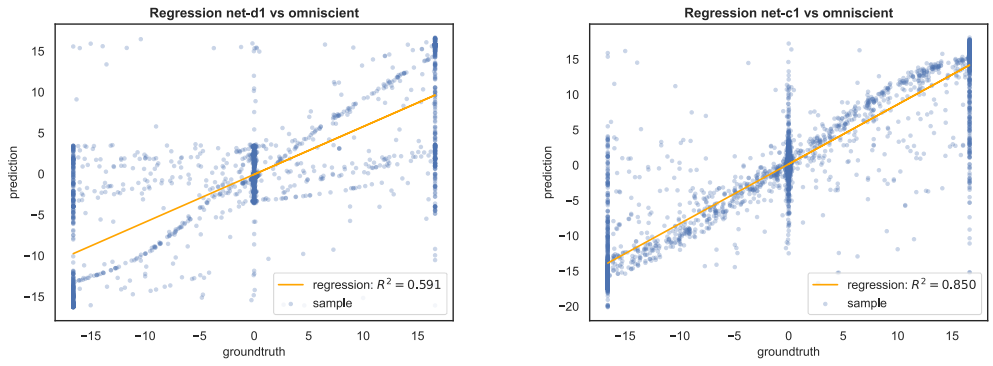

Figure 5.53. Comparison of the R^2 coefficients of the controllers learned from `net-d1` and `net-c1`, with respect to the omniscient one.

In Figure 5.54 are visualised the trajectories of the agents, in a sample simulation, over time. The agents moved using the omniscient controller are those that reach the target faster. Those moved using the manual controller approach the goal position, on average in 10 time steps, but never reach it. The controller learned from `net-d1` in about 25 time steps is able to let the agents arrive in the correct final configuration. Instead, the new controller, learned from `net-c1`, is faster than both the previous and the manual one: in less than 5 time steps the robots reach their goal.

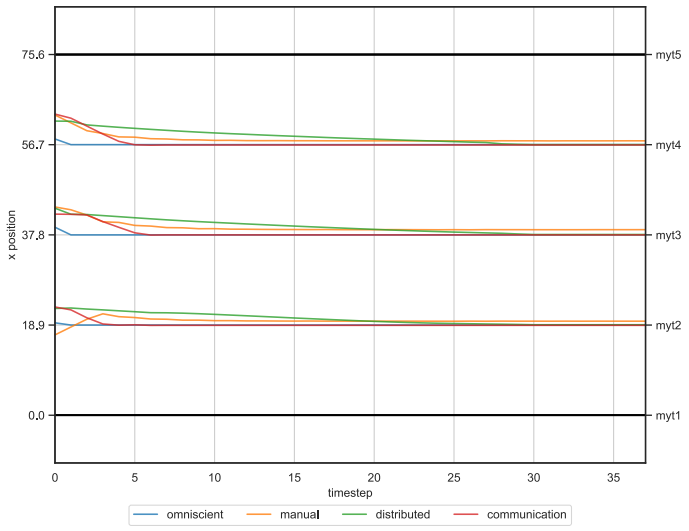

Figure 5.54. Comparison of trajectories, of a single simulation, generated using four controllers: the expert, the manual and the two learned from `net-d1` and `net-c1`.

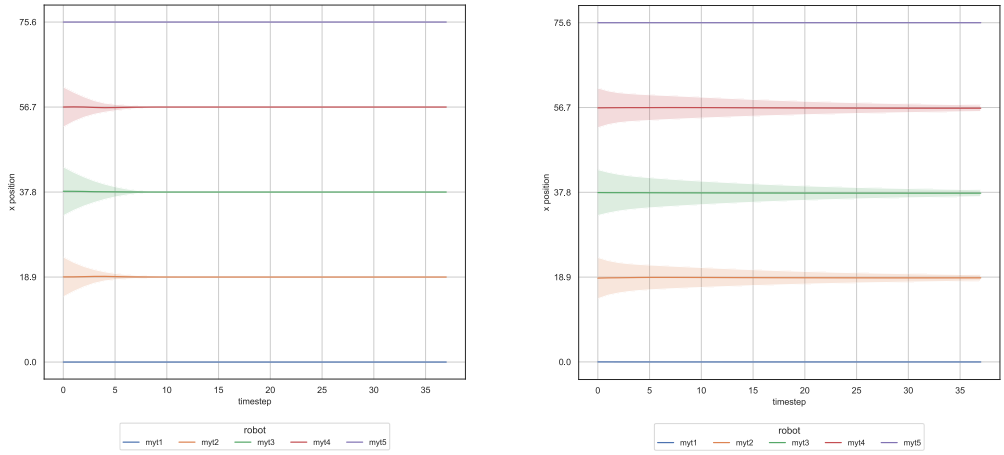

(a) Expert controller trajectories. **(b)** Distributed controller trajectories.

Figure 5.55. Comparison of trajectories, of all the simulation runs, generated using four controllers: the expert, the manual and the two learned from `net-d1` and `net-c1`.

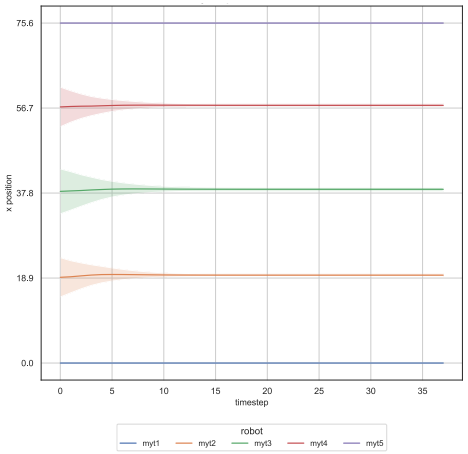

(c) Manual controller trajectories.

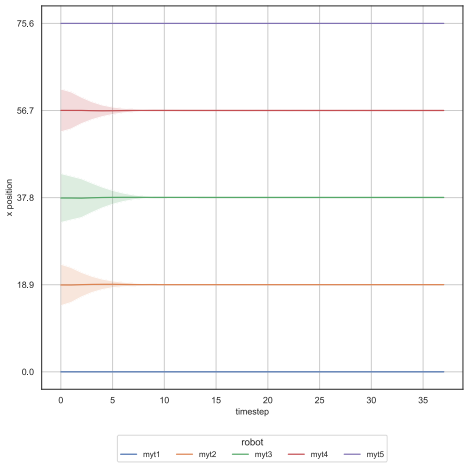

(d) Communication controller trajectories.

Figure 5.55. Comparison of trajectories, of all the simulation runs, generated using four controllers: the expert, the manual and the two learned from `net-d1` and `net-c1` (cont.).

To confirm this improvement, we show in Figure 5.55 the trajectories obtained employing the four controllers. Clearly, the convergence of the robots to the target using the communication is much faster that with the distributed controller alone, but it is even better than the manual, to such an extent that it can be compared to the expert.

Moreover, analysing the evolution of the control over time, in Figure 5.56, we observe that the control learned from the network with communication is much more similar to that decided by the expert. After about 10 time steps both reach the target and set the speed at 0, while the manual and the distributed need more time.

In Figure 5.57 is shown the behaviour, in terms of response of the controllers, of a robot located between other two which are already in the correct position.

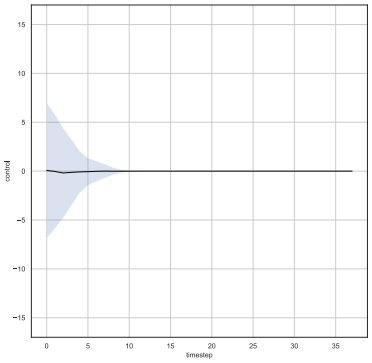

(a) Expert control.

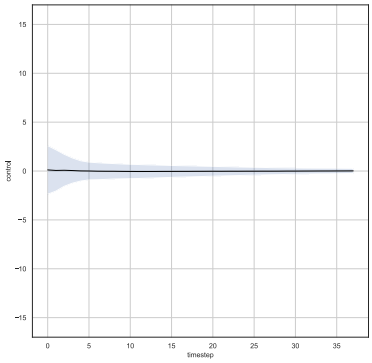

(b) Distributed control.

Figure 5.56. Comparison of output control decided using four controllers: the expert, the manual and the two learned from `net-d1` and `net-c1`.

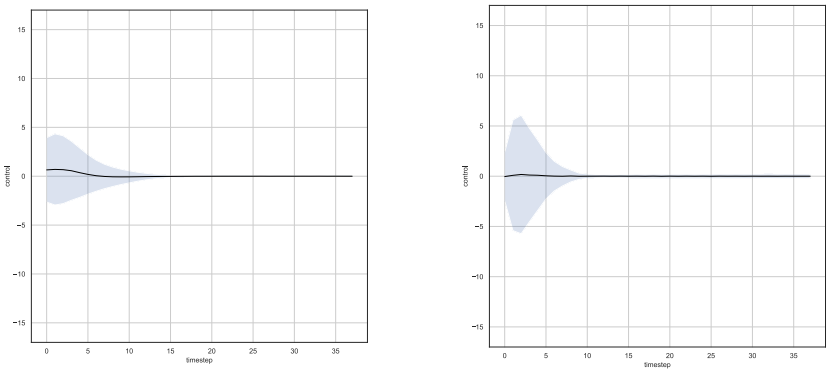

(c) Manual control. **(d)** Communication control.

Figure 5.56. Comparison of output control decided using four controllers: the expert, the manual and the two learned from `net-d1` and `net-c1` (cont.).

on the y-axis, by varying the position of the moving robot, on the x-axis. As expected, the output is a high value, positive or negative when the robot is near to an obstacle on the left or on the right, or close to 0 when the distance is equal on both side. When the moving robot is located halfway between the two stationary agents, the behaviour of the controller with communication is more similar to the one desired.

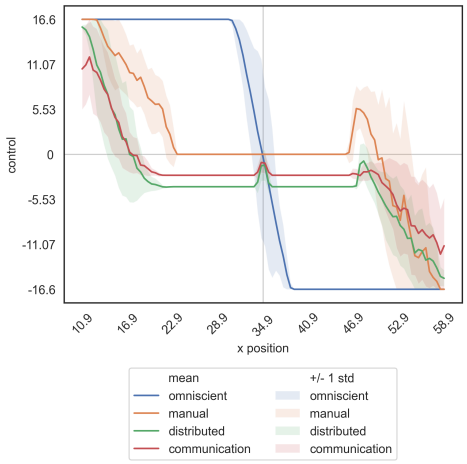

Figure 5.57. Response of `net-c1` by varying the initial position.

Finally, in Figure 5.58 are presented the absolute distances of each robot from the target, visualised on the y-axis, over time. On average, the distance from goal of the communication controller is far better than that obtained with the distributed and the manual. After about 5 time steps, the robots are in the final configuration, while using the distributed alone, 25 time steps are necessary to get closer to the target. Instead, the manual controller does not reach the goal, remaining 1cm away.

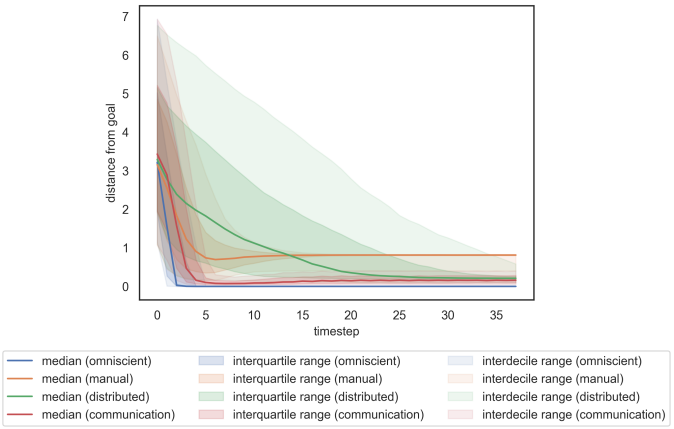

Figure 5.58. Comparison of performance in terms of distances from goal obtained using four controllers: the expert, the manual and the two learned from `net-d1` and `net-c1`.

For this experiment, it seems that the addition of the communication allowed the distributed controller to assume an efficient behaviour, for this reason it is interesting to investigate how this happens since the communication protocol is inferred and learned from the network. Analysing the graph in Figure 5.59, which shows the trajectories of

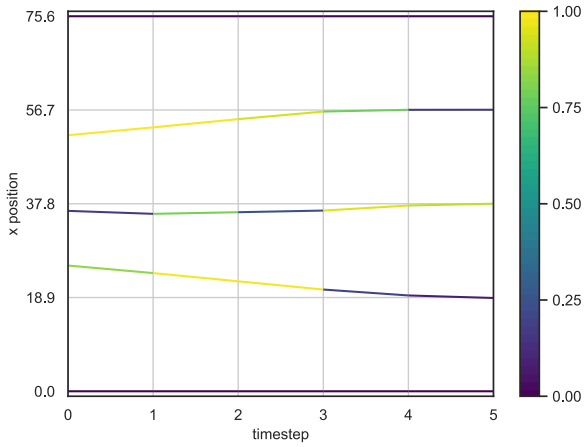

Figure 5.59. Visualisation of the communication values transmitted by each robot over time using the controller learned from `net-c1`.

the agents over time coloured in such a way that the messages transmitted are shown through a colour bar whose spectrum is included in the range $[0, 1]$, i.e., the maximum and minimum value of communication transmitted. We observe that the second and fourth robots in the first time steps transmit values close to one, while the central one transmits a value very close to 0. The agents begin to move towards the desired position and, as they approach the target, the extreme ones transmit decreasing values while the central one transmits a higher value. In this case, 5 time steps are sufficient to reach

the final configuration. It is difficult, however, only from this image to understand the criteria which the network uses to decide the communication. From a further analysis in fact it would seem that the value predicted by the network is not linearly correlated neither to the distance from the goal nor to the speed assumed by the agents.

Results using `prox_comm` input Following are presented the results of the experiments performed using `prox_comm` readings.

In Figure 5.60, are shown the losses by varying the average gap, as before the blue, orange and green lines represent respectively gaps of 8, 13 and 24cm. From a first observation, the network seems to be able to work with all the gaps and the approach with communication demonstrate lower loss values than the previous one.

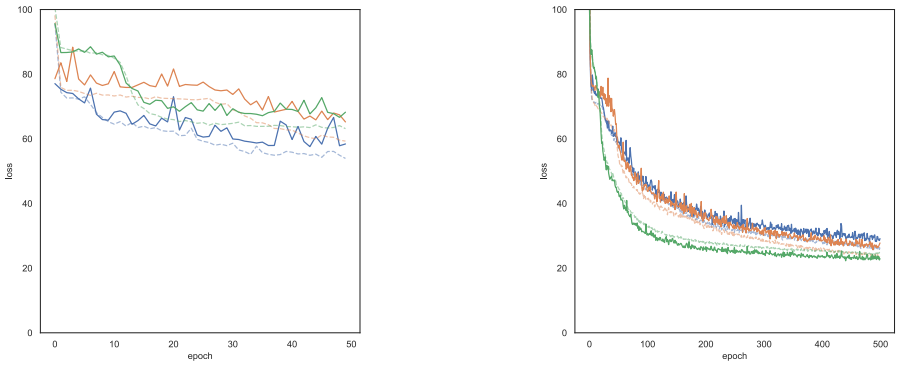

(a) Distributed approach. **(b)** Distributed approach with communication.

Figure 5.60. Comparison of the losses of the models that use `prox_comm` readings.

Focusing on the models trained on the dataset with average gap 24cm, in Figure 5.61 we observe the R^2 of the manual and the learned controllers, both the one with

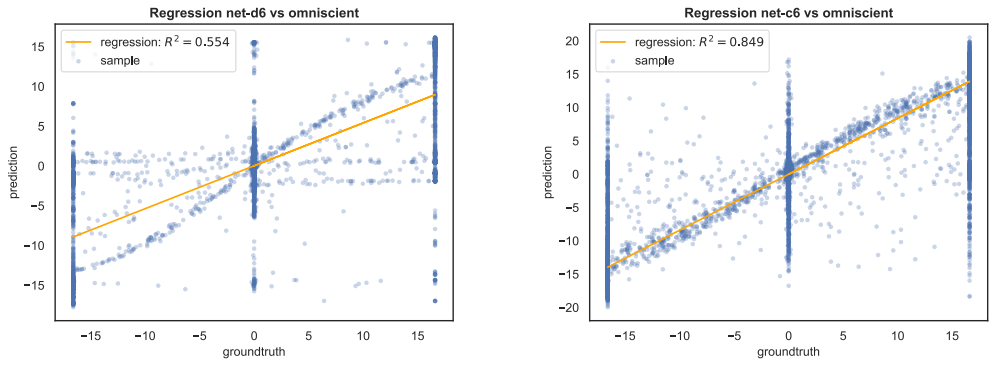

Figure 5.61. Comparison of the R^2 coefficients of the controllers learned from `net-d6` and `net-c6`, with respect to the omniscient one.

and the one without communication, on the validation sets. Once again, we expect better performance using the new approach than the previous, given the fact that the coefficient is increased from 0.55 up to 0.85.

In Figure 5.62 we show a comparison of the trajectories obtained for a sample simulation, using the four controllers. We immediately see that the omniscient controller and the two `net-d6` and `net-c6` are the fastest and allow agents to always reach the target. Instead, those moved using the manual controller did not approach the goal, even if they try to position themselves at equal distances.

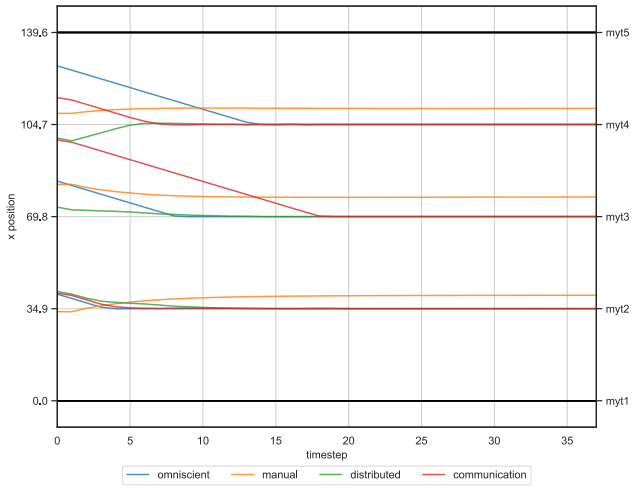

Figure 5.62. Comparison of trajectories, of a single simulation, generated using four controllers: the expert, the manual and the two learned from `net-d6` and `net-c6`.

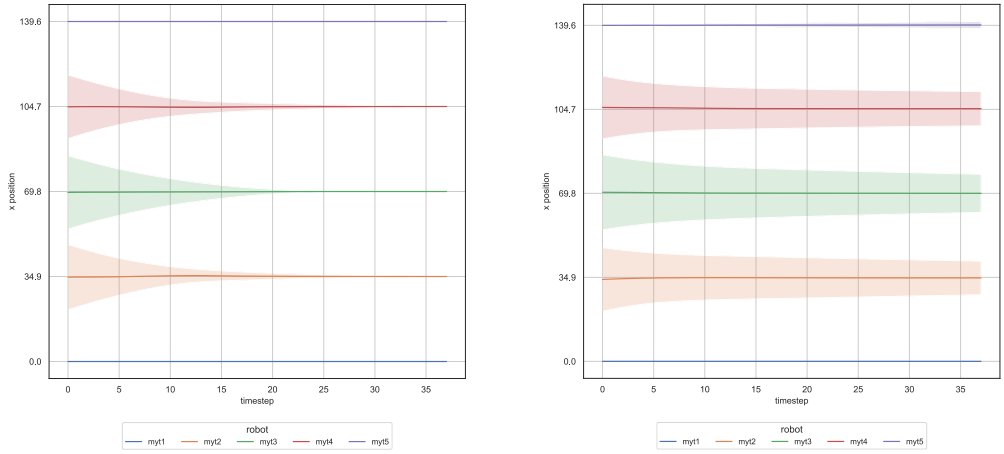

(a) Expert controller trajectories. **(b)** Distributed controller trajectories.

Figure 5.63. Comparison of trajectories, of all the simulation runs, generated using four controllers: the expert, the manual and the two learned from `net-d6` and `net-c6`.

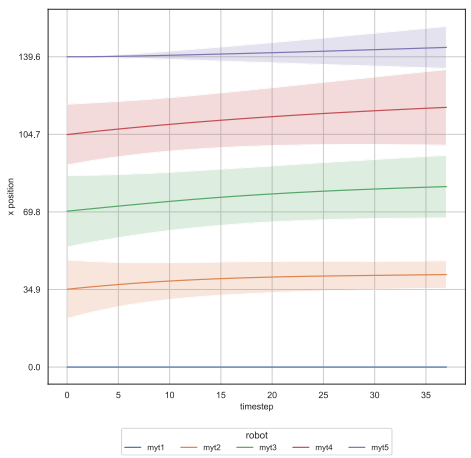

(c) Manual controller trajectories.

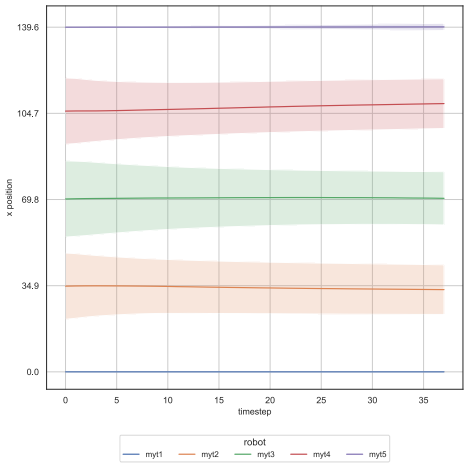

(d) Communication controller trajectories.

Figure 5.63. Comparison of trajectories, of all the simulation runs, generated using four controllers: the expert, the manual and the two learned from `net-d6` and `net-c6` (cont.).

In Figure 5.63 are shown the trajectories obtained employing the four controllers. Even for the expert, the convergence to the target is slower than before, since the distance between the robots is greater, but it is still much faster than with the other two controllers. As we said for Figure 5.13, the manual controller has serious problems in reaching the goal. The two learned controllers can still try to approach the desired position employing more time steps.

In addition, the analysis of the evolution of the control over time in Figure 5.64 suggests that the reason for this behaviour is the fact the both the learned controllers use a lower speed than expected.

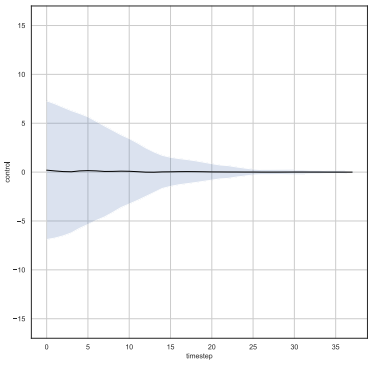

(a) Expert control.

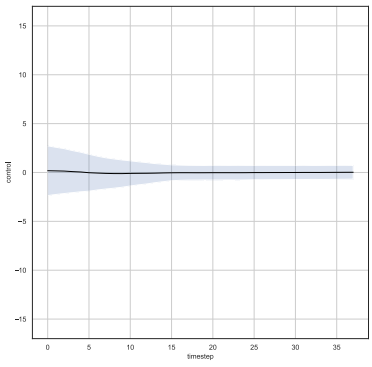

(b) Distributed control.

Figure 5.64. Comparison of output control decided using four controllers: the expert, the manual and the two learned from `net-d6` and `net-c6`.

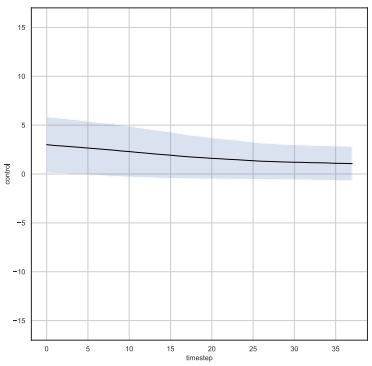

(c) Manual control.

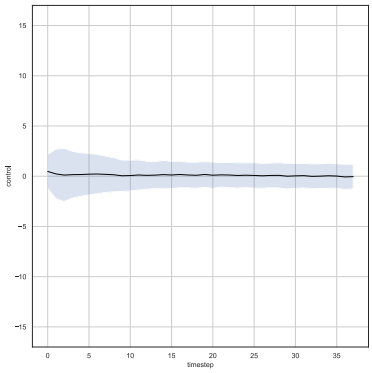

(d) Communication control.

Figure 5.64. Comparison of output control decided using four controllers: the expert, the manual and the two learned from `net-d6` and `net-c6` (cont).

In Figure 5.65 is displayed the behaviour of a robot located between other two stationary agents, showing the response of the controllers, on the y-axis, by varying the position of the moving robot, on the x-axis. As expected, the output is a high positive value when the robot is close to an obstacle on the left, negative when there is an obstacle in front and not behind, and 0 when the distance from right and left is equal.

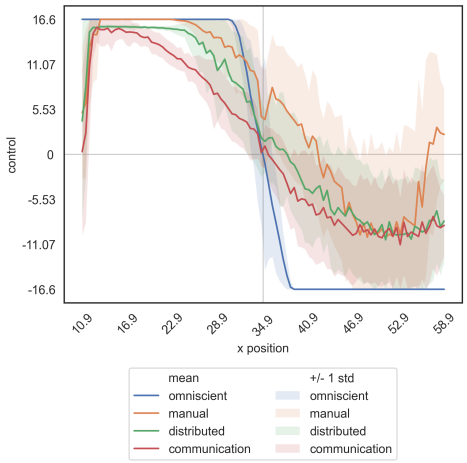

Figure 5.65. Response of `net-c6` by varying the initial position.

The behaviour of the controller that uses the communication is most accurate when the moving robot is halfway between the two stationary.

Finally, in Figure 5.66 is presented a metric that measures the absolute distance of each robot from the target over time. Unlike the non-optimal performances obtained with the manual and distributed controllers, in which in both cases the robots in the

final configuration are located on average at about 5cm from the target, the distance from goal of the communication controller is far better. In just 11 time steps, 4 more than the expert, the agents reach the goal position.

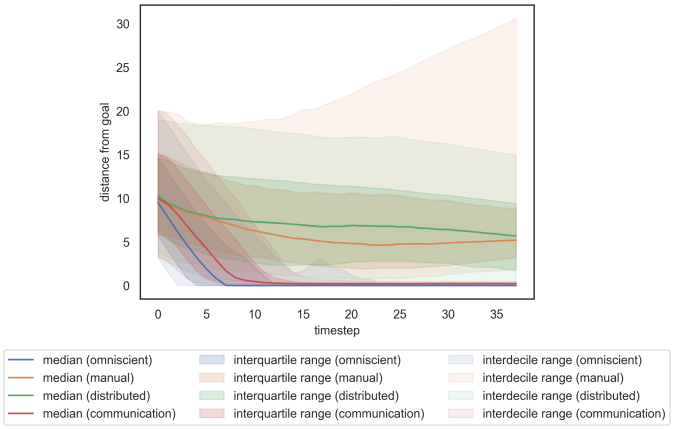

Figure 5.66. Comparison of performance in terms of distances from goal obtained using four controllers: the expert, the manual and the two learned from `net-d6` and `net-c6`.

As before, it is very difficult to analyse the communication transmitted over time through the visualisation in Figure 5.67. In this case, the agents seem to communicate initially a high value, except the central one that is sending values in the range $[0.6, 1]$.

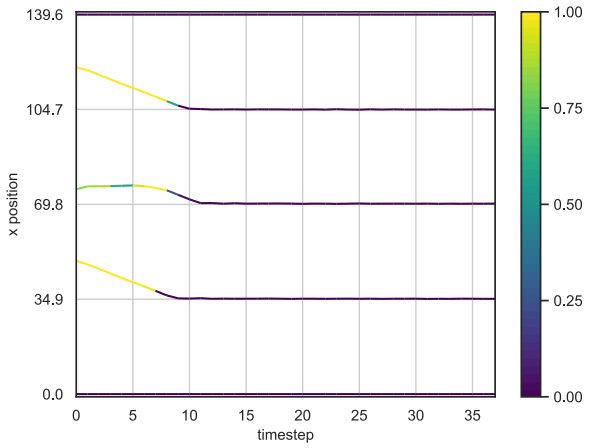

Figure 5.67. Visualisation of the communication values transmitted by each robot over time using the controller learned from `net-c6`.

In all the cases, these values decrease as the robots approach the target position.

Results using `all_sensors` input We conclude the first group of experiments presenting the results obtained using both types of input together from which we expect a more

stable and robust behaviour.

In Figure 5.68 are summarised the performance, in terms of loss, of the models trained using `all_sensors` input and different gaps: the blue, orange and green lines represent respectively average gaps of 8, 13 and 24cm. It is immediately evident that using the new approach the trend of the curves are very similar to each other, and in general the loss is considerably decreased down to 20.

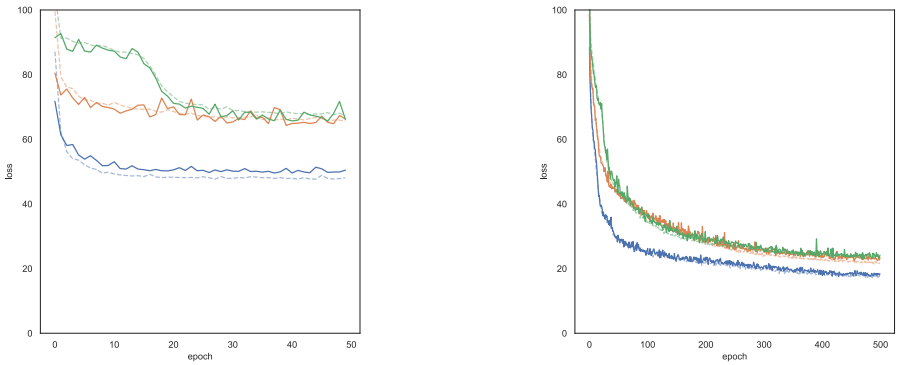

(a) Distributed approach. **(b)** Distributed approach with communication.

Figure 5.68. Comparison of the losses of the models that use `all_sensors` readings.

Considering, as before, the more complex case, for instance the one with the greatest average gap, in Figure 5.69 are visualised the R^2 of the manual and the learned controllers, with and without communication. The superiority of the new approach is once again confirmed by the increase in the coefficient R^2 from 0.56 to 0.84.

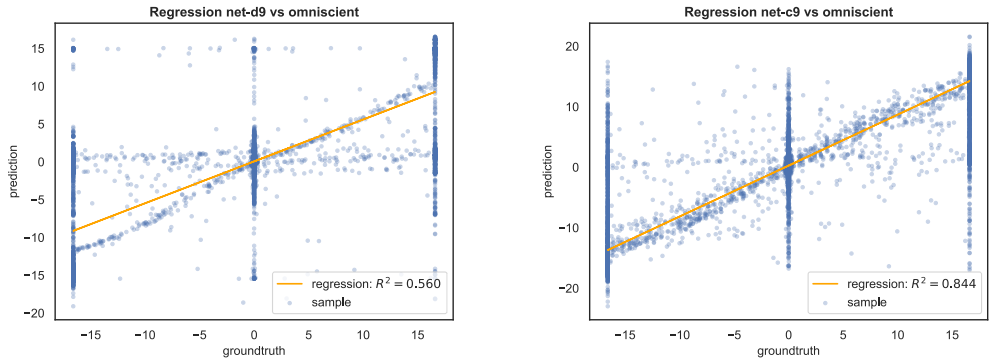

Figure 5.69. Comparison of the R^2 coefficients of the controllers learned from `net-d9` and `net-c9`, with respect to the omniscient one.

In Figure 5.70 is shown a comparison of the trajectories obtained for a sample simulation. As before, the performance obtained using the omniscient and the learned controllers are comparable: they all are very fast and reach the target in less than 10 time steps.

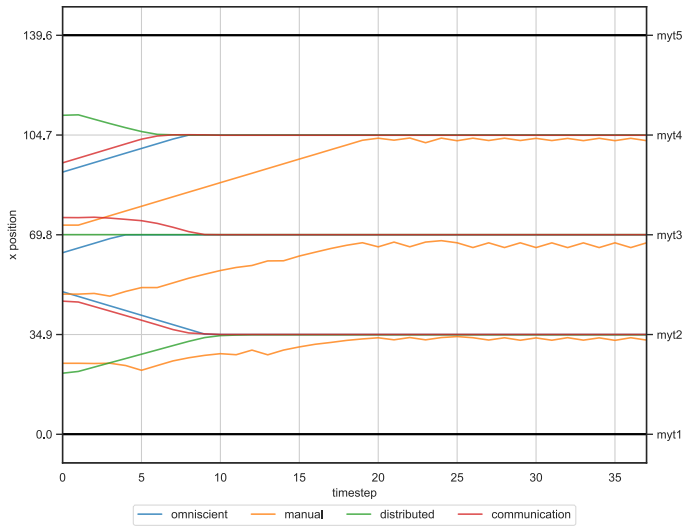

Figure 5.70. Comparison of trajectories, of a single simulation, generated using four controllers: the expert, the manual and the two learned from `net-d9` and `net-c9`.

This improvement is further supported by the trajectories shown in Figure 5.71. The convergence to the target is still slow due to the high distance between the robots, but this time the controller with communication is much faster than the distributed controller but also than the manual. The bands of the deviation show that this approach can reach the same results of the expert.

Moreover, from the evolution of the control over time in Figure 5.72, we observe that the control learned from the communication network is very similar to the expert.

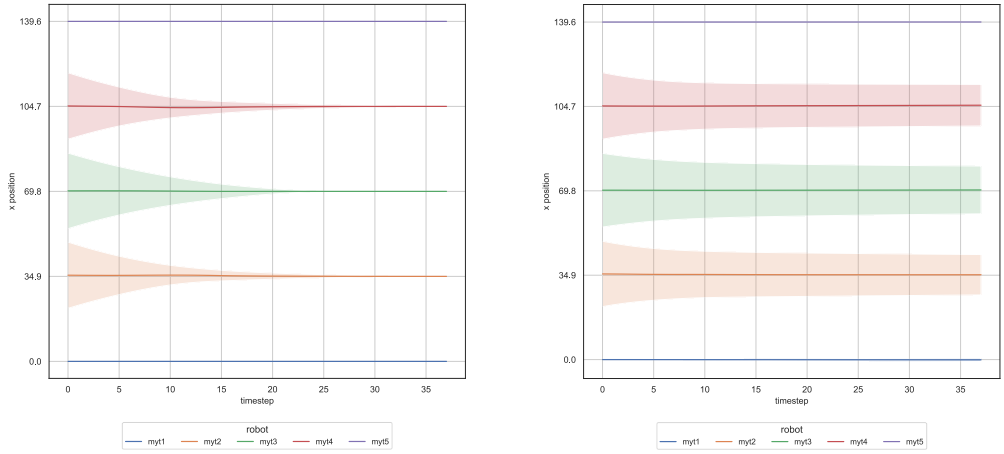

(a) Expert controller trajectories. **(b)** Distributed controller trajectories.

Figure 5.71. Comparison of trajectories, of all the simulation runs, generated using four controllers: the expert, the manual and the two learned from `net-d9` and `net-c9`.

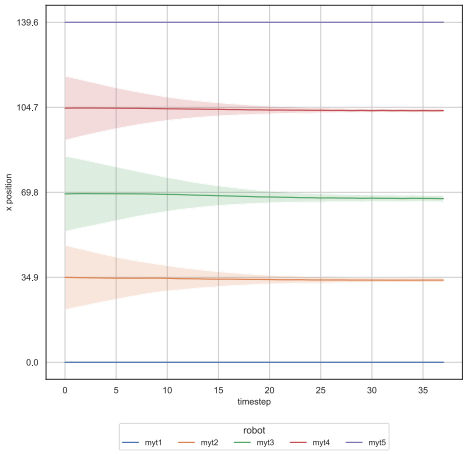

(c) Manual controller trajectories.

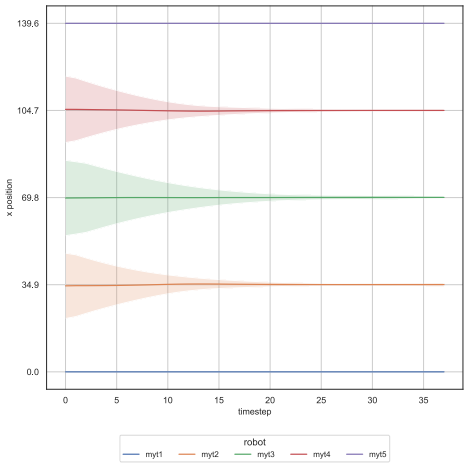

(d) Communication controller trajectories.

Figure 5.71. Comparison of trajectories, of all the simulation runs, generated using four controllers: the expert, the manual and the two learned from `net-d9` and `net-c9` (cont.).

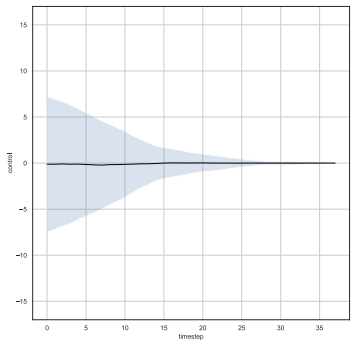

(a) Expert control.

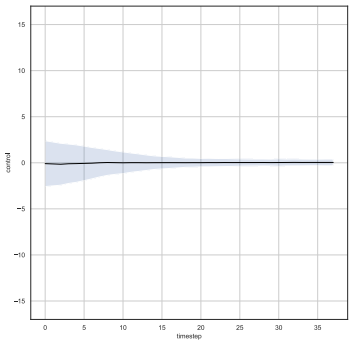

(b) Distributed control.

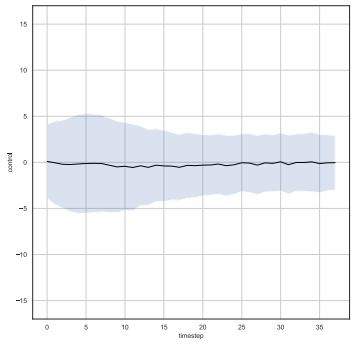

(c) Manual control.

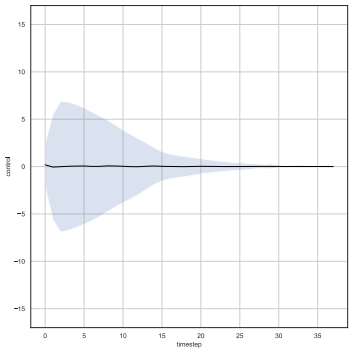

(d) Communication control.

Figure 5.72. Comparison of output control decided using four controllers: the expert, the manual and the two learned from `net-d9` and `net-c9`.

In Figure 5.73 is displayed the behaviour of a robot located between other two stationary agents which are already in the correct position, showing the response of the controllers, on the y-axis, by varying the position of the moving robot, visualised on the x-axis. As expected, the output is a high value, positive or negative respectively when the robot is close to an obstacle on the left or on the right, or it is close to 0 when the distance from right and left is equal.

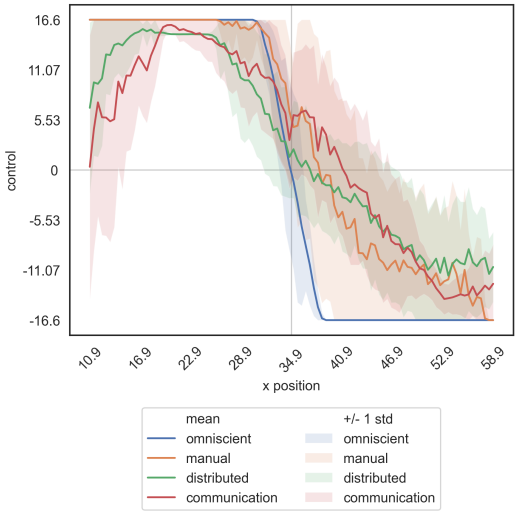

Figure 5.73. Response of `net-c9` by varying the initial position.

Finally, in terms of absolute distance of each robot from the target, in Figure 5.74 we show that exploiting the communication, the robots are able to end up in the correct position by using a couple more time steps than expert does.

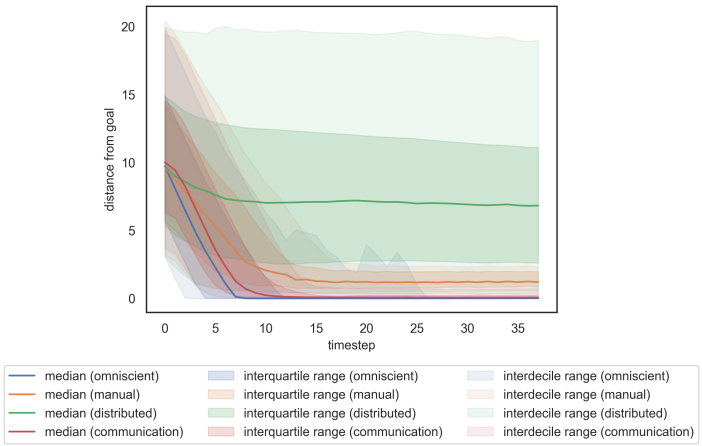

Figure 5.74. Comparison of performance in terms of distances from goal obtained using four controllers: the expert, the manual and the two learned from `net-d9` and `net-c9`.

In this case, the analysis of the communication transmitted over time, in Figure 5.75, contradicts the hypotheses made for the previous experiments. The robots do not decrease or increase the value transmitted by approaching the target, demonstrating, as anticipated that this value is uncorrelated to the distance from goal, reaffirming the difficulty of understanding the protocol learned from the network.

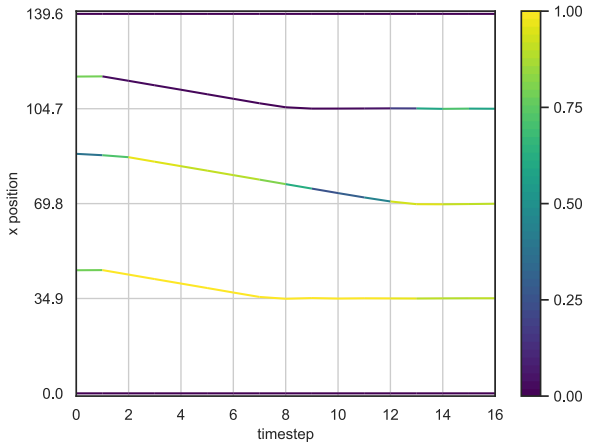

Figure 5.75. Visualisation of the communication values transmitted by each robot over time using the controller learned from `net-c9`.

Summary To sum up, we show in the figures below the losses of the trained models as the different inputs vary for each gap. In all the figures the blue line represents the loss using `prox_values` as input, in orange `prox_comm` and finally in green `all_sensors`. In both approaches, with `avg_gap` of 8cm, the model trained using `prox_values` has a lower loss, followed, with a very close value, by the network that employ `all_sensors`.

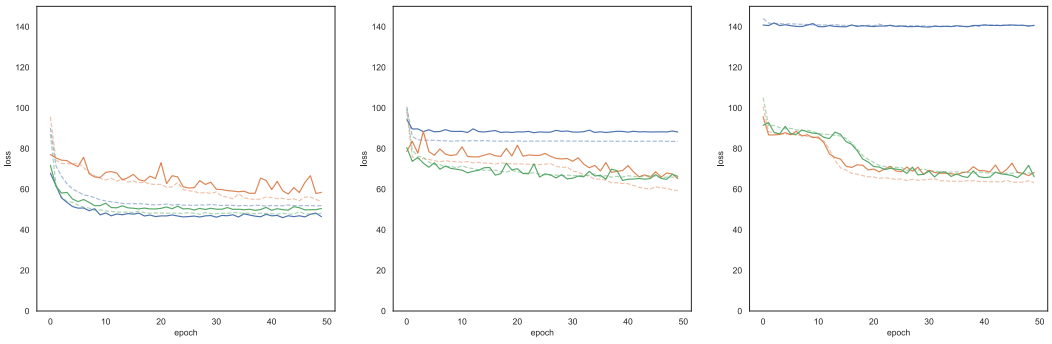

(a) `avg_gap` of 8cm. **(b)** `avg_gap` of 13cm. **(c)** `avg_gap` of 24cm.

Figure 5.76. Comparison of the losses of the model trained without communication, by varying the input of the networks for the three gaps.

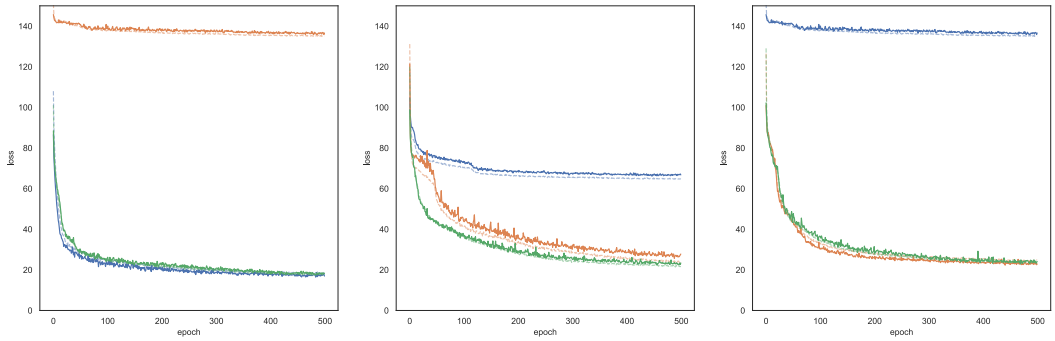

(a) `avg_gap` of 8cm. **(b)** `avg_gap` of 13cm. **(c)** `avg_gap` of 24cm.

Figure 5.77. Comparison of the losses of the model trained with communication, by varying the input of the networks for the three gaps.

Next is the model that works with `prox_comm`, that is not able to work well with small gaps, even when using communication. Similarly, by increasing the gap to 13cm, `prox_values` is not able to achieve satisfactory results in both approaches, while used together with `prox_comm`, `all_sensors` reaches good performances, which can even be improved by using communication. Finally, by increasing the gap even more, up to 24cm, `prox_values` becomes completely unusable, while `prox_comm` and `all_sensors` have excellent responses, in particular with the new approach.

5.1.2.2 Experiment 2: variable number of agents

The second group of experiments we carried out using a distributed approach with communication, summarised in Table 5.4, examines the behaviour of the control learned using `all_sensors` inputs.

Model	network_input	input_size	avg_gap	N
net-c10	all_sensors	14	8	5
net-c11	all_sensors	14	20	5
net-c12	all_sensors	14	variable	5
net-c13	all_sensors	14	8	8
net-c14	all_sensors	14	20	8
net-c15	all_sensors	14	variable	8
net-c16	all_sensors	14	8	variable
net-c17	all_sensors	14	20	variable
net-c18	all_sensors	14	variable	variable

Table 5.4. List of the experiments carried out using a variable number of agents and of gaps.

The objective of this set of experiments is to verify the robustness of the models,

proving that it is possible to train networks that use a variable number of agents.

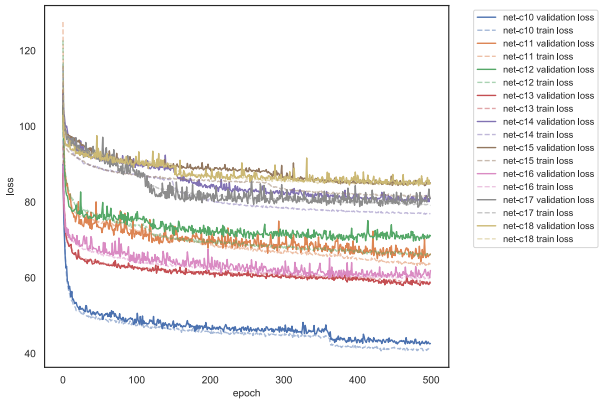

Figure 5.78. Comparison of the losses of the models carried out using a variable number of agents and of average gap.

We analyse the same experiments of the previous approach, presented in Section 5.1.2. We focus our examination by inspecting the behaviour of the network trained on simulations with different number of robots N and variable average gap, i.e `net-c12`, `net-c15` and `net-c18`. Then we compare the performances obtained for these models to the corresponding distributed networks, i.e., `net-d12`, `net-d15` and `net-d18`. In Figure 5.78 os shown an overview of the train and validation losses obtained for these models.

Results using 5 agents Proceeding step by step, we summarise in Figure 5.79 the losses of the experiments carried out using a 5 agents, the same of the first group of experiments presented above, in order to highlight the difference of performance using a gap that is first small, then large and finally variable, respectively represented by the

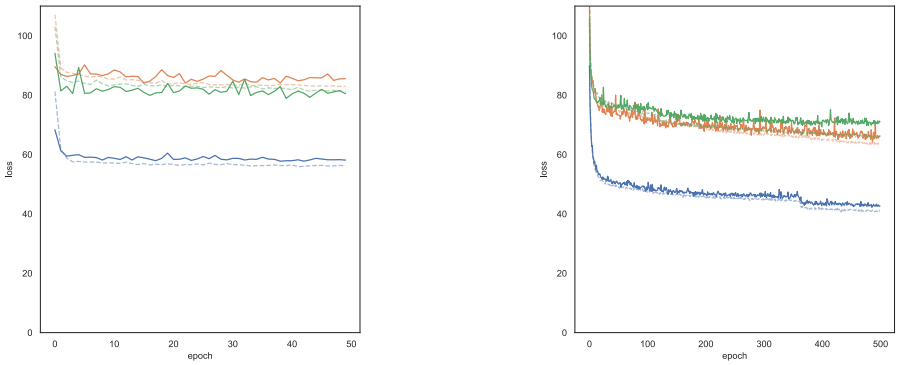

(a) Distributed approach. **(b)** Distributed approach with communication.

Figure 5.79. Comparison of the losses of the models that use 5 agents as the gap varies.

blue, the orange and the green lines. These results are also compared to those obtained without employing the communication. Clearly, in case of small gaps the network performs better. We can also note that in general by enabling the communication, the losses decrease, meaning an improvement over the previous approach.

Considering the model trained using a variable gap, in Figure 5.80 are shown the R^2 coefficients of the manual and the learned controllers, for both approaches. From these we expect that the behaviour of the robots using the learned controller with communication instead of the manual or the distributed alone is better, even if far from the expert. The new model produces an increase in the coefficient from 0.41 to 0.49.

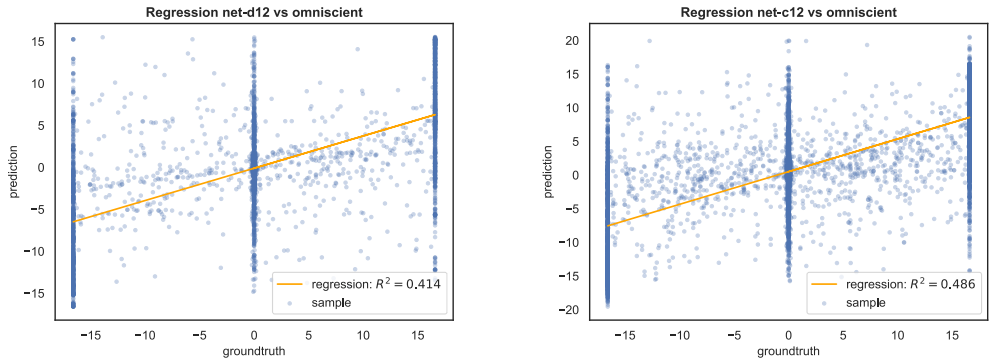

Figure 5.80. Comparison of the R^2 coefficients of the controllers learned from `net-d12` and `net-c12`, with respect to the omniscient one.

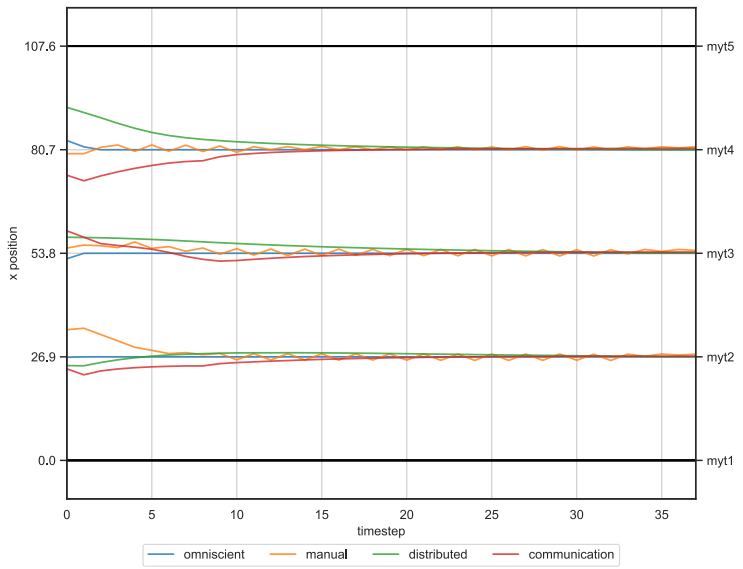

Figure 5.81. Comparison of trajectories, of a single simulation, generated using four controllers: the expert, the manual and the two learned from `net-d12` and `net-c12`.

In Figure 5.81 we first show a sample simulation: on the y-axis are visualised the positions of the agents, while on the x-axis the simulation time steps. The behaviour of the agents moved using the new learned controller seems very similar to that obtained using the distributed one.

Analysing in Figure 5.82 the trajectories obtained employing the four controllers, it is difficult to demonstrate the improvement over the previous approach as having a variable gap we observe a deviation of the position of the robots with respect to the average that in this case it does not indicate a limitation of the model but just that the target positions are different among the simulation runs.

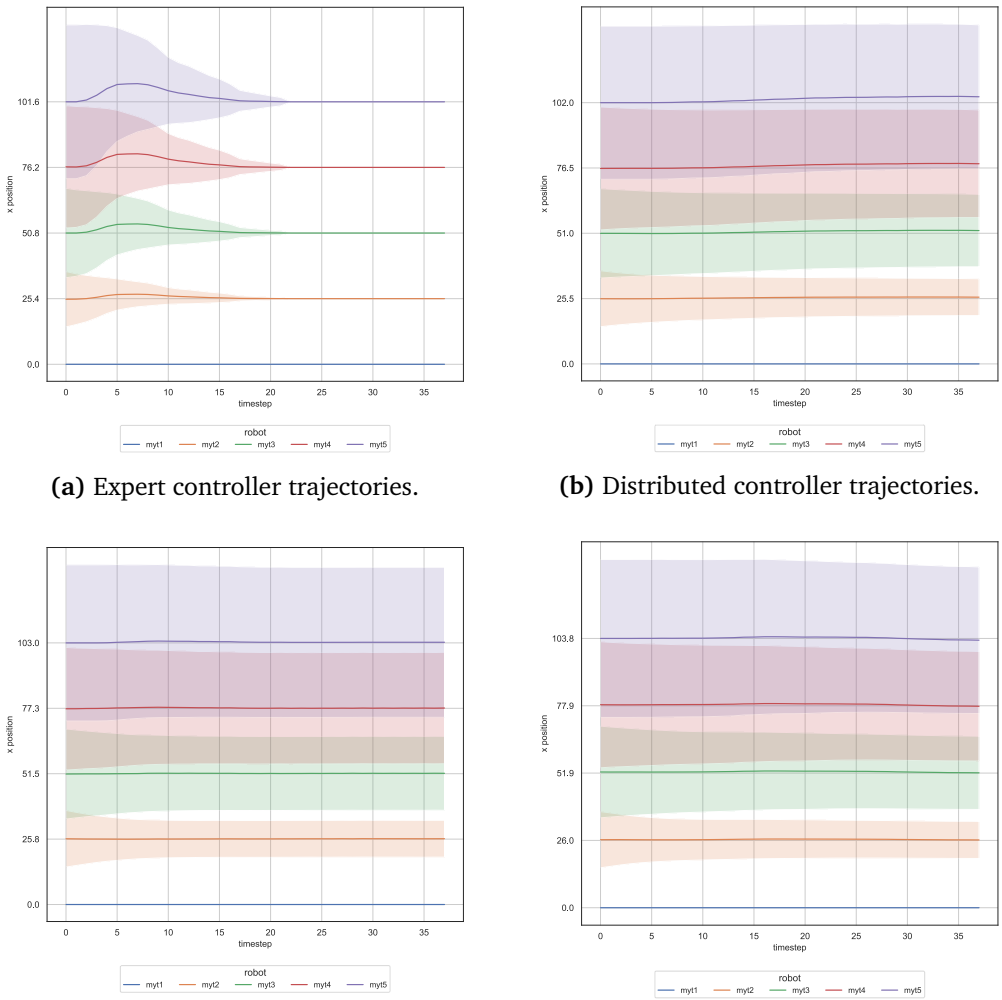

(a) Expert controller trajectories.

(b) Distributed controller trajectories.

(c) Manual controller trajectories.

(d) Communication controller trajectories.

Figure 5.82. Comparison of trajectories, of all the simulation runs, generated using four controllers: the expert, the manual and the two learned from `net-d12` and `net-c12`.

An analysis of the evolution of the control over time in Figure 5.83 evidence that the control decided by the communication network is similar to that set by the expert.

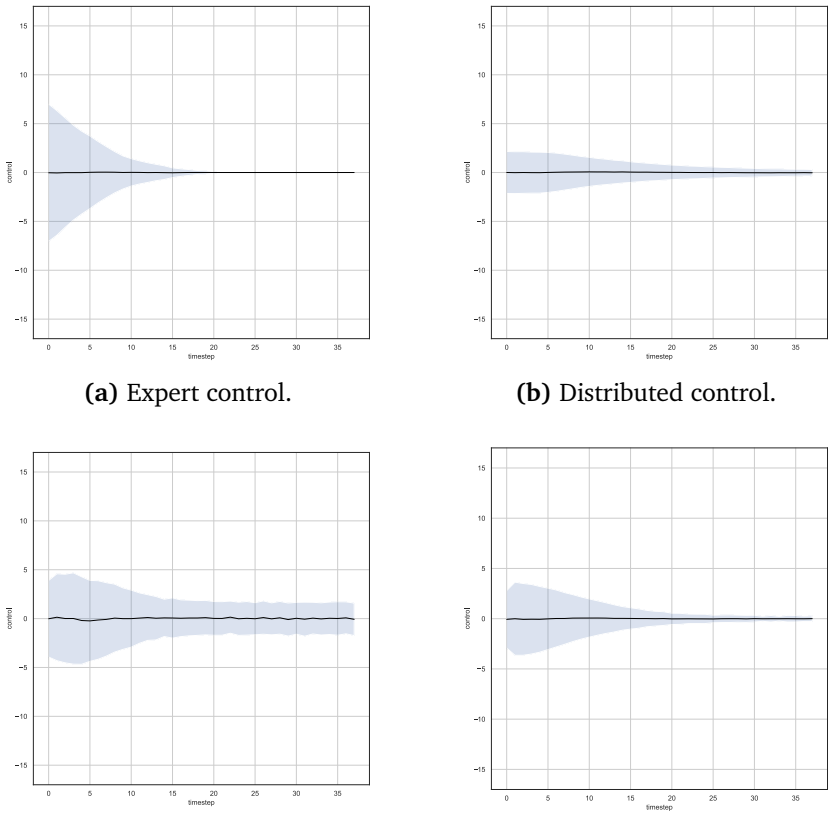

(a) Expert control.

(b) Distributed control.

(c) Manual control.

(d) Communication control.

Figure 5.83. Comparison of output control decided using four controllers: the expert, the manual and the two learned from `net-d12` and `net-c12`.

In Figure 5.84 is displayed the behaviour of a robot located between other two stationary agents which are already in the correct position, showing the response of the controllers, on the y-axis, by varying the position of the moving robot, on the x-axis. As expected, the output is a high positive value when the robot is close to an obstacle on the left, negative when there is an obstacle in front and not behind, and 0 when the distance from right and left is equal. The behaviour of the controller that uses the communication is the most accurate when the moving robot is halfway between the two stationary.

Finally, in Figure 5.85 are presented the absolute distances of each robot from the target, visualised on the y-axis, over time. On average, the distance from goal of the communication controller is a bit better than that obtained with the distributed while similar to the manual, even if slower. In the final configuration in all three cases the agents are 1cm away from the target.

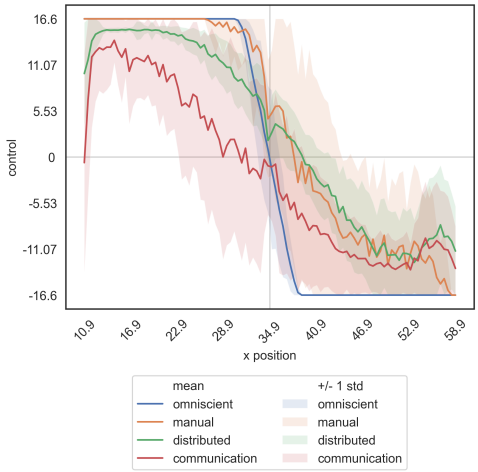

Figure 5.84. Response of `net-c12` by varying the initial position.

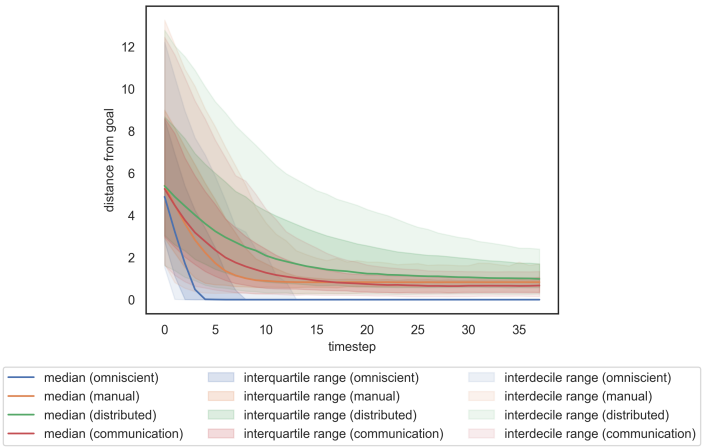

Figure 5.85. Comparison of performance in terms of distances from goal obtained using four controllers: the expert, the manual and the two learned from `net-d12` and `net-c12`.

Results using 8 agents Following are presented the results of the experiments performed using 8 agents. In Figure 5.86, are shown the losses by varying the average gap, as before the blue, orange and green lines represent respectively gaps of 8cm, 20cm and variable. From a first observation we see that the networks perform better in case of small gaps and when using communication.

Focusing on the models that use the dataset generate using a variable average gap, in Figure 5.87 we observe the R^2 of the manual and the learned controllers, both the one with and the one without communication, on the validation sets. Given the fact that the coefficient is increased from 0.23 up to 0.32, we expect superior performance.

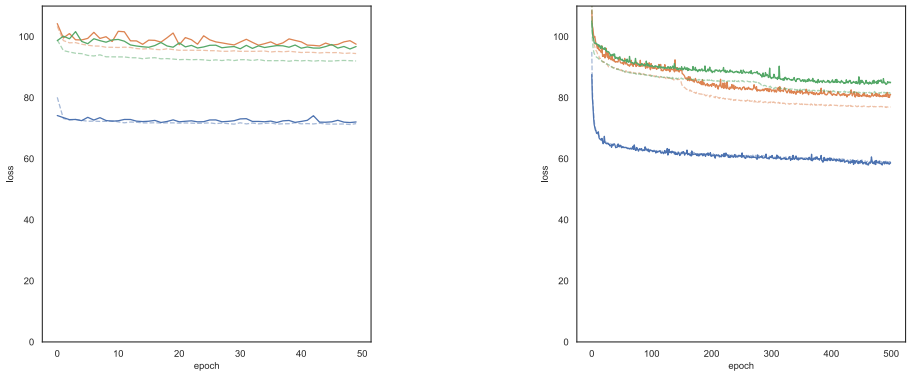

(a) Distributed approach. **(b)** Distributed approach with communication.

Figure 5.86. Comparison of the losses of the models that use 8 agents as the gap varies.

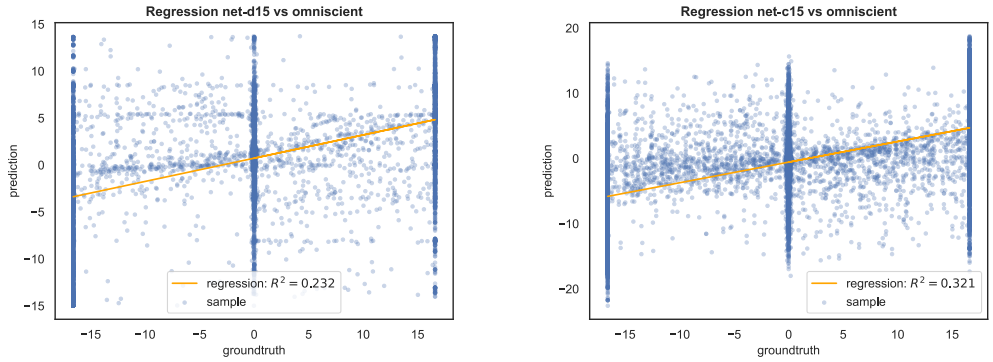

Figure 5.87. Comparison of the R^2 coefficients of the controllers learned from `net-d15` and `net-c15`, with respect to the omniscient one.

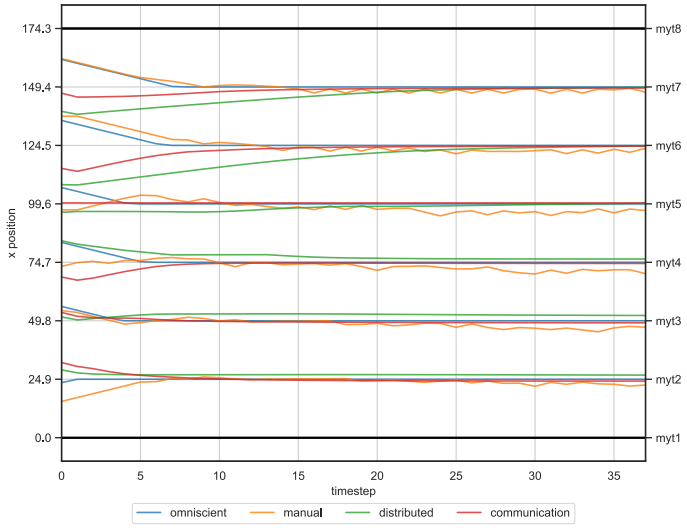

Figure 5.88. Comparison of trajectories, of a single simulation, generated using four controllers: the expert, the manual and the two learned from `net-d15` and `net-c15` .

In Figure 5.88 is visualised a sample simulation that shows on the y-axis position of each agent, while on the x-axis the simulation time steps. The agents moved using the manual controller, when have almost approached the target, they start to oscillate. those that use the distributed controller, even if in the initial configuration are far from the target, they are able to reach the goal. Instead, the communication controller has a more promising behaviour: the convergence is faster than before.

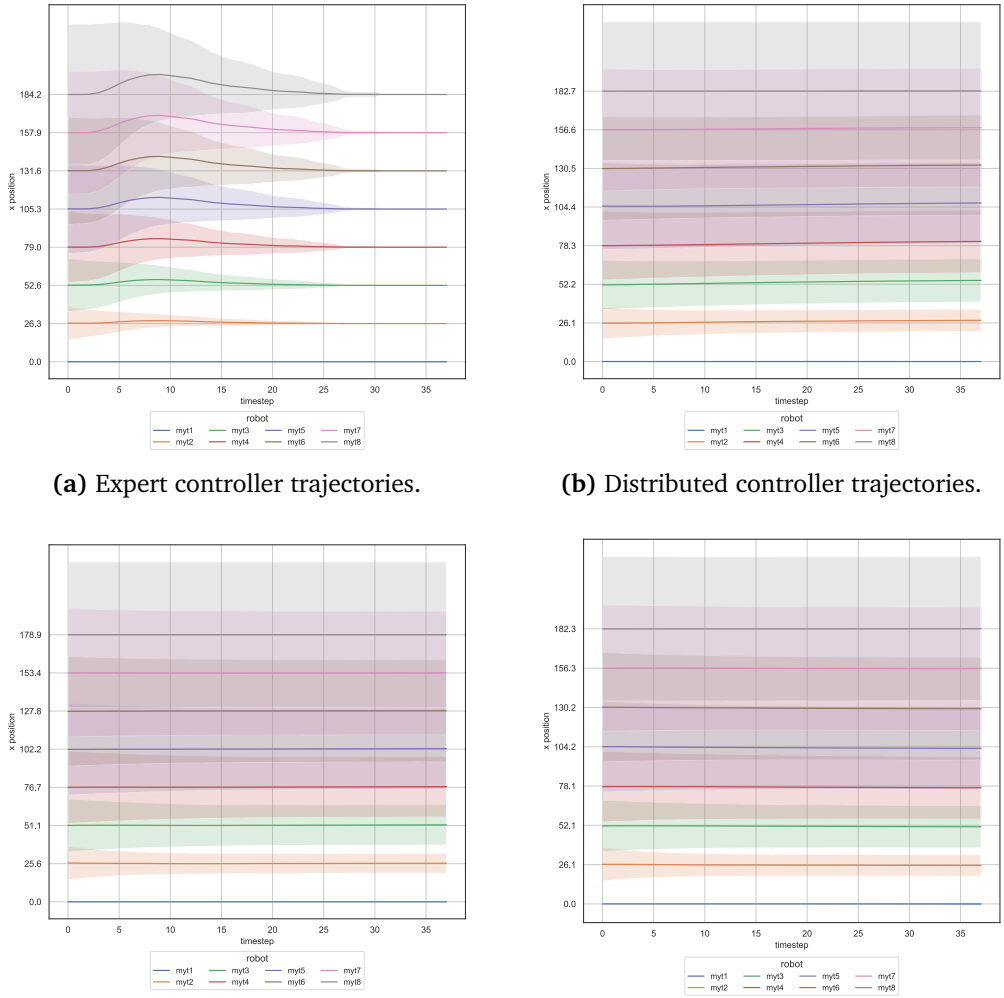

(a) Expert controller trajectories.

(b) Distributed controller trajectories.

(c) Manual controller trajectories.

(d) Communication controller trajectories.

Figure 5.89. Comparison of trajectories, of all the simulation runs, generated using four controllers: the expert, the manual and the two learned from `net-d15` and `net-c15`.

In Figure 5.89 are shown the trajectories obtained employing the four controllers. On average, all the robots seems to approach the desired position, some with less and some with more time steps, but is still difficult to demonstrate improvement over the previous approach due to the deviation in the graph caused by the different target

positions.

Even the analysis of the evolution of the control over time in Figure 5.90 is not able to provide further considerations.

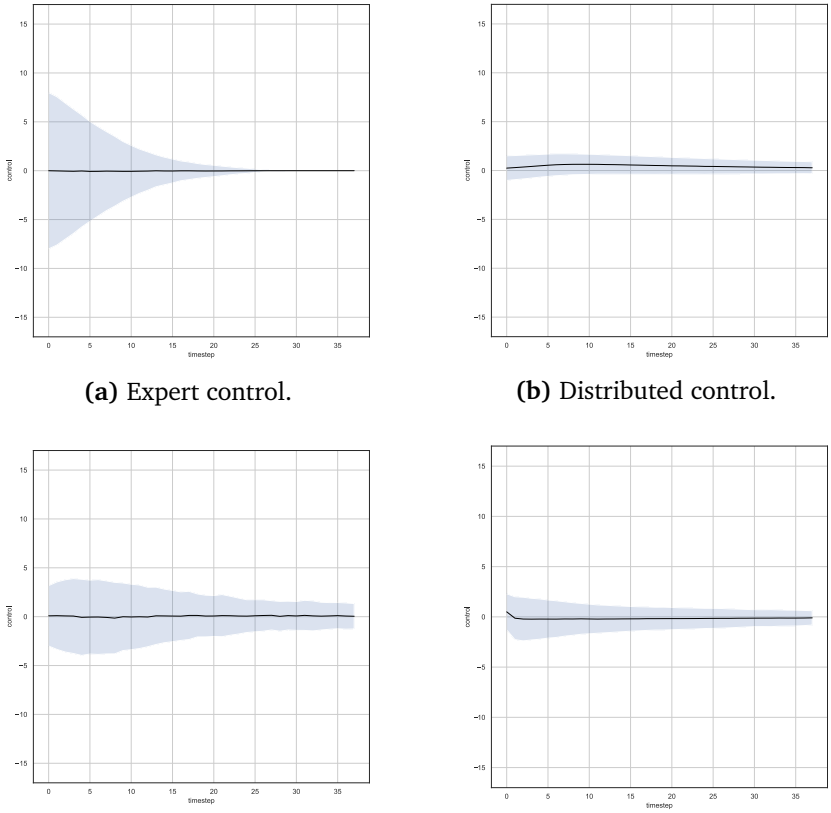

(a) Expert control.

(b) Distributed control.

(c) Manual control.

(d) Communication control.

Figure 5.90. Comparison of the output control decided using four controllers: the expert, the manual and the two learned from `net-d15` and `net-c15`.

In Figure 5.91 is displayed the behaviour of a robot located between other two stationary agents, showing the response of the controllers, on the y-axis, by varying the position of the moving robot, visualised on the x-axis. This time the trend of the curve obtained from the communication controller is different than the desired one.

Finally, in Figure 5.92 is presented a metric that measures the absolute distance of each robot from the target over time. Unlike the non-optimal performance obtained with the distributed controller, in which the robots in the final configuration are located on average at about 5cm from the target, the distance from goal of the communication controller is far better but similar to that obtained with the manual. Even if the new approach need more time to converge, at the end the robots are 2 away from the goal.

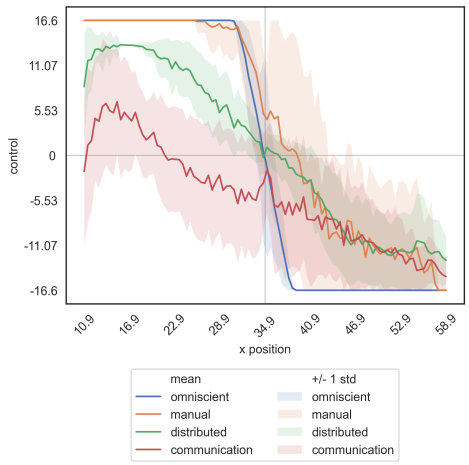

Figure 5.91. Response of `net-c15` by varying the initial position.

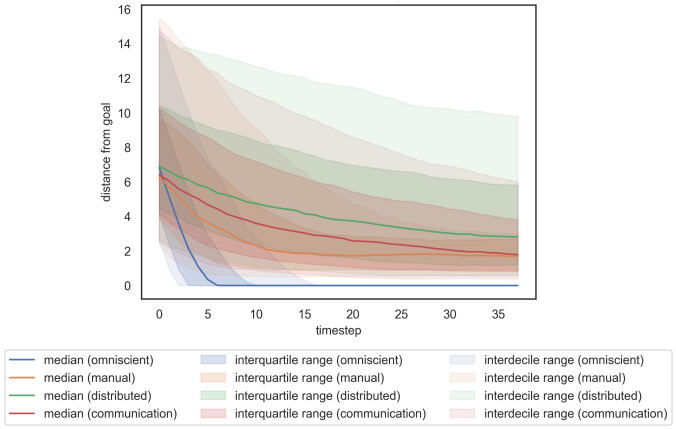

Figure 5.92. Comparison of performance in terms of distances from goal obtained using four controllers: the expert, the manual and the two learned from `net-d15` and `net-c15`.

Results using variable agents We conclude the experiments on task 1 presenting the results obtained using variable number of agents, in particular, in Figure 5.93 are summarised the performance in terms of loss, as before we used blue, orange and green lines to represent respectively average gaps of 8cm, 13cm and variable. Using the new approach we observe from the trend of the curves that in general the losses are decreased and for the network it is easier to perform the task by using a smaller gap.

Considering, as before, the more complex case, for instance the one with variable average gap, in Figure 5.94 are visualised the R^2 of the manual and the learned controllers, with and without communication. A small improvement in the new approach is confirmed by the increase in the coefficient R^2 from 0.23 to 0.30.

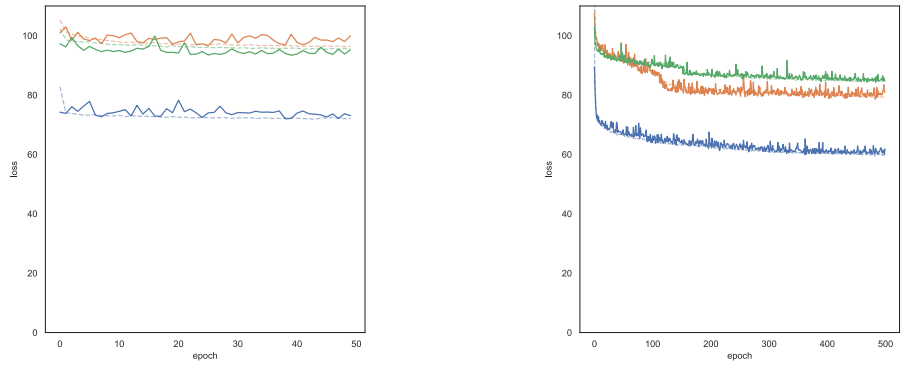

(a) Distributed approach. **(b)** Distributed approach with communication.

Figure 5.93. Comparison of the losses of the models that use variable agents and gaps.

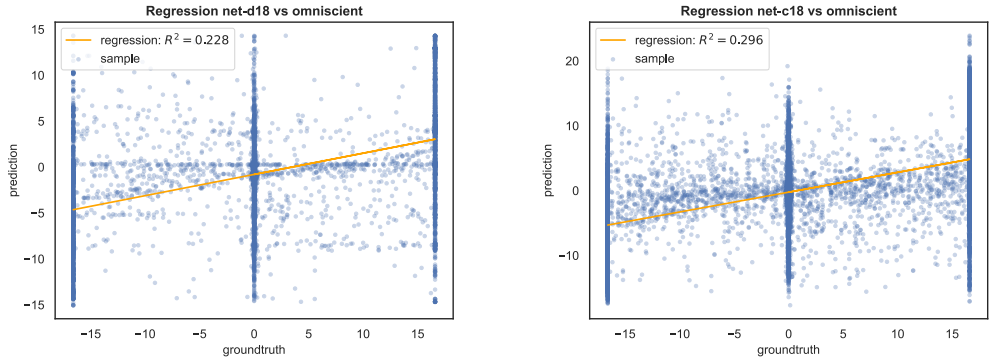

Figure 5.94. Comparison of the R^2 coefficients of the manual and the controllers learned from `net-d18` and `net-c18`, with respect to the omniscient one.

In this experiment is difficult to demonstrate improvement over the previous approach through the trajectories plots, as well as by the evolution of the control, due to the variable average gap. For this reason we show, in Figure 5.95 is shown a comparison of the trajectories obtained for a sample simulation. In this example, the simulation presents 10 agents. They are always able to reach the target when moved using the omniscient controller, this is not always true for others. When they use the manual controller, the same oscillation issue occurs in proximity to the goal. The distributed controller is certainly the slowest, and after 38 time steps not all robots are in the correct position. Instead, adding the communication speeds up the achievement of the goal. In fact, this controller seems to behave in most cases better than the previous two, although with results that are still lower than those obtained by the expert.

We move on analysing in Figure 5.96 the behaviour of a robot located between other two stationary agents which are already in the correct position, showing the response of the controllers by varying the position of the moving robot. As expected, the output

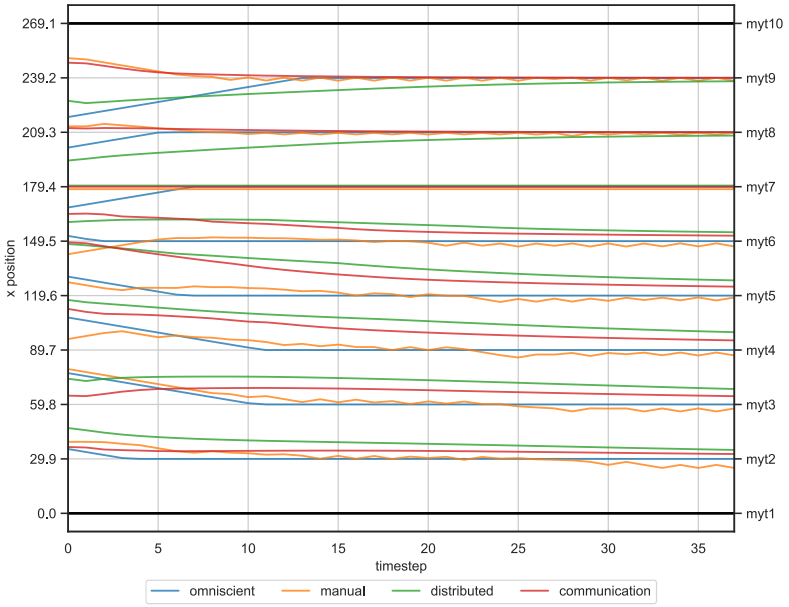

Figure 5.95. Comparison of trajectories, of a single simulation, generated using four controllers: the expert, the manual and the two learned from `net-d18` and `net-c18`.

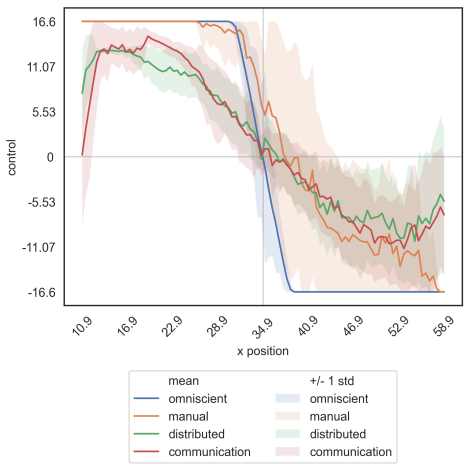

Figure 5.96. Response of `net-c18` by varying the initial position.

is a high value, positive or negative respectively when the robot is close to an obstacle on the left or on the right, or it is close to 0 when the distance from right and left is equal.

Finally, in terms of absolute distance of each robot from the target, in Figure 5.97

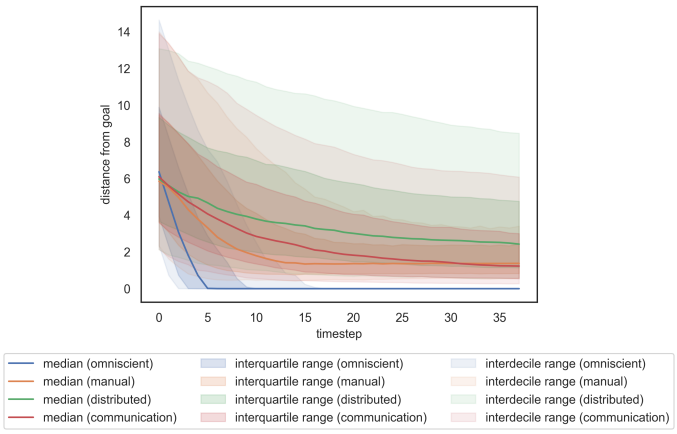

Figure 5.97. Comparison of performance in terms of distances from goal obtained using four controllers: the expert, the manual and the two learned from `net-d18` and `net-c18`.

is shown that, exploiting the communication, the robots in the final configuration are closer to the target than those moved using the distributed or even the manual controller.

Summary To sum up, we finally show in the figures below the losses of the trained models as the number of agents vary for each gap. In all the figures are represented the losses of the models that use 5, 8 and variable agents, respectively in blue, orange and green. In case of an `avg_gap` of 8cm, with or without communication, the model trained using a minor number of agents, as expected, has a lower loss. Instead, very similar are the losses obtained in case of 8 or variable agents, in which the model with less robots is still the better. In general, using the communication has improved the performance.

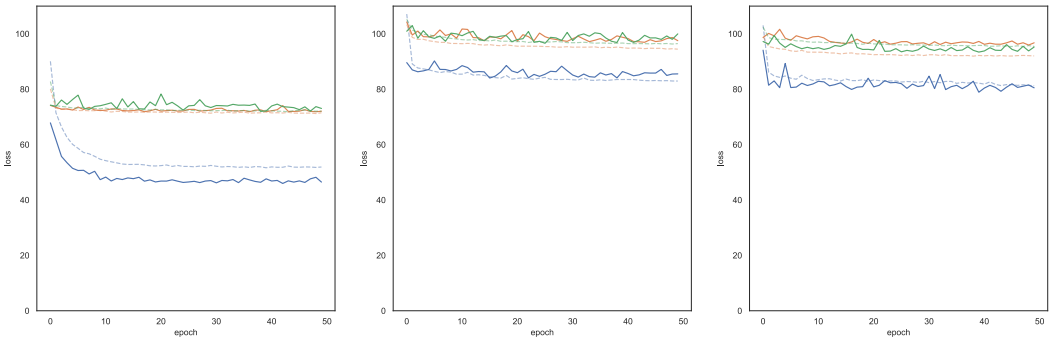

(a) `avg_gap` of 8cm. **(b)** `avg_gap` of 20cm. **(c)** `avg_gap` variable.

Figure 5.98. Comparison of the losses of the model trained without communication, by varying the number of agents for the three gaps.

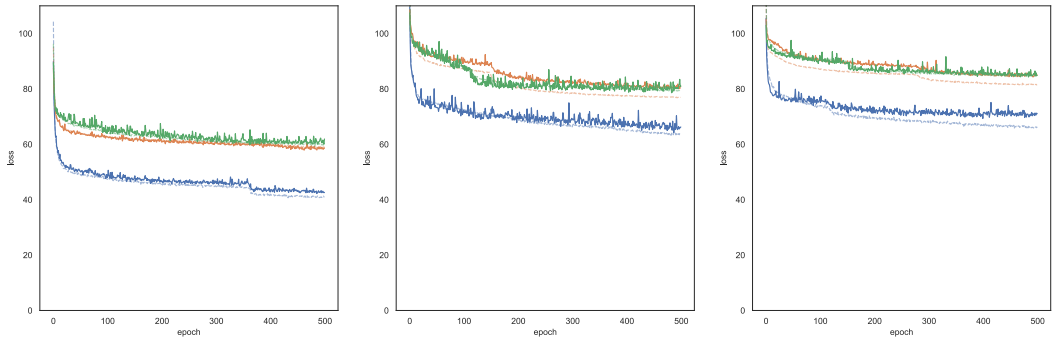

(a) `avg_gap` of 8cm. **(b)** `avg_gap` of 20cm. **(c)** `avg_gap` variable.

Figure 5.99. Comparison of the losses of the model trained with communication, by varying the number of agents for the three gaps.

5.1.2.3 Experiment 3: increasing number of agents

The last group of experiments focuses on the scalability properties of a multi-agent system, showing the behaviour of the network trained using `all_sensors` input, variable gaps and number of agents, applied on simulations with a higher number of robots, from 5 up to 50. In Figure 5.100 is visualised, for 5 different experiments, the absolute

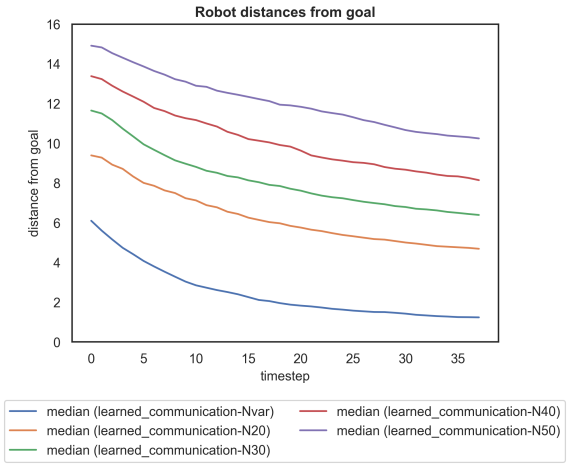

Figure 5.100. Comparison of performance in terms of distances from goal obtained on simulations with an increasing number of robots.

distance of each robot from the target over time. This value is averaged on all robots among all the simulation runs. The results obtained using the communication approach are a bit better then the previous, even if increasing the number of robots still produces a slowdown in reaching the correct positions. In the final configuration, the robots are on average at about 1cm from the from the goal position, instead of 3 as before. In-

creasing the number of agents, first to 20, then 30, 40 and finally 50, the robots are in the worst case 10cm from the target, 3cm closer than without using communication.

5.1.2.4 Remarks

In this section, we have shown that using a distributed controller learned by imitating an expert and exploiting a communication protocol among the agents, it is possible to obtain results more or less comparable to those reached employing an expert controller, albeit a bit worse when using variable number of agents and gaps.

5.2 Task 2: Colouring the robots in space

The second scenario tackles another multi-agent coordination task, assuming that the agents are divided into groups, their purpose is to colour themselves, by turning on their top RGB LED, depending on their group membership. As for the previous task, the problem can be solved performing imitation learning, but the role of communication is fundamental. In fact, what makes the difference are not the distances perceived by the robot sensors but the messages exchanged between the agents, which are they only mean to determine their order. In this scenario, the two "dead" robots play an important role: they always communicate a message that indicates that they are the only two agents that receive communication just from one side.

5.2.1 Distributed approach with communication

5.2.1.1 Experiment 1: variable number of agents

In this section, we explore the experiments carried out using the communication approach, in particular, examining the behaviour of the control learned from 9 networks

Model	avg_gap	N
net-v1	8	5
net-v2	20	5
net-v3	variable	5
net-v4	8	8
net-v5	20	8
net-v6	variable	8
net-v7	8	variable
net-v8	20	variable
net-v9	variable	variable

Table 5.5. List of the experiments carried out using a variable number of agents and of gaps.

based on different simulation runs that use a number of robots N that can be fixed at 5 or 8 for the entire simulation, or even vary in the range $[5, 10]$, and an `avg_gap` that can be a fixed value in all the runs, chosen between 8 or 20, but also vary in the range $[5, 24]$. The objective of this set of experiments, summarised in Table 5.5, is to verify the robustness of the communication protocol and prove also the scalability of the network on the number of agents.

First of all, we show in Figure 5.101 an overview of the train and validation losses obtained for these models.

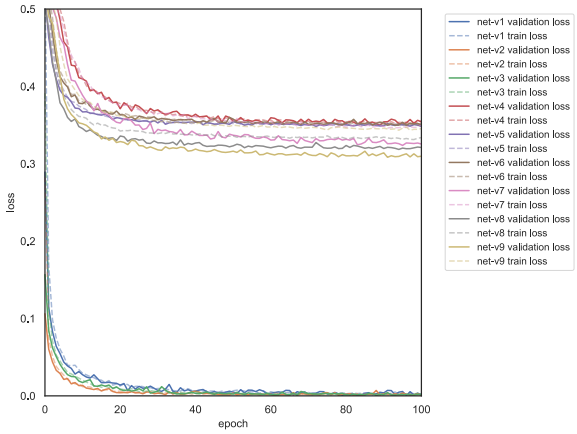

Figure 5.101. Comparison of the losses of the models carried out using a variable number of agents and of average gap.

Results using 5 agents We start our examination by inspecting the behaviour of the network trained on simulations with variable average gap, i.e., `net-v3`, `net-v6` and

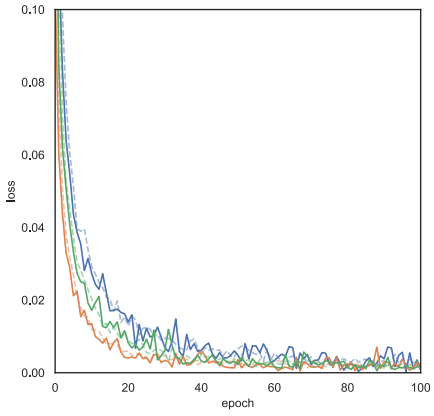

Figure 5.102. Comparison of the losses of the models that use 5 agents as the gap varies.

net-v9, summarising, in Figure 5.102, the losses of these experiments in order to highlight the difference of performance using a gap that is first small, then large and finally variable, respectively represented by the blue, the orange and the green lines. Clearly, in case of small gaps the network performs better, albeit slightly, as the agents are already close to the target.

Then, we move to explore the results of the experiments by showing in Figure 5.103 the ROC curve of the model [Fawcett, 2006], a visualisation of the performance of our classification model, in terms of True Positive Rate (TPR) versus False Positive Rate (FPR), at all classification thresholds. In particular we use the Area Under the ROC Curve (AUC) to evaluate the classifier: by measuring the two-dimensional (2D) area under the ROC curve, from $[0,0]$ to $[1,1]$, the AUC is able to provide an aggregate measure of performance as the discrimination threshold varies. We assume that a model whose predictions are 100% correct has an AUC of 1, as in this case.

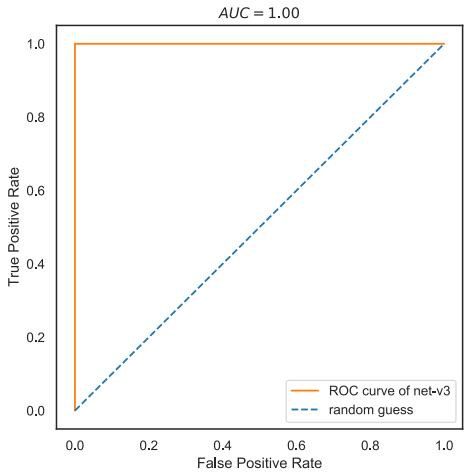

Figure 5.103. Visualisation of the ROC curve of net-v3.

Also for this task, it is interesting to analyse the type of communication protocol inferred by the network, also comparing it with the one implemented by the manual controller. In Figure 5.104 are shown, for a simulation run, first the messages transmitted by the agents over time, through a colour bar whose spectrum is included in the range [0, 1], i.e.,the maximum and minimum value of communication transmitted, and then the colour assumed by the robot in a certain time step, for both the manual and the learned controllers. The extreme robots always transmit the same message using both controllers, while using the learned one, the central robots seems to transmit the same value, i.e.,1, but despite this they are able to achieve their goal in only two time steps, one less than with the manual. This behaviour cannot scale to a number of robot higher then 5. For instance, in case of 5 agents, in the first time step, myt2 and myt4 receive respectively the messages $(0,1)$ and $(1,0)$, so they immediately know

their position with respect to the central robot, which in turn knows its position since it receives $(1, 1)$. Then they communicate their message and in the following time step all the agents have coloured themselves in the right way, achieving the goal. Consequently if the number of robots is greater, the central robots are not able to localise themselves.

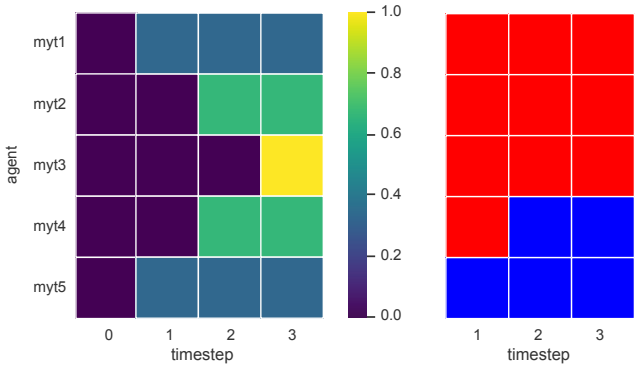

(a) Communication and colour decided using the manual controller.

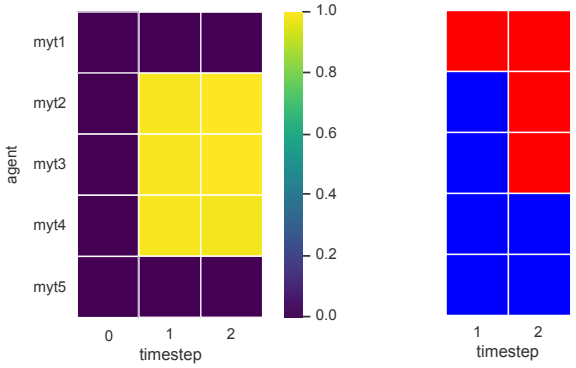

(b) Communication and colour decided using the learned controller.

Figure 5.104. Visualisation of the communication transmitted by each robot over time and the colour decided by the controller learned from `net-v3`.

In Figure 5.105 is presented a useful metric that measures the amount of wrong expected colours, on the y-axis, over time, averaged for all the robots among the simulation runs. In particular, at each time step we count the number of agents that have the wrong colour and divide it by the number of simulations. The mean value is shown as well as the bands representing minus and plus the standard deviation. On average, the amount of correct colours is higher for the manual controller than the learned one.

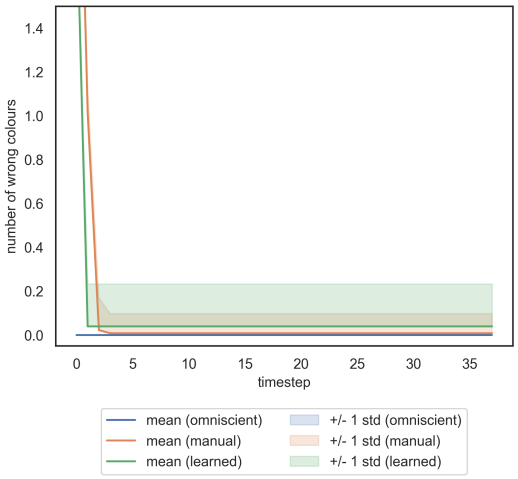

Figure 5.105. Comparison of performance in terms of amount of wrong expected colours obtained using the controller learned from `net-v3`.

Results using 8 agents Following are presented the results of the experiments performed using 8 agents.

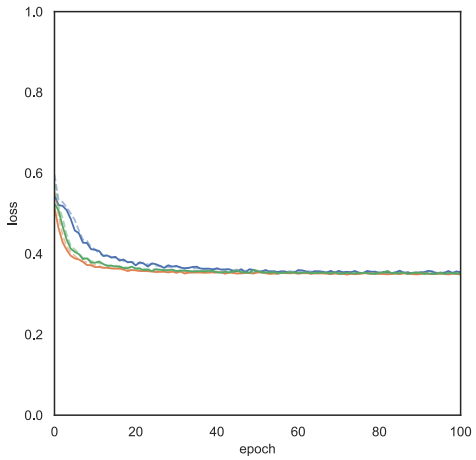

Figure 5.106. Comparison of the losses of the models that use 8 agents as the gap varies.

In Figure 5.106 are summarised the performance in terms of train and validation losses, by varying the average gap, as before the blue, orange and green lines represent respectively gaps of 8cm, 20cm and variable. From a first observation we see that the losses are higher than before, this is because a great number of agents reduce the performance, since more time steps are necessary to achieve the goal.

From the ROC curve of the model in Figure 5.107 we observe that this time the AUC is decreased from 1 to 0.87 with respect to the previous model examined.

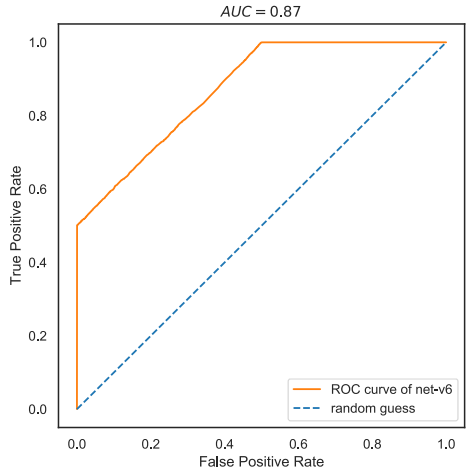

Figure 5.107. Visualisation of the ROC curve of `net-v6` based on BCE Loss.

In Figure 5.108 is presented the measure of the amount of wrong expected colours, on the y-axis, over time, averaged on all robots among all the simulation runs.

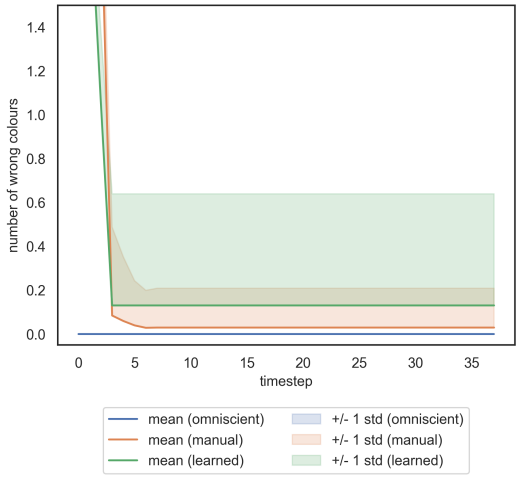

Figure 5.108. Comparison of performance in terms of amount of wrong expected colours obtained using the controller learned from `net-v6`.

As expected, the number of colours correctly predicted by the learned controller is lower than before, while the manual controller still has the same performance.

Finally, we visualise, in Figure 5.109, the communication protocol inferred by the network and the one chosen by the manual controller, as well as the colour assumed by each robot, we immediately see a difference in both the figures. This time it is possible to hypothesize the policy adopted by the network to send messages: as before, the extreme robots always send the same message but this time the central ones

communicate a value interpreted as a reward. In detail, starting from the edges, the value 0 is transmitted, then, once the robot that follows or precedes receives this value in turn communicates 0, until all the agents have received the message and therefore have clear their positional order. This type of reward acts in such a way as to colour as desired the following robot, for those in the first half, or the one that precedes, for those in the second, communicating 0 respectively when there is a red agent behind it or when in front there is a blue one. In this way the control is able to stabilise and achieve its goal.

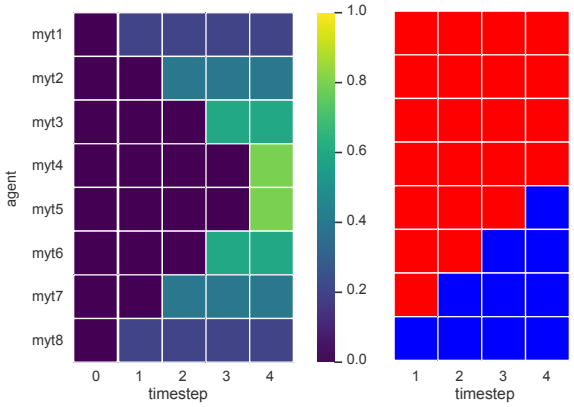

(a) Communication and colour decided using the manual controller.

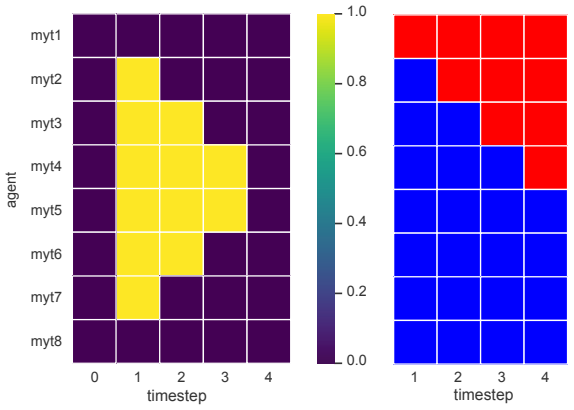

(b) Communication and colour decided using the learned controller.

Figure 5.109. Visualisation of the communication transmitted by each robot over time and the colour decided by the controller learned from `net-v6`.

Results using variable agents We conclude the experiment on this task by presenting the results obtained using variable number of agents. In Figure 5.110 are summarised the performance in terms of loss, as before we used blue, orange and green lines to represent respectively average gaps of 8cm, 13cm and variable. As before we observe that

in general the losses are increased respect the first experiment that use a smaller number of agents, since a higher amount of robots reduce the performance of the models, instead it is decreased respect the last experiment examined.

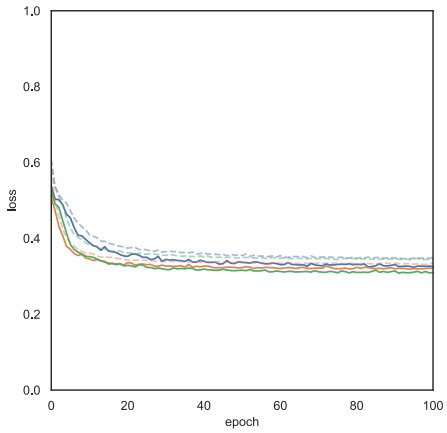

Figure 5.110. Comparison of the losses of the models that use variable agents as the gap varies.

From the ROC curve of the model in Figure 5.111 we observe that this time the AUC is a bit increased respect the previous experiment, going from 0.87 up to 0.89, but still worse than the first one.

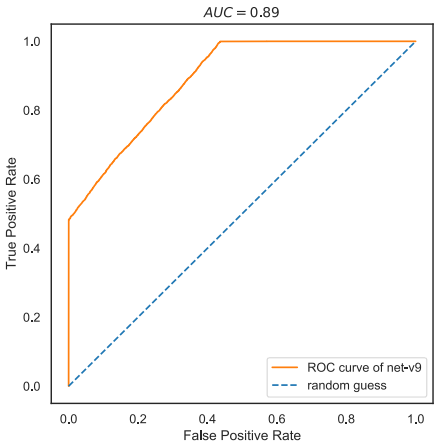

Figure 5.111. Visualisation of the ROC curve of `net-v9`.

This time we visualise in Figures 5.112 and 5.113 two examples of communication protocol inferred by the network and the one chosen by the manual controller, as well as the colour assumed by each robot. The first visualisation is obtained from a simulation with 10 agents. As before, the policy adopted by the network to send messages is very similar to the previous one. The robots at the edges start to transmit the value 0. Then,

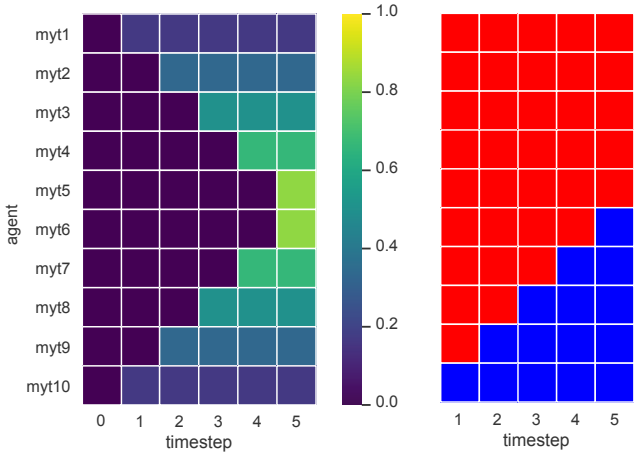

(a) Communication and colour decided using the manual controller.

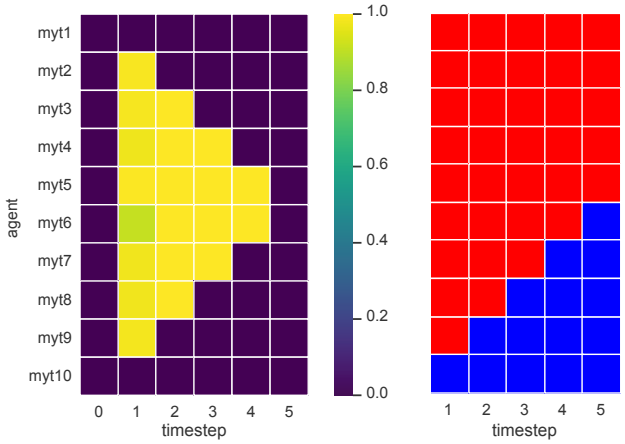

(b) Communication and colour decided using the learned controller.

Figure 5.112. Visualisation of the communication transmitted by each robot over time and the colour decided by the controller learned from `net-v9`.

once the next robots receive the message in turn they communicates 0 or a value very close to it, until all the agents have received and sent the the message and have finally clear their positional order. This time the manual and learned controllers achieve the goal in the same number of time steps. The second visualisation is obtained from a simulation with 6 agents. The policy adopted by the network is the same as before, this time is even more efficient than the protocol used from the manual controller. In fact, in 2 time steps, one less then the other controller, the model is able to achieve the goal.

Finally, in Figure 5.114 is presented the measure of the amount of wrong expected colours, on the y-axis, over time, averaged on all robots among all the simulation runs.

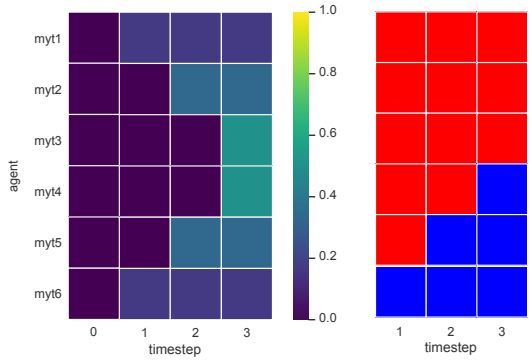

(a) Communication and colour decided using the manual controller.

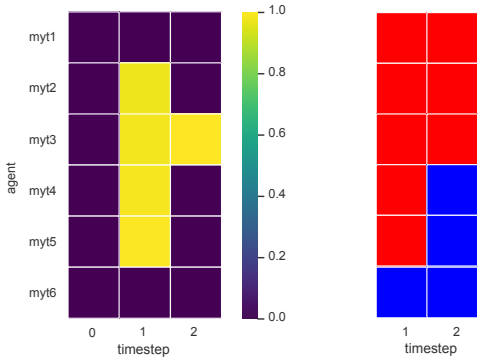

(b) Communication and colour decided using the learned controller.

Figure 5.113. Visualisation of the communication transmitted by each robot over time and the colour decided by the controller learned from `net-v9`.

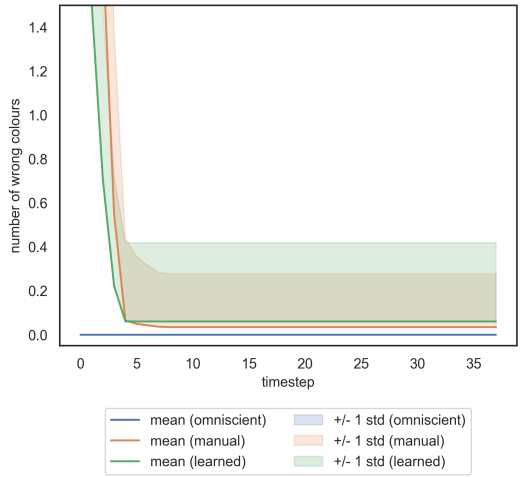

Figure 5.114. Comparison of performance in terms of amount of wrong expected colours obtained using the controller learned from `net-v9`.

for this experiment the number of colours correctly predicted by the learned controller is a bit less than that obtained by the manual controller, and even if the variance for the model is higher the performance are acceptable.

Summary To sum up, we show the losses of the trained models as the number of robots vary for each gap, in particular, in blue, orange and green we refer to the simulation with 5, 8 and variable agents. Unlike the previous task, here no clear differences are highlighted varying the gap. The performance obtained with a smaller number of agents are clearly superior, while the other two, obtained by increasing the amount of robots, are very similar and tend to move away from each other as the gap grows.

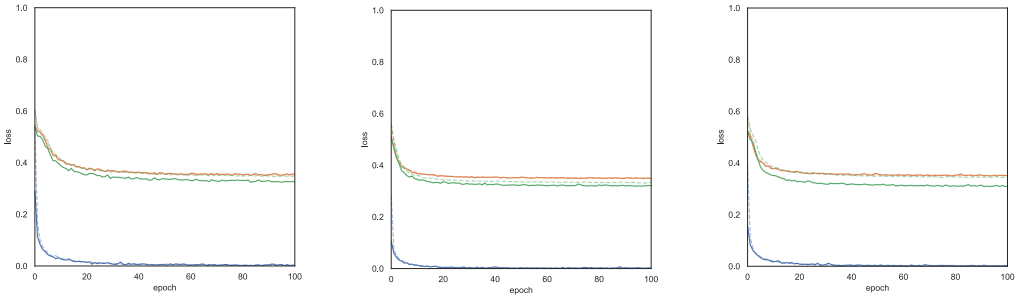

(a) `avg_gap` of 8cm. **(b)** `avg_gap` of 20cm. **(c)** `avg_gap` variable.

Figure 5.115. Comparison of the losses of the model trained with communication, by varying the number of agents for the three gaps.

5.2.1.2 Experiment 2: increasing number of agents

The last group of experiments focuses on the scalability properties of a multi-agent system, showing the behaviour of the network trained using variable gaps and number of agents, applied on simulations with a higher number of robots, from 5 up to 50.

In Figure 5.116 is visualised, for 5 different experiments, the expected percentage of wrong colours over time, averaged for all the robots among the simulation runs. In all experiments, the number of errors in the simulation corresponds to 50%, i.e.,half of the colours are wrong. This results are expected since the colours at the first time step are chosen randomly. As the time steps pass, the number of errors decreases at a constant speed, about two robots per time step. In general, $\frac{N}{2}$ time steps are required to achieve convergence, sometimes $\frac{N}{2} - 1$ when the number of agents is odd. Despite this, when using a number of robots between 5 and 10, on average 1% of the colours are wrong in the final configuration. Increasing the amount of agents this value increases, reaching 10% in the case of 50 robots. Despite this, the performances are very promising and the network is able to scale well by increasing the number of robots.

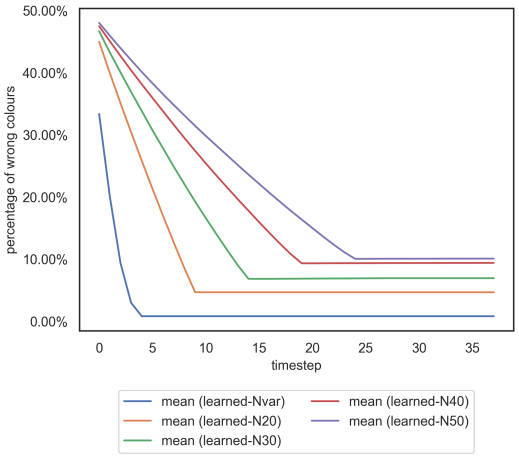

Figure 5.116. Comparison of performance in terms of distances from goal obtained on simulations with an increasing number of robots.

5.2.1.3 Remarks

In this section we have shown that, for some problems, communication is a necessity. Therefore, using a controller learned through imitation learning, which autonomously infers a communication protocol between the agents, it is possible to obtain excellent results and solve the task in many cases more effectively than the baseline. Moreover, the network is able to scale with the increase of the number of robots, without worsening performance.

Conclusion and perspectives

This chapter presents first, in Section 5.3, our concluding thoughts and finally suggestions for possible future research lines in Section 5.4.

5.3 Concluding thoughts

Robotics research has dedicated extensive attention to cooperative multi-agent problems, proposing different approaches that allow the collaboration and communication of swarm of robots to achieve a common goal.

Our work makes a further step in the direction of Imitation Learning (IL) approaches, and aims to find feasible solutions to different multi-agent scenarios.

We explore two alternative tasks: distributing the robots in space such that they stand at equal distance from each other, and, assuming that the agents are divided into two sets, colouring the robots in space depending on their group membership. To solve these examples of cooperative tasks, we propose two main models: both learn decentralised controllers, via observation of the demonstrations of a centralised controller, by training end-to-end Neural Networks (NNs) in which is possible to introduce a communication protocol, is inferred by the network, consisting in an explicit exchange of messages between the robots.

For the first task, we build two models: one that at each time step takes as input an array containing the response values of the sensors for each robot and produces as output the speed of the agent, the other one that as input takes also the messages received in the previous time step, communicated by the nearest agents (on the left and on the right), and produces as output, in addition to the control, the communication, i.e.,the message transmitted by the robot to the two neighbours.

For the second task, we implement a single model, similar to the previous, but this time ignoring the sensors readings. Thus, the network, at each time step, takes as input for each robot only the message received in the previous time step, communicated by the nearest agents, and returns as output an array of 2 floats, the first one is the probability of the agent top LED to be blue and the second is the communication, i.e.,the message to be transmitted by the robot.

Throughout the experiments, in addition to comparing the approach with or with-

out communication, we also analyse the effects of varying the inputs of the networks, the average gap and the number of agents chosen.

First of all, we examine the behaviour of the learned controllers by varying the input of the network — either `prox_values`, `prox_comm` or `all_sensors`. Since at each input corresponds a different range of the proximity sensors, the performance mainly depends on the average gap chosen: for `prox_values` the best results are obtained by using small gaps, less than 12cm, while with `prox_comm` using larger ones. In general, `all_sensors` input is able to work with arbitrary gaps, obtaining more stable behaviours and achieving satisfactory results in both approaches.

We continue analysing the performance by varying the average gap between the agents — either fixed to a certain value or variable in the range $[5, 24]$. Similarly to the previously mentioned experiment, the results are heavily influenced by the input used this time too. Considering `all_sensors` input, the networks have excellent performance with any gap, from a smaller to a larger one, even with a variable one. Unlike in the first task, in the second one, no clear differences emerge varying the gap.

Then, we proceed to compare the behaviour of the models varying the number of agents — either fixed among the simulation runs or variable in the range $[5, 10]$. The main reason of these experiments is to verify the robustness of the models and proving that it is possible to train networks that handle a variable number of agents. The results show, as expected, that in both approaches it is easier to obtain a correct behaviour of the controller using a small number of agents.

Finally, since multi-agent systems present interesting scalability challenges, we focus on the behaviour of a network that takes as input `all_sensors`, variable gaps and number of agents applied on simulations with a higher number of robots, from 5 up to 50. In the first task, a greater number of robots implies a slowdown in reaching the correct positions in both approaches, even when using an expert controller. In fact, the complexity grows rapidly as the number of robots increases and it is common for biases to add up and for the error to become more significant. In the second scenario, regardless the number of agents, the goal is reached at constant speed: in general, $\frac{N}{2}$ time steps, sometimes $\frac{N}{2} - 1$, are necessary to reach the correct final configuration. Therefore the network is able to scale with the increase of the number of robots, without worsening performance.

In conclusion, using a distributed controller learned by imitating an expert, the first task obtains performance more or less comparable to those reached with a manual controller. Instead, applying a communication strategy improves the performance of the distributed model, letting it decide which actions to take almost as precisely and quickly as the expert controller. The second task shows that it is possible to let the network autonomously infer a communication protocol, obtaining excellent results and solving the task more effectively, in many cases, than the baseline.

5.4 Future works

We demonstrated the effectiveness of our method in a couple of simulated scenarios, so a following experiment could be implemented to prove the power of our model in the real world. Another possible expansion of our work could be the application of our models to new problems and scenarios, such as colouring the robots using different criteria and supporting their repositioning in the row. In this study we focus on relatively simple environments, indeed an interesting extension of this approach would be consider more realistic situations, moving to multi-dimensional environments, first 2D and then 3D, working with drones rather than differential drive robots.

Appendix A

List of Acronyms

1D one-dimensional

2D two-dimensional

3D three-dimensional

AI Artificial Intelligence

ANN Artificial Neural Network

AUC Area Under the ROC Curve

BCE Binary Cross Entropy

CE Cross Entropy

DAI Distributed Artificial Intelligence

Dec-POMDP Decentralised partially observable Markov decision process

DL Deep Learning

DNN Deep Neural Network

ECAL Lausanne Arts School

EPFL Swiss Federal Institute of Technology in Lausanne

FPR False Positive Rate

GPU Graphics Processing Unit

GUI Graphical User Interface

ICC Instantaneous Center of Curvature

IL Imitation Learning

IR Infrared

IRL Inverse Reinforcement Learning

LED Light Emitting Diode

MA Multi-Agent

MAL Multi-Agent Learning

MAS Multi-Agent System

ML Machine Learning

MSE Mean Squared Error

NN Neural Network

PID Proportional–Integral–Derivative

R^2 R Squared

RGB Red Green Blue

RL Reinforcement Learning

RNN Recurrent Neural Network

ROC Receiver Operating Characteristic

ROS Robot Operating System

TPR True Positive Rate

Bibliography

Giorgia Adorni. Simulation of robot swarms for learning communication-aware coordination (GitHub repository of the master thesis project: learning-robot-swarm-controllers), 2020a. URL https://github.com/GiorgiaAuroraAdorni/learning-robot-swarm-controllers.

Giorgia Adorni. PyEnki simulation of a multi-agent system in which a manual proportional controller moves the robots such that they stand at equal distances from each other without using communication., 2020b. URL https://www.youtube.com/watch?v=jNkt7xf6pUU.

Javier Alonso-Mora, Eduardo Montijano, Tobias Nägeli, Otmar Hilliges, Mac Schwager, and Daniela Rus. Distributed multi-robot formation control in dynamic environments. *Autonomous Robots*, 43(5):1079–1100, 2019.

Samuel Barrett, Avi Rosenfeld, Sarit Kraus, and Peter Stone. Making friends on the fly: Cooperating with new teammates. *Artificial Intelligence*, 242:132–171, 2017.

Mordechai Ben-Ari and Francesco Mondada. Elements of Robotics, 2018.

Aude Billard, Sylvain Calinon, Ruediger Dillmann, and Stefan Schaal. Survey: Robot programming by demonstration. *Handbook of robotics*, 59(BOOK_CHAP), 2008.

Sylvain Calinon. *Robot programming by demonstration*. EPFL Press, 2009.

Sylvain Calinon and Aude Billard. Learning of gestures by imitation in a humanoid robot. Technical report, Cambridge University Press, 2007.

Gianni Di Caro. Autonomous Swarm/Multi-robot systems and human-in-the-loop, 2006. URL http://www.giannidicaro.com/robotics.html.

Gregory Dudek and Michael Jenkin. *Computational principles of mobile robotics*. Cambridge University Press, 2010.

Tom Fawcett. An introduction to ROC analysis. *Pattern recognition letters*, 27(8):861–874, 2006.

King Sun Fu, Ralph Gonzalez, and CS George Lee. *Robotics: Control, Sensing, Vision, and Intelligence*. Tata McGraw-Hill Education, 1987.

Robin Gasser and Michael N Huhns. *Distributed Artificial Intelligence*, volume 2. Morgan Kaufmann, 2014.

Raúl Gómez. Understanding categorical cross-entropy loss, binary cross-entropy loss, softmax loss, logistic loss, focal loss and all those confusing names. 2018. URL `https://gombru.github.io/2018/05/23/cross_entropy_loss`.

Plerre-P Grassé. La reconstruction du nid et les coordinations interindividuelles chezBellicositermes natalensis etCubitermes sp. la théorie de la stigmergie: Essai d'interprétation du comportement des termites constructeurs. *Insectes sociaux*, 6(1): 41–80, 1959.

Carlos Guestrin, Michail Lagoudakis, and Ronald Parr. Coordinated reinforcement learning. In *ICML*, volume 2, pages 227–234. Citeseer, 2002.

Jérôme Guzzi, Alessandro Giusti, Luca M Gambardella, and Gianni A Di Caro. A model of artificial emotions for behavior-modulation and implicit coordination in multi-robot systems. In *Proceedings of the Genetic and Evolutionary Computation Conference*, pages 21–28, 2018.

Jérôme Guzzi. Thymio II support for Enki simulator, 2020. URL `https://jeguzzi.github.io/enki/intro.html`.

Dylan Hadfield-Menell, Smitha Milli, Pieter Abbeel, Stuart J Russell, and Anca Dragan. Inverse reward design. In *Advances in neural information processing systems*, pages 6765–6774, 2017.

Jun Han and Claudio Moraga. The influence of the sigmoid function parameters on the speed of backpropagation learning. In *International Workshop on Artificial Neural Networks*, pages 195–201. Springer, 1995.

Jonathan Ho and Stefano Ermon. Generative adversarial imitation learning. In *Advances in neural information processing systems*, pages 4565–4573, 2016.

Owen E Holland. Multiagent systems: Lessons from social insects and collective robotics. In *Adaptation, Coevolution and Learning in Multiagent Systems: Papers from the 1996 AAAI Spring Symposium*, pages 57–62, 1996.

Zool Hilmi Ismail and Nohaidda Sariff. A survey and analysis of cooperative multi-agent robot systems: challenges and directions. In *Applications of Mobile Robots*. IntechOpen, 2018.

D Ya Ivanov. Distribution of roles in groups of robots with limited communications based on the swarm interaction. *Procedia Computer Science*, 150:518–523, 2019.

Arthur Juliani. ML-Agents Toolkit v0.3 Beta released: Imitation Learning, feedback-driven features, and more., 2018. URL https://blogs.unity3d.com/2018/03/15/ml-agents-v0-3-beta-released-imitation-learning-feedback-driven-features-and-more/.

Barry L Kalman and Stan C Kwasny. Why tanh: choosing a sigmoidal function. In *[Proceedings 1992] IJCNN International Joint Conference on Neural Networks*, volume 4, pages 578–581. IEEE, 1992.

Diederik P Kingma and Jimmy Ba. Adam: A method for stochastic optimization. *arXiv preprint arXiv:1412.6980*, 2014.

Hoang M Le, Yisong Yue, Peter Carr, and Patrick Lucey. Coordinated multi-agent imitation learning. In *Proceedings of the 34th International Conference on Machine Learning-Volume 70*, pages 1995–2003. JMLR. org, 2017.

Jie Li and Ying Tan. A two-stage imitation learning framework for the multi-target search problem in swarm robotics. *Neurocomputing*, 334:249–264, 2019.

Ilya Loshchilov and Frank Hutter. Decoupled weight decay regularization. *arXiv preprint arXiv:1711.05101*, 2017.

Ryan Lowe, Yi I Wu, Aviv Tamar, Jean Harb, OpenAI Pieter Abbeel, and Igor Mordatch. Multi-agent actor-critic for mixed cooperative-competitive environments. In *Advances in neural information processing systems*, pages 6379–6390, 2017.

Stéphane Magnenat, Philippe Rétornaz, Michael Bonani, Valentin Longchamp, and Francesco Mondada. ASEBA: A modular architecture for event-based control of complex robots. *IEEE/ASME transactions on mechatronics*, 16(2):321–329, 2010.

Stéphane Magnenat. asebaros, 2010. URL https://github.com/ethz-asl/ros-aseba.git.

Stéphane Magnenat et al. Enki: A fast 2D robot simulator, 1999. URL https://github.com/enki-community/enki.

Qi Meng, Wei Chen, Yue Wang, Zhi-Ming Ma, and Tie-Yan Liu. Convergence analysis of distributed stochastic gradient descent with shuffling. *Neurocomputing*, 337:46–57, 2019.

Francesco Mondada, Michael Bonani, Fanny Riedo, Manon Briod, Léa Pereyre, Philippe Rétornaz, and Stéphane Magnenat. Bringing robotics to formal education: The Thymio open-source hardware robot. *IEEE Robotics & Automation Magazine*, 24(1): 77–85, 2017.

Frans A Oliehoek. Decentralized POMDPS. In *Reinforcement Learning*, pages 471–503. Springer, 2012.

Liviu Panait and Sean Luke. Cooperative multi-agent learning: The state of the art. *Autonomous agents and multi-agent systems*, 11(3):387–434, 2005.

Emanuele Pesce and Giovanni Montana. Improving coordination in multi-agent deep reinforcement learning through memory-driven communication, 2019.

Morgan Quigley, Josh Faust, Tully Foote, and Jeremy Leibs. ROS: an open-source Robot Operating System. 2009.

Stéphane Ross, Geoffrey Gordon, and Drew Bagnell. A reduction of imitation learning and structured prediction to no-regret online learning. In *Proceedings of the fourteenth international conference on artificial intelligence and statistics*, pages 627–635, 2011.

Peter Sadowski. Notes on backpropagation. 2016. URL `https://www.ics.uci.edu/pjsadows/notes.pdf`.

Guillaume Sartoretti, William Paivine, Yunfei Shi, Yue Wu, and Howie Choset. Distributed learning of decentralized control policies for articulated mobile robots. *IEEE Transactions on Robotics*, 35(5):1109–1122, 2019.

Stefan Schaal. Is imitation learning the route to humanoid robots? *Trends in cognitive sciences*, 3(6):233–242, 1999.

Stefan Seefeld. Boost.Python, 2002-2015. URL `https://www.boost.org/doc/libs/1_70_0/libs/python/doc/html/index.html`.

Khoshnam Shojaei, Alireza Mohammad Shahri, Ahmadreza Tarakameh, and Behzad Tabibian. Adaptive trajectory tracking control of a differential drive wheeled mobile robot. *Robotica*, 29(3):391–402, 2011.

Bruno Siciliano, Lorenzo Sciavicco, Luigi Villani, and Giuseppe Oriolo. *Robotics: modelling, planning and control*. Springer Science & Business Media, 2010.

Roland Siegwart, Illah Reza Nourbakhsh, and Davide Scaramuzza. *Introduction to autonomous mobile robots*. MIT press, 2011.

Jiaming Song, Hongyu Ren, Dorsa Sadigh, and Stefano Ermon. Multi-agent generative adversarial imitation learning. In *Advances in neural information processing systems*, pages 7461–7472, 2018.

Adrian Šošić, Wasiur R KhudaBukhsh, Abdelhak M Zoubir, and Heinz Koeppl. Inverse reinforcement learning in swarm systems. *arXiv preprint arXiv:1602.05450*, 2016.

Bradly C Stadie, Pieter Abbeel, and Ilya Sutskever. Third-person imitation learning. *arXiv preprint arXiv:1703.01703*, 2017.

Simon Stepputtis, Joseph Campbell, Mariano Phielipp, Chitta Baral, and Heni Ben Amor. Imitation Learning of Robot Policies by Combining Language, Vision and Demonstration. *arXiv preprint arXiv:1911.11744*, 2019.

Peter Stone and Manuela Veloso. Multiagent systems: A survey from a machine learning perspective. *Autonomous Robots*, 8(3):345–383, 2000.

Sainbayar Sukhbaatar, Rob Fergus, et al. Learning multiagent communication with backpropagation. In *Advances in neural information processing systems*, pages 2244–2252, 2016.

Ming Tan. Multi-agent reinforcement learning: Independent vs. cooperative agents. In *Proceedings of the tenth international conference on machine learning*, pages 330–337, 1993.

Ekaterina Tolstaya, Fernando Gama, James Paulos, George Pappas, Vijay Kumar, and Alejandro Ribeiro. Learning decentralized controllers for robot swarms with graph neural networks. In *Conference on Robot Learning*, pages 671–682, 2020.

Faraz Torabi, Garrett Warnell, and Peter Stone. Behavioral cloning from observation. *arXiv preprint arXiv:1805.01954*, 2018.

Marco Verna. Learning distributed controllers by backpropagation, 2020.

Zhou Wang and Alan C Bovik. Mean squared error: Love it or leave it? A new look at signal fidelity measures. *IEEE signal processing magazine*, 26(1):98–117, 2009.

Tianhao Zhang, Zoe McCarthy, Owen Jow, Dennis Lee, Xi Chen, Ken Goldberg, and Pieter Abbeel. Deep imitation learning for complex manipulation tasks from virtual reality teleoperation. In *2018 IEEE International Conference on Robotics and Automation (ICRA)*, pages 1–8. IEEE, 2018.

Jinming Zou, Yi Han, and Sung-Sau So. Overview of artificial neural networks. In *Artificial Neural Networks*, pages 14–22. Springer, 2008.